THE UNIVERSITY OF OKLAHOMA

GRADUATE COLLEGE

# COMPARTMENTAL BILINEAR MODELS AND TRACER TECHNIQUES IN THE ANALYSIS OF BIOLOGICAL CONTROL SYSTEMS

A DISSERTATION

SUBMITTED TO THE GRADUATE FACULTY

in partial fulfillment of the requirements for the

degree of

DOCTOR OF PHILOSOPHY

BY

WARREN DREW SMITH

Norman, Oklahoma

1971

COMPARTMENTAL BILINEAR MODELS AND TRACER TECHNIQUES

IN THE ANALYSIS OF BIOLOGICAL CONTROL SYSTEMS

APPROVED BY

DISSERTATION COMMITTEE

## ACKNOWLEDGEMENT

First, I would like to express sincere appreciation to my chairman and advisor, Dr. R. R. Mohler. Not only has Dr. Mohler provided guidance throughout my entire doctoral program, but also it was through him that this work was supported in part on NSF Grant Number 17866.

I also thank Dr. George Ewing, Dr. James Payne, Dr. Nicolas Tzannes, and Dr. Roger Thies for their services as advisory committee members. I especially appreciated Dr. Thies' encouragement in my venture into the realm of physiology.

It was a pleasure associating with Dr. Howard Haines. He graciously shared his research on the wild house mouse. Moreover, his willingness, even eagerness, to combine our resources proved to me that the engineer and the life scientist both profit by working together.

I feel grateful in having secured the most competent typing of Mrs. Joanne Long.

Finally, I deeply thank my wife, Judy, for continuing, throughout this long task, to see something else in me besides a dissertation writer.

TABLE OF CONTENTS

LIST OF TABLES

## LIST OF ILLUSTRATIONS

# PREFACE

This dissertation is based on the broad system concept that, rather than having to consider each physiological process separately, it should be possible to develop concepts of biological modeling and analysis which can be applied to a wide variety of problems. One characteristic common to organisms is homeostasis, that is, a tendency to maintain a constant internal environment. Another common trait is compartmentedness. Anatomical and physiological compartments can be seen ranging from intracellular and cellular processes to the gross structure and environmental relationships of an organism.

When related to compartmentation, homeostasis implies the regulation of substance amounts and/or concentrations within the various compartments of an organism. As a regulatory mechanism, a living organism adjusts not only the rates of production and destruction of substances within compartments but also varies the substance fluxes between compartments and exchange with the environment. This regulation-through-fluxes leads to the presence, in mathematical models of the associated processes, of multiplicative modes of control, wherein the regulated quantities (state variables) and

the available control variables appear as products. Linear control models cannot account for such products; the simplest control models which do allow products of state and control variables are bilinear control systems.

The union of the above concepts of homeostasis, compartmentedness, and bilinearity precipitated the present interest in compartmental bilinear physiological systems.

There are particular problems associated with the analysis of physiological control systems. It is not easy to isolate the controlled process, or plant, from the rest of the system. That is, it may not be possible to manipulate the system control variables. In fact, it may be impossible even to observe control and state variables. These problems preclude the application of much of the theory of identification and modeling to physiological systems. This dissertation suggests that these problems can be resolved for compartmental bilinear systems by utilizing their compartmental structure, and in particular by tracer analysis of this structure. Hence, the emphasis is on the generalization and development of tracer methods applicable to the analysis of compartmental bilinear systems.

In Chapter I, the concepts of compartmental bilinear systems and tracer analysis are formally introduced. Chapter II discusses the first problem in fitting a compartmental bilinear model to a physiological system, that of determining the model order. It is shown that, using tracers, the system

order can be estimated while the system is held in steady state, thus circumventing the problems of system nonlinearity and complexity. In Chapter III, methods, again based on tracers, are developed for obtaining the dynamical behavior of a compartmental bilinear system. That is, when the state and control variables of such a system functioning in a living organism are not directly accessible, their behaviors can nevertheless be derived from tracer data as shown in Chapter III. Chapters IV and V consist of an analysis of water acclimation in the wild house mouse. Necessary background physiology is presented in Chapter IV, and models of water exchange in the mouse are derived. Then, in Chapter V, this physiological background and the theory of Chapters II and III are applied to experimental data obtained on water acclimation. Chapter VI contains both a summary with conclusions and suggestions for future work.

Equations, figures, tables, and references to the literature are numbered sequentially within each chapter and appendix; the references are listed at the end of the dissertation according to chapter.

# COMPARTMENTAL BILINEAR MODELS AND TRACER TECHNIQUES IN THE ANALYSIS OF BIOLOGICAL CONTROL SYSTEMS

## CHAPTER I

## INTRODUCTION

### 1.1 Objectives

The fundamental objective of this dissertation is to facilitate the application of compartmental bilinear models to the study of physiological control systems. Bilinear models are known to be appropriate for representing a wide variety of physical phenomena, including nuclear reactor neutron kinetics [1.1],[1] economic and population growth [1.2], and, of special interest here, physiological regulatory systems [1.2, 1.3]. Questions of controllability [1.4], optimal control [1.5, 1.6], and identification [1.7] of bilinear systems are considered in the literature. The available theory, however, is not directly applicable to the immediate problems in physiology of system modeling and analysis. This dissertation, as a partial answer to this need, presents methods of developing and analyzing bilinear models for physiological control systems which possess compartmental forms. In particular, tracer techniques are

[1] References to the literature are given in brackets.

derived for studying the compartmental structures of such systems, which are then related to the bilinear control forms.

The remainder of this chapter introduces the concepts of compartmentation, bilinearity, and tracer analysis. In Section 1.2, compartmental models and bilinear control models are defined. Then the existence and interrelatedness of these two concepts in physiological systems are discussed. The fundamentals of tracer methods for the analysis of compartmental physiological systems are presented in Section 1.3.

## 1.2 Compartmental Bilinear Control Models

Compartmental models for physiological systems are suggested on the basis of anatomy, physiology, and mathematics. They have been applied in the study of such diverse problems as thermal regulation [1.8], body fluid and electrolyte balance [1.9], the kinetics of material injected or ingested into or excreted from the body [1.10], and the kinetics of metabolites in cell suspensions or tissues [1.11]. Though some of these processes have been approximated by noncompartmental integral equations [1.12] and stochastic models [1.13], such techniques have been hindered by their mathematical complexity or their failure to describe desired parameters [1.14].

The simplest compartmented system model consists of a single substance X which is distributed among n compartments

(phases, spaces, pools). The elements of such an ideal system are related by the following conservation equations:[1]

$$\dot{x}_i = \sum_{p=1}^{n}{}' \phi_{ip}(t) - \sum_{q=1}^{n}{}' \phi_{qi}(t) + \phi_{ia}(t) - \phi_{ai}(t)$$

$$+ P_i(t) - D_i(t) , \quad i = 1, \cdots, n . \tag{1.1}$$

In (1.1) $\dot{x}_i$ means $dx_i/dt$, the primed sigma means that the ith term of the summation is deleted, and

$x_i(t)$ is the amount of substance X in compartment i,

$\phi_{ij}(t)$ is the flux of X to compartment i from compartment j,[2]

$\phi_{ia}(t)$ $(\phi_{ai}(t))$ is the flux of X into (out of) compartment i from (to) the environment,

$P_i(t)$ $(D_i(t))$ is the rate of production (destruction) of X in compartment i.

Only single-substance compartmental systems of form (1.1) are considered in this study.

The system described by (1.1) can also be represented by the following abbreviated form: Define the generalized fluxes,

---

[1]Following the notation of system theory, the time dependence of state variables and control variables is not explicitly indicated in dynamical equations.

[2]This order of flux subscripts is the reverse of that sometimes found in the literature on compartmental theory. It is chosen here to be consistent with the matrix notation to follow.

$$\phi_{i,n+1}(t) = \phi_{ia}(t) \ ,$$

$$\phi_{n+1,i}(t) = \phi_{ai}(t) \ ,$$

$$\phi_{i,n+2}(t) = P_i(t) \ , \tag{1.2}$$

and

$$\phi_{n+2,i}(t) = D_i(t) \ , \quad i = 1, \cdots, n \ .$$

Then, (1.1) becomes

$$\dot{x}_i = \sum_{p=1}^{n+2}{}' \phi_{ip}(t) - \sum_{q=1}^{n+2}{}' \phi_{qi}(t) \ , \quad i = 1, \cdots, n \ . \tag{1.3}$$

Form (1.3) is used later in this section in relating compartmental and bilinear structures. Both forms (1.1) and (1.3) express the conservation of substance X in terms of substance amounts, $x_i(t)$, $i = 1, \cdots, n$, within the compartments. In some compartmental systems, substance X may be uniformly distributed within each compartment, and concentrations rather than total amounts of X in the compartments may be regulated. In these cases, it may be desired to express the conservation equations in terms of compartmental concentrations, $\xi_i(t)$, $i = 1, \cdots, n$, where, with volume or capacity $C_i(t)$ of compartment i,

$$x_i(t) = C_i(t)\xi_i(t) \ , \quad i = 1, \cdots, n \ . \tag{1.4}$$

When fitting (1.1) to a real physiological system, the mathematical compartments and fluxes chosen should correspond to meaningful biological quantities. Also, it must be possible to take measurements on the system, preferably in a manner not harmful to the organism. There should be negligible X stored in the interfaces between the physiological compartments, and the changes in X in these compartments should be approximately continuous with time. When a distributed system is compartmentized, the choice and number of compartments is determined by the sites of interest of the behavior of X and the desired accuracy of the model. Also, it is often desirable to represent several physiological compartments by a single compartment in the model; some considerations and criteria for combining compartments are given in [1.15] and [1.16].

Homeostasis operating in the above system implies regulation of the $x_i(t)$, $i = 1, \cdots, n$. Such regulation could be effected through variation of any or all of the intercompartmental fluxes, the system environment fluxes, and the rates of production and destruction of X within the compartments. The fact that organisms use all these modes of control leads to the interrelationship of bilinear control models with compartmental physiological systems.

First, a bilinear control system is defined as a control system linear in state, and linear in control, but not jointly

linear in state and control. A finite dimensional bilinear system can be expressed as

$$\dot{\bar{x}} = A(t)\bar{x} + \sum_{k=1}^{m} u_k B_k(t)\bar{x} + C(t)\bar{u} + \bar{g}(t) \ , \qquad (1.5)$$

where

$\bar{x}$ is an $n \times 1$ state vector,

$\bar{u}$ is an $m \times 1$ control vector with elements $u_k$,

$A(t)$ and the $B_k(t)$'s are $n \times n$ matrices,

$C(t)$ is an $n \times m$ matrix,

and

$\bar{g}(t)$ is a given $n \times 1$ time function.

Sometimes it is convenient to express bilinear system (1.5) in the form

$$\dot{\bar{x}} = A(t)\bar{x} + \sum_{j=1}^{n} x_j E_j(t)\bar{u} + C(t)\bar{u} + \bar{g}(t) \ , \qquad (1.6)$$

where the elements of the $n \times n$ matrices $E_j(t) = (e_{j,ik}(t))$, $j = 1, \cdots, n$, are related to the elements of matrices $B_k(t) = (b_{k,ij}(t))$, $k = 1, \cdots, m$, by

$$e_{j,ik}(t) = b_{k,ij}(t) \ . \qquad (1.7)$$

The interesting feature in (1.5) (or (1.6)) is the set of terms involving products of state and control variables. It is these bilinear terms which permit the modeling of controllable fluxes in the compartmented systems; without them,

(1.5) becomes again simply a linear control system. Fluxes of X leaving a particular compartment, say the ith, to other compartments or to the environment often depend on the amount of X, $x_i(t)$, within that compartment. These substance amounts are the natural state variables of a compartmental system. Furthermore, the fluxes are regulated by varying the effective conductivity or permeability of the compartment boundary to the passage of X. A bilinear structure is the simplest form which can account for this multiplicative type of control in compartmented control systems. Physiological examples of multiplicative or bilinear control include passive thermal conduction or mass diffusion through a region of controllable conductivity or permeability, respectively. A thermal process of this type occurs, for example, in the human body where vasomotor routing of blood flow controls the effective thermal conductivities of the body. An analogous process occurs in mass diffusion through cell membranes where enzymes can control fluxes by changing membrane permeabilities.

More generally, a simple membrane model including active transport also fits this form directly. Assume, for example, two compartments with capacities $C_1$ and $C_2$ and respective uniform concentrations $\xi_1(t)$ and $\xi_2(t)$ of substance X, separated by a membrane capable of active transport. The simplest model describing the net flux through the membrane from $C_2$ to $C_1$ is

$$\phi_{net}(t) = \rho_{12}\xi_1(t) - \rho_{21}\xi_2(t)$$

$$= \frac{\rho_{12}}{c_2} x_2(t) - \frac{\rho_{21}}{c_1} x_1(t) \ , \qquad (1.8)$$

where the exchange coefficients $\rho_{12}$ and $\rho_{21}$ are generally not equal. By definition, the active transport mechanism is directly coupled to the metabolic energy chain. By varying this energy link, the rates of active transport, and hence the values of $\rho_{12}$ and $\rho_{21}$ can be controlled.

In general, a generalized flux, $\phi_{ip}(t)$, of compartmental system (1.3) is in bilinear form if it can be expressed in terms of state variables (substance amounts) $x_i$, $i = 1, \cdots, n$, and control variables $u_k$, $k = 1, \cdots, m$, as

$$\phi_{ip}(t) = \sum_{j=1}^{n} a_{ip,j}(t)x_j(t) + \sum_{j=1}^{n}\sum_{k=1}^{m} b_{ip,jk}(t)x_j(t)u_k(t)$$

$$+ \sum_{k=1}^{m} c_{ip,k}(t)u_k(t) + g_{ip}(t) \ , \qquad (1.9)$$

$$i,p = 1, \cdots, n+2, \ i \neq p \ ,$$

$$(i,p) \neq (n+1, n+2)$$

$$\neq (n+2, n+1) \ .$$

In (1.9), $a_{ip,j}(t)$, $b_{ip,jk}(t)$, $c_{ip,k}(t)$, and $g_{ip}(t)$, $i,p = 1, \cdots, n+2$, $i \neq p$, $(i,p) \neq (n+1, n+2)$, $(i,p) \neq (n+2, n+1)$, $j = 1, \cdots, n$, $k = 1, \cdots, m$, are given time functions. Mechanisms of thermal and material exchange within organisms and

their environments are generally complex. Thermal exchange includes the processes of convection, radiation, evaporation, and bulk transfer as well as conduction. Material transport is induced by hydrostatic pressure, diffusion, and active transport. Complex transport mechanisms, however, can be approximated by bilinear expressions. For example, a general expression for the net flux through a membrane possessing active transport [1.17] is

$$\phi_{net}(t) = \frac{a\xi_2(t) - b\xi_1(t)}{c + d\xi_1(t) + e\xi_2(t)} , \tag{1.10}$$

where $\xi_1(t)$ and $\xi_2(t)$ are the substance concentrations on either side of the membrane. One approximation to this expression is the first few terms of a two-dimensional Taylor series in $\xi_1(t)$, $\xi_2(t)$ about $\xi_{10}$, $\xi_{20}$, giving

$$\begin{aligned}\phi_{net}(t) \simeq{}& \frac{a\xi_{20} - b\xi_{10}}{c + d\xi_{10} + e\xi_{20}} \\ &+ \frac{ac + (ad + be)\xi_{10}}{(c + d\xi_{10} + e\xi_{20})^2}(\xi_2(t) - \xi_{20}) \\ &- \frac{bc + (ad + be)\xi_{20}}{(c + d\xi_{10} + e\xi_{20})^2}(\xi_1(t) - \xi_{10}) .\end{aligned} \tag{1.11}$$

If a and/or b are controls, then (1.11) is in bilinear form.

Particular cases of bilinear compartmented physiological control systems are discussed in the literature. For instance,

compartmented models of the human thermo-regulator are in this form [1.8, 1.18]. As mentioned above, bilinear control in this system occurs through adjustable thermal conductivities. Another example of a bilinear compartmented system is the respiratory chemostat for $CO_2$ modeled by Grodins [1.19]. Here, the bilinear controls are lung ventilation rate and heart output. In general, if every process of compartmental system (1.1) has the mathematical bilinear form of (1.9), then the total system is a bilinear control system of form (1.5). That is, insert (1.9) into (1.3) and collect terms. Then, (1.3) has bilinear form (1.5), where the elements of $A(t) = (a_{ij}(t))$, $B_k(t) = (b_{k,ij}(t))$, $C(t) = (c_{ik}(t))$, and $\bar{g}(t) = (g_i(t))$ are given, respectively, by

$$a_{ij}(t) = \sum_{p=1}^{n+2}{}' a_{ip,j}(t) - \sum_{q=1}^{n+2}{}' a_{qi,j}(t) , \tag{1.12}$$

$$b_{k,ij}(t) = \sum_{p=1}^{n+2}{}' b_{ip,jk}(t) - \sum_{q=1}^{n+2}{}' b_{qi,jk}(t) , \tag{1.13}$$

$$k = 1, \cdots, m ,$$

$$c_{ik}(t) = \sum_{p=1}^{n+2}{}' c_{ip,k}(t) - \sum_{q=1}^{n+2}{}' c_{qi,k}(t) , \tag{1.14}$$

and

$$g_i(t) = \sum_{p=1}^{n+2}{}' g_{ip}(t) = \sum_{q=1}^{n+2}{}' g_{qi}(t) . \tag{1.15}$$

Alternately, the elements of $E_j(t) = (e_{j,ik}(t))$ in form (1.6) are given by

$$e_{j,ik}(t) = \sum_{p=1}^{n+2}{}' b_{ip,jk}(t) - \sum_{q=1}^{n+2}{}' b_{qi,jk}(t) , \qquad (1.16)$$

$$j = 1, \cdots, n .$$

A comprehensive theory of the identification and analysis of bilinear models of form (1.5) is not developed here. Instead, techniques of modeling and studying such models are developed, based on the additional assumption of a compartmental structure. An important tool of these techniques is tracer analysis.

## 1.3 Tracer Analysis

A tracer is a labeled substance which can be used to follow the behavior of the substance of interest. (A classic example is the belling of a sheep so that the wanderings of the flock may be traced.) Supplementing the direct methods of obtaining compartmental capacities and substance amounts and concentrations, tracer methods, especially using isotopic tracers, can often yield information conveniently and harmlessly. For example, in dilution analysis a known quantity of tracer is injected into the system. Samples from the compartments provide not only substance and tracer concentrations but also information on compartmental capacities and, hence, substance amounts. Moreover, as is shown later, tracer

methods are uniquely suited to determining the fluxes in a compartmented system.

When applying tracers to compartmental analysis, it is usually assumed that the tracer in every compartment is distributed uniformly through the substance X, that labeled and unlabeled X behave identically in the system, and that the presence of tracer does not affect system behavior [1.20, 1.21, 1.22]. This last assumption includes the requirement that the fraction of labeled X in a compartment is negligible. With these assumptions, the tracer dynamics associated with compartmental system (1.1) are described in terms of tracer specific activities, $a_i$, $i = 1, \cdots, n$, by (1.17). (Specific activity $a_i$ is the fraction of tracer in the total amount of X in compartment i.)

$$\frac{d}{dt}(x_i a_i) = \sum_{p=1}^{n}{}' \phi_{ip}(t) a_p - \sum_{q=1}^{n}{}' \phi_{qi}(t) a_i + \phi_{ia}(t) a_{ia}(t)$$

$$- \phi_{ai}(t) a_i - D_i(t) a_i + f_i(t) , \qquad (1.17)$$

$$i = 1, \cdots, n .$$

Tracer can enter a compartmental system either via substance fluxes from the environment or by direct insertion into compartments. In (1.17), $a_{ia}(t)$ is the specific activity of the substance in influx $\phi_{ia}(t)$ ($\phi_{ia}(t) \equiv 0$ implies $a_{ia}(t) \equiv 0$), and $f_i(t)$ is the influx of tracer directly inserted into compartment i. Using matrix notation, (1.17) becomes

$$\dot{\bar{a}} = S(t)\bar{a} + X^{-1}(t)\Phi_{.a}(t)\bar{a}_{.a}(t) + X^{-1}(t)\bar{f}(t) \ , \qquad (1.18)$$

where $\bar{a}$ and $\bar{a}_{.a}(t)$ are n-vectors of tracer specific activities within the compartments and in the influxes, respectively, and $\bar{f}(t)$ is the n-vector of directly inserted tracer influxes. The n-square matrices $S(t) = (s_{ij}(t))$, $X(t)$, and $\Phi_{.a}(t)$ of (1.18) are defined, respectively, by

$$s_{ij}(t) = \frac{\phi_{ij}(t)}{x_i(t)} \geq 0 \ , \quad i, j = 1, \cdots, n, \ i \neq j \ , \qquad (1.19)$$

$$s_{ii}(t) = -\frac{1}{x_i(t)}\left( \sum_{p=1}^{n}{}' \phi_{ip}(t) + \phi_{ia}(t) + P_i(t) \right) \ , \qquad (1.20)$$

$$i = 1, \cdots, n \ ,$$

$$= -\frac{1}{x_i(t)}\left( \sum_{q=1}^{n}{}' \phi_{qi}(t) + \phi_{ai}(t) + D_i(t) \right.$$

$$\left. + \dot{x}_i(t) \right) \ , \quad i = 1, \cdots, n \ , \qquad (1.21)$$

$$X(t) = \mathrm{diag}(x_1(t), \cdots, x_n(t)) \ , \qquad (1.22)$$

and

$$\Phi_{.a}(t) = \mathrm{diag}(\phi_{1a}(t), \cdots, \phi_{na}(t)) \ . \qquad (1.23)$$

Note that even if compartmental system (1.1) describes a physiological system involving highly nonlinear and complex transport and regulatory mechanisms, the corresponding tracer system in (1.18) (or (1.17)) is linear in specific activity.

It is this linearity which makes tracer analysis such a useful tool in compartmental analysis.

Most of the available theory on using tracer methods to analyze compartmental systems is for steady state ($\dot{x}_i = \dot{\phi}_{ij} = \dot{\phi}_{ai} = \dot{\phi}_{ia} = \dot{P}_i = \dot{D}_i = 0$, $i, j = 1, \cdots, n$, $i \neq j$),[1] closed ($\phi_{ai} = \phi_{ia} = 0$, $i = 1, \cdots, n$), conservative ($P_i = D_i = 0$, $i = 1, \cdots, n$) systems. In this case, (1.1) becomes

$$0 = \sum_{p=1}^{n}{}' \phi_{ip} - \sum_{q=1}^{n}{}' \phi_{qi} , \quad i = 1, \cdots, n , \tag{1.24}$$

and the associated tracer dynamics are described by the time-invariant system,

$$\dot{\bar{a}} = S\bar{a} . \tag{1.25}$$

Work has been done, for example, on the specification of required data to obtain fluxes $\phi_{ij}$, $i, j = 1, \cdots, n$, $i \neq j$, from tracer observations and on the solution for the fluxes with complete [1.16, 1.23] and incomplete [1.24] data. Also, some general theorems on the response of this tracer system have been derived [1.25, 1.26]. Only a few special cases of nonsteady state compartmental systems have been analyzed [1.16, 1.21, 1.27]. The system of interest in this dissertation, however, has general compartmental form (1.1) and,

---

[1] Steady state is used in physiology not in the engineering sense of forced response but to mean that all the system parameters, including state, are time-invariant. The term equilibrium is not applied because, as used in biology, it would imply no net flux between each pair of compartments and between each compartment and the environment.

through (1.9) and (1.12)-(1.16), bilinear form (1.5). Therefore, portions of the next two chapters are devoted to generalizing and developing the concepts of tracer analysis so that it may be applied to the identification and investigation of general compartmental system (1.1).

# CHAPTER II

# DETERMINATION OF SYSTEM ORDER

## 2.1 Introduction

When fitting a compartmental bilinear model to a physiological controlled process, the first task is to determine the order or number of compartments, n, to be used. Usually, the compartments chosen are to have physiological significance, and, of course, any physiological insight should be utilized. This chapter, however, focuses on the problem of estimating n from experimental observations on the physiological system. Recall that the model to be applied is assumed to have both bilinear form (1.5) and the compartmental structure (1.1).

The problem of estimating the system order, n, can be approached via either the bilinear form in (1.5) or the compartmental form in (1.1). Techniques for finding the order, n, of bilinear system (1.5) can be developed based on the application of test inputs and the fact that (1.5) reduces to a linear system when $\bar{u}$ is held constant. These methods are not described here, however, because they are not well suited to estimating n for system (1.5) when it is the controlled

process of a physiological system. The physiological system under study is generally a functioning homeostatic system, complete with unknown, nonlinear feedback paths. In this condition, it may not be possible to drive controlled process (1.5) externally by means of the control variables, and the system automatically compensates for any disturbances of the state variables. Hence, it is not possible at present to estimate the order of such a bilinear physiological system from direct observations on the state variables.

It is often possible, however, to investigate the order of a compartmental bilinear physiological system by tracer analysis of compartmental structure (1.1). Recall from Chapter I that tracer system (1.18) associated with compartmental structure (1.1) is linear in specific activity and has the same order, n, as the original compartmental system. Furthermore, the dynamics of (1.18) can be studied while maintaining (1.1) in steady state. Under this condition, (1.18) is a time-invariant linear system, regardless of the complex nonlinear structure of (1.1) with its associated controller and feedback paths.

The problem of finding the order of a time-invariant linear system consists of two parts: verification that there is adequate experimental access to the system and estimation of system order from experimental data. The first of these two aspects of finding the order of tracer system (1.18) is

discussed in Section 2.2. Consider the general time-invariant nth-order linear system,

$$\dot{\bar{x}} = A\bar{x} + C\bar{u}$$
$$\bar{y} = D\bar{x} + E\bar{u} \ , \tag{2.1}$$

with n-dimensional state vector $\bar{x}$, m-dimensional input or control vector $\bar{u}$, q-dimensional output vector $\bar{y}$, and matrices A, C, D, and E of appropriate dimensions. The order, n, of system (2.1) can be obtained from input-output observations if and only if (2.1) is completely controllable (CC) and completely observable (CO) [2.1].[1] Moreover, define $n \times m(n - r + 1)$ matrix $U_{n-r}(A, C)$ by

$$U_{n-r}(A, C) = (C \ AC \ \cdots \ A^{n-r}C) \ , \tag{2.2}$$

and define $q(n - s + 1) \times n$ matrix $V_{n-s}(A, D)$ by

$$V_{n-s}(A, D) = (D^* \ A^*D^* \ \cdots \ A^{n-s^*}D^*)^* \ , \tag{2.3}$$

where the asterisk denotes matrix transpose. Then, (2.1) is CC if and only if

$$\rho(U_{n-r}(A, C)) = n \ , \tag{2.4}$$

---

[1] Heuristically, a system is CC if every "mode" of state behavior can be excited by the input and CO if every "mode" of state behavior influences the output. This result and other properties of linear systems used here are referenced in [2.1] only for convenience; many other texts on linear system theory are also available.

where $1 \leq r \leq \rho(C)$, and $\rho(G)$ denotes the rank of matrix G [2.1, pp. 178 and 181]. Similarly, for system (2.1) to be CO, it is necessary and sufficient that

$$\rho(V_{n-s}(A, D)) = n \ , \tag{2.5}$$

where $1 \leq s \leq \rho(D)$ [2.1, pp. 188 and 189]. Based on (2.2)-(2.5), conditions are derived in Section 2.2 describing the necessary experimental access to linear tracer system (1.18) to obtain the order n.

Methods for estimating the order, n, of a linear system from input-output data yield, in fact, $n_o$, the order of the lowest-order linear system which could generate or "realize" the given data.[1] When the linear system is CC-CO, $n = n_o$; otherwise, $n > n_o$ [2.1]. Section 2.3 relates general linear system techniques for finding system order to tracer system (1.18). Also, special methods are described for estimating the system order of a linear system whose state matrix has only nonpositive, distinct, real eigenvalues.[2] Conditions on the compartmental structure are then derived under which the associated tracer system satisfies this latter requirement.

---

[1] Such a lowest-order system is called a minimal realization and is usually not unique.

[2] See [2.1] for definitions of the eigenvalues and eigenvectors of a matrix.

## 2.2 Tracer System Controllability and Observability

As with the general linear system, the first step in finding the order, n, of tracer system (1.18) is to attempt to assure that, under the available experimental access, the system is CC-CO. The relation between controllability and observability on one hand and the structure of the original compartmental system and experimental access on the other is now developed.

Recall from Chapter I that tracer can be applied to a physiological system in two ways. Tracer can be inserted via special routes, such as by injection, directly into particular portions of the system; or normally existing pathways into the system can be used, such as when the system is subjected to a tracer-labeled environment. For simplicity, these two experimental procedures are considered separately in Sections 2.2.1 and 2.2.2, respectively.

### 2.2.1 Direct Tracer Insertion

Assume $\bar{a}_{.a} \equiv \bar{0}^{1}$ and that tracer can be directly inserted into p system compartments and that tracer behavior can be experimentally monitored in q compartments. Define an n × p input matrix, P, having zero elements except for a unity element in each row corresponding to a compartment accessible for tracer insertion. Each column of P has exactly one unity

[1] The n elements of n-vector $\bar{0}$ are all zero.

element, and $\rho(P) = p$. Also, define $q \times n$ output matrix $Q$ with zero elements except for a one in each column which corresponds to an observable compartment. Then, the above experimental access to system (1.18) can be described by

$$\begin{aligned} \dot{\bar{a}} &= S\bar{a} + X^{-1}P\bar{F} \\ \bar{w} &= Q\bar{a} \ . \end{aligned} \tag{2.6}$$

In (2.6), the $p \times 1$ vector $\bar{F}$ is the vector of inserted total activity fluxes, and, therefore, $X^{-1}P\bar{F}$ is the vector of inserted specific activity fluxes. The q-dimensional output vector, $\bar{w}$, consists of the compartmental specific activities which can be directly observed. For example, consider the general three-compartment system shown in Fig. 2.1. Assume that tracer can be inserted into compartments 1 and 2 and that tracer specific activity can be measured in compartment 1. Then, (2.6) becomes

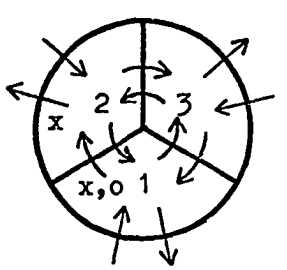


x denotes tracer insertion
o denotes tracer observation

Fig. 2.1. Tracer Insertion into a General Three-Compartment System.

$$\begin{pmatrix} \dot{a}_1 \\ \dot{a}_2 \\ \dot{a}_3 \end{pmatrix} = \begin{pmatrix} s_{11} & s_{12} & s_{13} \\ s_{21} & s_{22} & s_{23} \\ s_{31} & s_{32} & s_{33} \end{pmatrix} \begin{pmatrix} a_1 \\ a_2 \\ a_3 \end{pmatrix} + \begin{pmatrix} \frac{1}{x_1} & 0 & 0 \\ 0 & \frac{1}{x_2} & 0 \\ 0 & 0 & \frac{1}{x_3} \end{pmatrix} \begin{pmatrix} 1 & 0 \\ 0 & 1 \\ 0 & 0 \end{pmatrix} \begin{pmatrix} F_1 \\ F_2 \end{pmatrix} \tag{2.7}$$

$$w_1 = (1\ 0\ 0) \begin{pmatrix} a_1 \\ a_2 \\ a_3 \end{pmatrix} .$$

Conditions for the controllability and observability of system (2.6) can be obtained by comparing it with the general linear system in (2.1). That is, (2.6) is controllable if and only if

$$\rho[(X^{-1}P\ SX^{-1}P\ \cdots\ S^{n-p}X^{-1}P)] = n . \tag{2.8}$$

Condition (2.8) can be simplified. Because input matrix P has only a single nonzero entry (unity) in each column, each element in a given column of the controllability matrix in (2.8) is multiplied by the same element of diagonal matrix $X^{-1}$. But, the multiplication of a matrix column by a nonzero constant does not alter the rank of the matrix. Hence, the matrix in (2.8) can be replaced by the simplified controllability matrix,

$$U_{n-p}(S, P) = (P\ SP\ \cdots\ S^{n-p}P) . \tag{2.9}$$

Then, with the observability matrix, from (2.3),

$$V_{n-q}(S, Q) = (Q^* \; S^*Q^* \; \cdots \; S^{n-q^*}Q^*)^* , \qquad (2.10)$$

the tracer system is CC-CO under the experimental access given by (2.6) if and only if

$$\rho(U_{n-p}(S, P)) = \rho(V_{n-q}(S, Q)) = n . \qquad (2.11)$$

Necessary conditions for CC and CO can also be derived from physical reasoning. For the compartmental tracer system to be controllable, it is necessary that the tracer specific activity in each compartment can be influenced by the specific activity in at least one of the p input compartments. That is, separate the compartments into two disjoint groups: the set $C = \{k_1, \cdots, k_p\}$ of compartments accessible for tracer insertion and the set $\tilde{C} = \{i_1, \cdots, i_{n-p}\}$ of compartments not accessible for insertion ($C \cup \tilde{C} = \{1, \cdots, n\}$; $C \cap \tilde{C} = \phi$[1]). Then, for <u>each</u> $i_u \varepsilon \tilde{C}$ and for <u>some</u> $k_v \varepsilon C$, there must exist a nonzero product of fluxes of the form

$$\phi_{i_u j_1} \phi_{j_1 j_2} \cdots \phi_{j_{r-1} j_r} \phi_{j_r k_v} > 0 , \quad r < n , \quad j_w \varepsilon \tilde{C} ,$$

$$w = 1, \cdots, r . \qquad (2.12)$$

Analogously, the tracer system can be observable only if the tracer specific activity in each compartment can affect the specific activity in at least one of the observable

---

[1]The empty set or null set is denoted by $\phi$.

compartments. As above, divide the compartments into the set $E = \{f_1, \cdots, f_q\}$ of compartments accessible for tracer observation and the set $\tilde{E} = \{h_1, \cdots, h_{n-q}\}$ not accessible for observation ($E \cup \tilde{E} = \{1, \cdots, n\}$; $E \cap \tilde{E} = \phi$). Then, to have an observable tracer system, it is necessary that, for <u>each</u> $h_u \varepsilon \tilde{E}$, there exist <u>some</u> $f_v \varepsilon E$ such that

$$\phi_{f_v g_1} \phi_{g_1 g_2} \cdots \phi_{g_{s-1} g_s} \phi_{g_s h_u} > 0 , \quad s < n , \quad g_w \varepsilon \tilde{E} ,$$

$$w = 1, \cdots, s . \qquad (2.13)$$

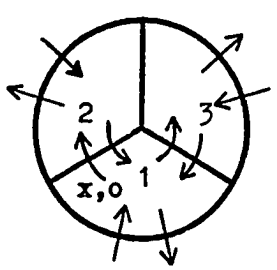


x denotes tracer insertion
o denotes tracer observation

Fig. 2.2. Tracer Insertion into a Special Compartmental System.

As an example of the application of condition (2.11), consider the system given by (2.7). In this case,

$$U_{n-2}(S, P) = \begin{pmatrix} 1 & 0 & s_{11} & s_{12} \\ 0 & 1 & s_{21} & s_{22} \\ 0 & 0 & s_{31} & s_{32} \end{pmatrix} , \qquad (2.14)$$

and

$$V_{n-1}(S, Q) = \begin{pmatrix} 1 & 0 & 0 \\ s_{11} & s_{12} & s_{13} \\ s_{11}^2+s_{12}s_{21} & s_{11}s_{12}+s_{12}s_{22} & s_{11}s_{13}+s_{12}s_{23} \\ +s_{13}s_{31} & +s_{13}s_{32} & +s_{13}s_{33} \end{pmatrix} . \tag{2.15}$$

It is seen from (2.14) and (2.11) that (2.7) is not controllable if and only if $s_{31} = s_{32} = 0$ ($\phi_{31} = \phi_{32} = 0$). Analogously, from (2.15) and (2.11), (2.7) is not observable if $\phi_{12} = \phi_{13} = 0$. Moreover, if say $\phi_{12} = 0$, then (2.7) is not observable unless $\phi_{13} \neq 0$ and $\phi_{32} \neq 0$. These conclusions could also have been obtained by applying conditions (2.12) and (2.13).

The system in Fig. 2.2 is an example of a tracer system under experimental access which satisfies the necessary conditions (2.12) and (2.13) and yet which is not CC-CO. For the system in Fig. 2.2, tracer is inserted and observed only in compartment 1, and the fluxes and production terms of the original steady state compartmental system are assumed to satisfy

$$\phi_{12} = \phi_{13}$$

$$\frac{\phi_{21}}{x_2} = \frac{\phi_{31}}{x_3}$$

$$\phi_{23} = \phi_{32} = 0$$

$$\phi_{2a} + P_2 = \phi_{3a} + P_3 \ . \tag{2.16}$$

It can be seen that conditions (2.12) and (2.13) are satisfied, respectively, by

$$\phi_{21} > 0$$

$$\phi_{31} > 0 \tag{2.17}$$

and

$$\phi_{12} > 0$$

$$\phi_{13} > 0 \ . \tag{2.18}$$

The tracer system matrix becomes

$$S = \begin{pmatrix} s_{11} & s_{12} & s_{12} \\ s_{21} & s_{22} & 0 \\ s_{21} & 0 & s_{22} \end{pmatrix} , \tag{2.19}$$

and the input and output matrices are, respectively,

$$P = \begin{pmatrix} 1 \\ 0 \\ 0 \end{pmatrix} \tag{2.20}$$

and

$$Q = (1 \quad 0 \quad 0) \ . \tag{2.21}$$

With (2.19), (2.20), and (2.21), the controllability (2.9) and observability (2.10) matrices become, respectively,

$$U_{n-p}(S, P) = \begin{pmatrix} 1 & s_{11} & s_{11}^2+2s_{12}s_{21} \\ 0 & s_{21} & s_{21}(s_{11}+s_{22}) \\ 0 & s_{21} & s_{21}(s_{11}+s_{22}) \end{pmatrix} \ , \tag{2.22}$$

and

$$V_{n-q}(S, Q) = \begin{pmatrix} 1 & 0 & 0 \\ s_{11} & s_{12} & s_{12} \\ s_{11}^2+2s_{12}s_{21} & s_{12}(s_{11}+s_{22}) & s_{12}(s_{11}+s_{22}) \end{pmatrix} \ . \tag{2.23}$$

The rank of neither (2.22) nor (2.23) can equal n = 3. Hence, under the specified experimental access, the tracer system is neither CC nor CO, even though conditions (2.12) and (2.13) are satisfied.

As a final example, to show how condition (2.11) for CC-CO can be related to a general class of compartmental systems, consider the n-compartment series system in Fig. 2.3. Let all the inter-compartmental fluxes be zero except

$$\phi_{i+1,i} > 0 \ , \quad i = 1, \cdots, n-1 \ , \tag{2.24}$$

so that the tracer matrix becomes

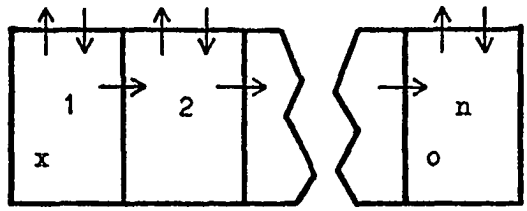


Fig. 2.3. A Uni-Directional Series Compartmental System.

$$S = \begin{pmatrix} s_{11} & & & & \\ s_{21} & s_{22} & & 0 & \\ & s_{32} & \ddots & & \\ & & \ddots & \ddots & \\ 0 & & s_{n,n1} & & s_{nn} \end{pmatrix} . \qquad (2.25)$$

It can then be shown by examining $U_{n-p}(S, P)$ that this tracer system is controllable if and only if compartment 1 is a site of insertion. Analogously, the tracer system is observable if and only if tracer behavior is monitored in the nth compartment. This experimental access is indicated in Fig. 2.3. Again, necessary conditions (2.12) for CC and (2.13) for CO are seen to be satisfied under the above access.

2.2.1.1 Access to a Single Compartment

In estimating the order of a tracer system, the case in which the same single compartment is available for tracer insertion and observation is of special interest. For this

case, the input and output matrices reduce, respectively, to column and row n-vectors, related by

$$P = \bar{p} = Q^* \ . \tag{2.26}$$

After the concept of a reducible matrix is introduced, it is shown that a necessary condition for a tracer system under the above experimental access to be CC-CO is that tracer matrix S in (1.18) be irreducible. By definition, a general n-square matrix $A = (a_{ij})$ is reducible (by a permutation) if the indices 1, 2, $\cdots$, n can be divided into two disjoint nonempty sets, $H = \{i_1, \cdots, i_u\}$ and $V = \{j_1, \cdots, j_{n-u}\}$ ($H \cup V = \{1, \cdots, n\}$; $H \cap V = \phi$) such that

$$a_{i_r j_s} = 0 \ , \quad \text{for all } i_r \varepsilon H \text{ and all } j_s \varepsilon V \ . \tag{2.27}$$

Otherwise, A is irreducible [2.2, p. 61]. Alternately, A is reducible if and only if there is a permutation of the indices which reduces it to the form

$$A_R = \begin{pmatrix} A_{11} & 0 \\ A_{21} & A_{22} \end{pmatrix} \ , \tag{2.28}$$

where $A_{11}$ and $A_{22}$ are square. As an illustration, Fig. 2.4 contains the three possible forms of reducible 4th-order S matrices and the associated compartmental structures. In the figure, the arrows in the diagrams correspond to intercompartmental fluxes which may be nonzero, and the X's in the matrices

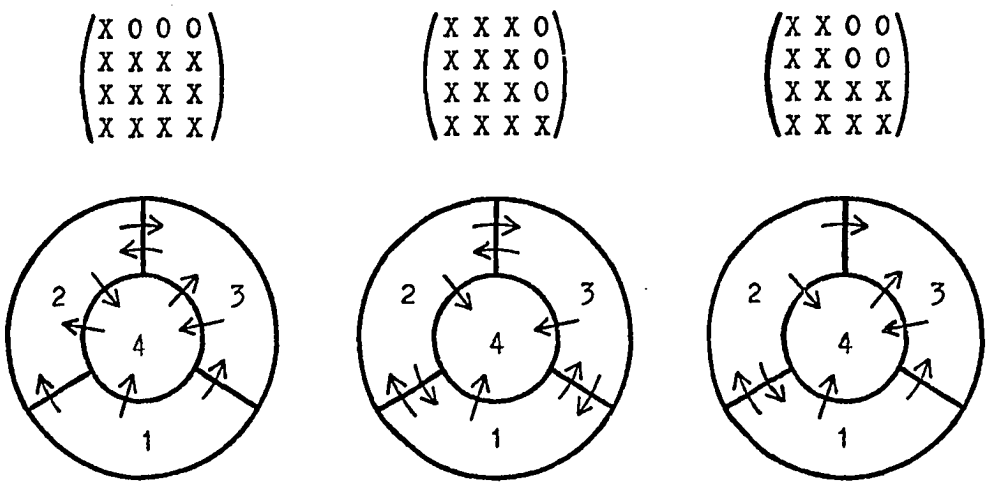


Fig. 2.4. The Three Forms of Reducible 4th-Order S Matrices and the Associated Compartmental Structures.

indicate possibly nonzero elements. For clarity, exchange with the environment is not shown.

That irreducible S is a necessary condition for CC-CO under condition (2.26) can be shown in two ways. First, note that in the case of a single accessible compartment, conditions (2.12) and (2.13) reduce to the following requirement: A necessary condition that a compartmental tracer system accessible according to (2.26) be CC-CO is that, for <u>each</u> distinct pair of compartments, say i and j, there must exist the nonzero products of fluxes,

$$\phi_{ij_1}\phi_{j_1j_2}\cdots\phi_{j_{r-1}j_r}\phi_{j_rj} > 0\ , \quad r < n\ ,$$

$$\phi_{jg_1}\phi_{g_1g_2}\cdots\phi_{g_{s-1}g_s}\phi_{g_si} > 0\ , \quad s < n\ , \tag{2.29}$$

$$1 \leq j_1, \cdots, j_r, \quad g_1, \cdots, g_s \leq n\ ,$$

$$j_u \neq j_v\ , \quad g_u \neq g_v \text{ when } u \neq v\ .$$

Condition (2.29) is equivalent to the condition that S is irreducible, as each is equivalent to specifying that no compartment or subsystem of compartments of the original compartmental system has only nonzero influxes from or only nonzero effluxes to the remaining compartments.

The second definition of reducibility can also be used to show that irreducible S is necessary for CC-CO when only a single tracer compartment is accessible. Assume, contrarily, that S is reducible and, by suitable compartmental numbering, is in the form

$$S = \begin{pmatrix} S_{11} & 0 \\ S_{21} & S_{22} \end{pmatrix}\ , \tag{2.30}$$

with submatrix $S_{11}$ of order r, $1 \leq r < n$. Then, powers of S have the form

$$S^i = \begin{pmatrix} S_{11}{}^i & 0 \\ C_i & S_{22}{}^i \end{pmatrix}\ , \quad i = 1, 2, \cdots, \tag{2.31}$$

where $C_i$ is a function of $S_{11}$, $S_{21}$, and $S_{22}$. Assume that tracer is inserted and observed in compartment k, so that the n columns of the controllability matrix, $U_{n-1}(S, P)$, are vector $P = \bar{p}$ and the kth columns of each of S, ..., $S^{n-1}$. Then, for $r < k \leq n$, (2.31) shows that the first r rows of $U_{n-1}(S, P)$ are zero, so that $\rho(U_{n-1}(S, P)) \leq n - r < n$, and the tracer system is not controllable. Analogously, the observability matrix, $V_{n-1}(S, Q)$, consists of row $Q = \bar{p}^*$ and the kth row of each of S, ..., $S^{n-1}$. Therefore, for $1 \leq k \leq r$, the last n-r columns of $V_{n-1}$ are zero, so that $\rho(V_{n-1}(S, Q)) \leq r < n$, and the tracer system is not observable. In conclusion, then, when P and Q satisfy (2.26), and S is reducible, the tracer system is not CC-CO.

The example associated with Fig. 2.2 shows that irreducible S is not a sufficient condition for CC-CO. The tracer matrix for this system is, indeed, irreducible and yet, with compartment 1 accessible, the tracer system is not CC-CO. This system does become CC-CO if the accessible compartment is 2 or, equivalently, 3. In the next example, however, S is irreducible, and yet the tracer system is not CC-CO for any single accessible compartment.

Consider the closed, conservative "parallel" compartmental system shown in Fig. 2.5. The intercompartmental fluxes are assumed to satisfy

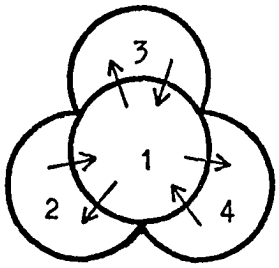


Fig. 2.5. A Closed, Conservative, Parallel Compartmental System.

$$\phi_{23} = \phi_{24} = \phi_{32} = \phi_{34} = \phi_{42} = \phi_{43} = 0$$

$$\frac{\phi_{12}}{x_1} = \frac{\phi_{13}}{x_1} = \frac{\phi_{14}}{x_1} = \frac{\phi_{21}}{x_2} = \frac{\phi_{31}}{x_3} = \frac{\phi_{41}}{x_4} = s \ , \tag{2.32}$$

so that the tracer matrix becomes

$$S = \begin{pmatrix} -3s & s & s & s \\ s & -s & 0 & 0 \\ s & 0 & -s & 0 \\ s & 0 & 0 & -s \end{pmatrix} . \tag{2.33}$$

Let $P = \bar{p} = Q^*$ (only one accessible compartment). Then, since $S = S^*$, the controllability matrix $U_{n-1}(S, P)$ and the observability matrix $V_{n-1}(S, Q)$ are related by

$$U_{n-1}(S, P) = V_{n-1}{}^*(S, Q) \ , \tag{2.34}$$

and so

$$\rho(U_{n-1}(S, P)) = \rho(V_{n-1}(S, Q)) \ . \tag{2.35}$$

With the central compartment accessible, i.e.,

$$P = \bar{p} = \begin{pmatrix} 1 \\ 0 \\ 0 \\ 0 \end{pmatrix}, \tag{2.36}$$

the controllability matrix becomes

$$U_{n-1}(S, P) = \begin{pmatrix} 1 & -3s & 12s^2 & -48s^3 \\ 0 & s & -4s^2 & 16s^3 \\ 0 & s & -4s^2 & 16s^3 \\ 0 & s & -4s^2 & 16s^3 \end{pmatrix}. \tag{2.37}$$

Hence, $\rho(U_{n-1}(S, P)) < 4$, and the system is neither controllable nor observable. Similarly, for an accessible peripheral compartment, e.g., compartment 2, so that

$$P = \bar{p} = \begin{pmatrix} 0 \\ 1 \\ 0 \\ 0 \end{pmatrix}, \tag{2.38}$$

then

$$U_{n-1}(S, P) = \begin{pmatrix} 0 & s & -4s^2 & 16s^3 \\ 1 & -s & 2s^2 & -6s^3 \\ 0 & 0 & s^2 & -5s^3 \\ 0 & 0 & s^2 & -5s^3 \end{pmatrix} . \qquad (2.39)$$

Again, $\rho(U_{n-1}(S, P)) < 4$, and the system is not CC-CO. For such a compartmental system, it is necessary to have access to at least two compartments in order for the tracer system to be CC-CO. For example, the tracer system is CC-CO when

$$P = Q^* = \begin{pmatrix} 0 & 0 \\ 1 & 0 \\ 0 & 1 \\ 0 & 0 \end{pmatrix} . \qquad (2.40)$$

### 2.2.2 "Natural" Tracer Absorption

The second method of subjecting a compartmental system to tracer analysis is to allow tracer to enter the system via naturally existing flux routes. Refer again to tracer system (1.18), and recall that, by definition, $a_{ia} \equiv 0$ whenever $\phi_{ia} = 0$, $i = 1, \cdots, n$. Assume that the fluxes $\phi_{ia}$ with specific activities $a_{ia}$, $i = 1, \cdots, n$, originate from $p'$ separate external sources of labeled substance, each with its own tracer specific activity $A_i$, $i = 1, \cdots, p'$. In this case, define $n \times p'$ input matrix, $P'$, which consists of zero elements except for a single "one" in each row, $i$, for which $a_{ia} \neq 0$. Unlike input matrix $P$ defined previously in Section 2.2.1, $P'$ may have more than a single "one" in a given column, for more than one compartment may receive substance from the

same external source. Output matrix Q, however, is defined as before. Then, (1.18), together with the equation describing observation access, can be written

$$\begin{aligned} \dot{\bar{a}} &= S\bar{a} + X^{-1}\Phi_{.a}P'\bar{A} \\ \bar{w} &= Q\bar{a} \ . \end{aligned} \tag{2.41}$$

where, as can be seen by comparing (2.41) and (1.18),

$$P'\bar{A} = \bar{a}_{.a} \ . \tag{2.42}$$

As seen from the theory of Section 2.1, system (2.41) is CC if and only if controllability matrix

$$U_{n-p'}(S,\ X^{-1}\Phi_{.a}P') = (X^{-1}\Phi_{.a}P'\ SX^{-1}\Phi_{.a}P'\ \cdots\ S^{n-p'}X^{-1}\Phi_{.a}P') \tag{2.43}$$

has rank n. Sometimes a simpler matrix than (2.43) can be used to test whether (2.41) is CC. For example, if no two system compartments receive tracer from the same external source, then each column of P' contains only a single nonzero (unity) element. Hence, by the same argument used to reduce the controllability matrix in (2.8) to (2.9), controllability matrix (2.43) can be reduced in this case to

$$U_{n-p'}(S,\ P') = (P'\ SP'\ \cdots\ S^{n-p'}P') \ . \tag{2.44}$$

In general, however, a given column of P' may contain more than a single nonzero entry, and controllability matrix (2.43) cannot be simplified as above. The observability matrix for

system (2.41) is still given by (2.10). Hence, in the general case, system (2.41) is CC-CO if and only if

$$\rho[U_{n-p'}(S, X^{-1}\Phi_{\cdot a}P')] = \rho[V_{n-q}(S, Q)] = n \ . \qquad (2.45)$$

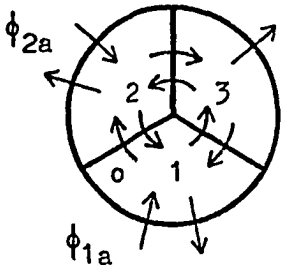


$a_a = A_1$

o denotes tracer observation

Fig. 2.6. Tracer Absorption into a Particular Three-Compartment System

As an example, consider the three-compartment system shown in Fig. 2.6. The nonzero influxes $\phi_{1a}$ and $\phi_{2a}$ ($\phi_{3a} = 0$) are both assumed to originate from the same environmental source at specific activity $A_1 = a_a$. The tracer specific activity of compartment 1 is assumed observable. Then, (2.41) becomes (compare with (2.7))

$$\begin{pmatrix} \dot{a}_1 \\ \dot{a}_2 \\ \dot{a}_3 \end{pmatrix} = \begin{pmatrix} s_{11} & s_{12} & s_{13} \\ s_{21} & s_{22} & s_{23} \\ s_{31} & s_{32} & s_{33} \end{pmatrix} \begin{pmatrix} a_1 \\ a_2 \\ a_3 \end{pmatrix} + \begin{pmatrix} \frac{1}{x_1} & 0 & 0 \\ 0 & \frac{1}{x_2} & 0 \\ 0 & 0 & \frac{1}{x_3} \end{pmatrix} \begin{pmatrix} \phi_{1a} & 0 & 0 \\ 0 & \phi_{2a} & 0 \\ 0 & 0 & 0 \end{pmatrix} \begin{pmatrix} 1 \\ 1 \\ 0 \end{pmatrix} A_1 \qquad (2.46)$$

$$w_1 = (1\ 0\ 0) \begin{pmatrix} a_1 \\ a_2 \\ a_3 \end{pmatrix} .$$

The controllability and observability matrices for (2.46) are given by

$$U_{n-1}(S,X^{-1}\Phi_{.a}P') = \begin{pmatrix} \frac{\phi_{1a}}{x_1} & s_{11}\frac{\phi_{1a}}{x_1} & [s_{11}^2+s_{12}s_{21}+s_{13}s_{31}]\frac{\phi_{1a}}{x_1} \\ & +s_{12}\frac{\phi_{2a}}{x_2} & +[s_{12}(s_{11}+s_{22})+s_{13}s_{32}]\frac{\phi_{2a}}{x_2} \\ \frac{\phi_{2a}}{x_2} & s_{21}\frac{\phi_{1a}}{x_1} & [s_{21}(s_{11}+s_{22})+s_{23}s_{31}]\frac{\phi_{1a}}{x_1} \\ & +s_{22}\frac{\phi_{2a}}{x_2} & +[s_{21}s_{12}+s_{22}^2+s_{23}s_{32}]\frac{\phi_{2a}}{x_2} \\ 0 & s_{31}\frac{\phi_{1a}}{x_1} & [s_{31}(s_{11}+s_{33})+s_{32}s_{21}]\frac{\phi_{1a}}{x_1} \\ & +s_{32}\frac{\phi_{2a}}{x_2} & +[s_{32}(s_{22}+s_{33})+s_{31}s_{12}]\frac{\phi_{2a}}{x_2} \end{pmatrix} \tag{2.47}$$

and by (2.15), respectively. The conditions for CO are the same for (2.46) as for (2.7). Also, as with (2.7), (2.46) is not CC if $\phi_{31} = \phi_{32} = 0$. Unlike for (2.7), however, this condition is not the only one for which (2.46) is not CC. Under the conditions

$$s_{12} = s_{21}$$

$$s_{13} = s_{23}$$

$$s_{31} = s_{32}$$

$$s_{11} = s_{22}$$

$$\frac{\phi_{1a}}{x_1} = \frac{\phi_{2a}}{x_2} , \qquad (2.48)$$

for example, $\rho[U_{n-1}(S, X^{-1}\Phi_{\cdot a}P')] < 3$ and (2.46) is not CC. The difference between the controllability of (2.7) and (2.46) lies, of course, in the fact that influxes $\phi_{1a}$ and $\phi_{2a}$ are constrained to have the same specific activity, $A_1$, whereas the inserted tracer fluxes, $F_1$ and $F_2$, in (2.7) were assumed independent. This comparison of systems (2.7) and (2.46) points out a general characteristic of the application of tracer to a compartmental system by means of natural flux routes: On the one hand, this method has the advantage of not requiring injections or some other potentially disturbing artificial means of inserting tracer; on the other hand, it can result in a less controllable tracer system, as more than one compartment may receive substance from the same environmental source.

The commonly used tracer soak up and washout experimental techniques to investigate compartmental structure fit into the category of "natural" tracer absorption. In a soak up experiment, a compartmental system is subjected to a labeled environment, such as a radioactive bath, and its absorption of tracer is monitored. For a tracer washout, the system is first saturated to a particular tracer specific activity. Then, the system is switched to a tracer-free environment and

the "washout" of tracer from the system is observed. In either case, the tracer system cannot be CC-CO, that is, the presence of all the compartments cannot be detected, unless (2.45) is satisfied.

## 2.3 Tracer System Order

Section 2.2 above considers the important questions of controllability and observability in the problem of finding the order, n, of an experimental tracer system having form (1.18). The other step in estimating n for tracer system (1.18) is the determination of the order, $n_o$, of a minimal realization from experimental data on the system. If the tracer system, under the available experimental access, such as (2.6) or (2.41), is known to be CC-CO, then $n = n_o$; otherwise, it is at least possible to say that $n_o \leq n$.

Some general time-domain techniques for determining $n_o$ from the $q \times m$ impulse response matrix, H(t) [2.1, p. 78], of a linear system are presented in [2.3]. Alternately, [2.1] contains some frequency-domain techniques for finding $n_o$ based on the Laplace transform of H(t), the transfer function matrix, H(s) [2.1, p. 84]. These techniques are applicable to tracer systems of form (2.6) and (2.41). In fact, (2.6) and (2.41) are seen to be special cases of the more general linear tracer system,

$$\begin{aligned} \dot{\bar{a}} &= S\bar{a} + R\bar{v} \\ \bar{w} &= Q\bar{a} \ , \end{aligned} \tag{2.49}$$

with $n \times \tilde{p}$ matrix R and $\tilde{p}$-dimensional input vector, $\bar{v}$, given, respectively, by

$$R = (X^{-1}P \; X^{-1}\Phi_{.a}P') \; , \tag{2.50}$$

and

$$\bar{v} = \begin{pmatrix} \bar{F} \\ \bar{A} \end{pmatrix} \; , \tag{2.51}$$

where $\tilde{p} = p + p'$. Experimentally, H(t) is obtained for (2.49) by applying an impulse (ideally a Dirac delta function, $\delta(t)$ [2.1]) to each input, say the ith, with the other inputs and initial system state set at zero; that is, $v_i(t) = \delta(t)$, $v_j(t) \equiv 0$, $j = 1, \cdots, \tilde{p}$, $j \neq i$, and $\bar{a}(0) = \bar{0}$. Then, under these conditions, the system output, $\bar{w}^i(t)$ becomes the ith column of H(t). Of course, H(t) can also be obtained from any output matrix, H'(t), consisting of the response vectors for a set of $\tilde{p}$ inputs of the form

$$\bar{v}^i(t) = \begin{pmatrix} \mu_1^i \\ \cdot \\ \cdot \\ \cdot \\ \mu_{\tilde{p}}^i \end{pmatrix} \delta(t) \; , \quad i = 1, \cdots, \tilde{p} \; , \tag{2.52}$$

where the vectors in set $\{\bar{\mu}^i\}$ are <u>linearly independent</u>.[1] In this case, H(t) is obtained from

[1] See [2.1] for the definition of linear independence of vectors.

$$H(t) = H'(t)M^{-1} ,$$

where $M \equiv (\bar{\mu}^1 \cdots \bar{\mu}^{\tilde{p}})$. Similarly, in the frequency domain, the transfer function matrix, $H(s)$, is related to the Laplace transforms of an arbitrary input vector, $\bar{V}(s)$, and the corresponding output vector, $\bar{W}(s)$, by

$$\bar{W}(s) = H(s)\bar{V}(s) .$$

Often, the compartmental analyst assumes the special case that, in essence, the S matrix of tracer system (1.18) or (2.49) has nonpositive, real, distinct eigenvalues. In this case, the specific activity transient responses to the homogeneous portion of (1.18) take the form

$$a_i(t) = \sum_{j=1}^{n} A_{ij} e^{\sigma_j t} \geq 0 , \quad i = 1, \cdots, n , \tag{2.53}$$

where $\{A_{ij}\}$ and $\{\sigma_j\}$ are sets of real constants with $\sigma_j \leq 0$, $j = 1, \cdots, n$, distinct. Hence, estimating n amounts to counting up the number of different exponential or <u>rate constants</u>, $\sigma_j$, appearing in the transient responses.

If, for example, the eigenvalues of S are real and distinct, and tracer system (1.18) is homogeneous, i.e.,

$$\Phi_{.a}\bar{a}_{.a} + \bar{f} = \bar{0} , \tag{2.54}$$

then the number of compartments equals the number of eigenvalues. Moreover, it is shown later in Section 2.3.1 that if

S is irreducible, then zero is an eigenvalue only if the compartmental system is closed and conservative. For nonhomogeneous tracer system (1.18), in which

$$\phi_{ia} a_{ia} + f_i \neq 0 , \quad \text{for some } i = 1, \cdots, n , \tag{2.55}$$

the transient responses can assume two different forms, depending on whether S is singular or not. If S is nonsingular, then $a_i(t)$ has the form

$$a_i(t) = \sum_{j=1}^{n} A_{ij} e^{\sigma_j t} + a_{iss} , \tag{2.56}$$

$$\sigma_j < 0 , \quad j = 1, \cdots, n ,$$

where $a_{iss} = a_i(\infty)$. Hence, only the nonconstant terms in the transient responses count towards the system order. On the other hand, if S is singular, $a_i(t)$ becomes

$$a_i(t) = \sum_{j=2}^{n} A_{ij} e^{\sigma_j t} + a_{iss} ,$$

$$\sigma_1 = 0 ,$$

$$\sigma_j < 0 , \quad j = 2, \cdots, n , \tag{2.57}$$

and any constant terms in the transient responses must be treated as though they correspond to the zero eigenvalue of S. It is seen, then, that methods for finding the order, $n_o$, of a minimal realization derived for data from a tracer

system whose S matrix has real, distinct eigenvalues can be based on the resolution of sums of exponentials into their components. For example, graphical, algebraic, and transform methods for obtaining $n_o$ are outlined in [2.4], [2.5], and [2.6], respectively. With these special techniques in mind, the remainder of this section is devoted to examining the properties of the S matrix in tracer system (1.18). The eigenvalues of S are related to the structure of the original compartmental system, and particular emphasis is placed on determining those conditions under which S has nonpositive, real, distinct eigenvalues. Throughout these developments, it is useful to recall that, from physical considerations, the elements of (1.18), (1.19), and (1.20) satisfy

$$\begin{aligned} & x_i > 0 \\ & P_i \geq 0 \\ & \phi_{ia} \geq 0 \\ & a_{ia} \geq 0 \\ & \phi_{ij} \geq 0 , \quad i, j = 1, \cdots, n , \quad i \neq j . \end{aligned} \tag{2.58}$$

### 2.3.1 General Properties of Tracer Matrix S

First, a theorem by Gersgorin can be used to show that the eigenvalues of matrix S of tracer system (1.18) always lie in the set consisting of the left half of the complex

plane together with the origin. The general theorem states that the eigenvalues of an n-square complex matrix $A = (a_{ij})$ lie in the closed region of the complex z-plane consisting of all the discs

$$|z - a_{ii}| \leq \sum_{j=1}^{n}{}' |a_{ij}| , \quad i = 1, \cdots, n . \tag{2.59}$$

If A is a real matrix, and the above Gersgorin discs are disconnected, then all the eigenvalues of A are real [2.7, p. 226]. When applied to S, (2.59) becomes

$$\left| z + \frac{1}{x_i}\left( \sum_{p=1}^{n}{}' \phi_{ip} + \phi_{ia} + P_i \right) \right| \leq \frac{1}{x_i} \sum_{p=1}^{n}{}' \phi_{ip} , \tag{2.60}$$

$$i = 1, \cdots, n .$$

Hence, by (2.58) and (2.60), each eigenvalue of S lies either in the left half of the complex plane or at the origin. Also, Gersgorin's theorem shows that if

$$\phi_{ia} + P_i > 0 , \quad i = 1, \cdots, n , \tag{2.61}$$

then S can have no zero eigenvalue; i.e., S is nonsingular.

A theorem by Frobenius for irreducible nonnegative matrices provides further insight into the nature of matrix S. Recall the definition of a reducible matrix given earlier in (2.27) or (2.28), and note that an n-square real matrix $A = (a_{ij})$ is <u>nonnegative</u> if $a_{ij} \geq 0$, i, j = 1, ···, n [2.2, p. 61]. Frobenius' theorem states that an irreducible

nonnegative matrix $A = (a_{ij})$ always has a positive real simple eigenvalue of value r, such that the moduli of all the other eigenvalues are at most r. To this dominant eigenvalue, there corresponds an eigenvector whose elements are all positive [2.2, p. 65]. Furthermore, r satisfies

$$\min_i \sum_{j=1}^{n} a_{ij} \leq r \leq \max_i \sum_{j=1}^{n} a_{ij} , \tag{2.62}$$

where the left or right equality sign holds only if both hold, i.e., when all the row sums of A are equal [2.2, p. 76].

In order to apply Frobenius' theorem to the S matrix of a tracer system, define n-square real matrix F by

$$F \equiv S + \sigma_o I_n , \tag{2.63}$$

where $I_n$ is the n-square identity matrix, and

$$\sigma_o > \max_i |s_{ii}| . \tag{2.64}$$

Then, F is nonnegative, F is reducible if and only if S is reducible, and the eigenvalues $\{\beta_i\}$ of F are related to those of S by

$$\sigma_i = \beta_i - \sigma_o , \quad i = 1, \cdots, n . \tag{2.65}$$

From (2.62), F, if irreducible, has a positive real simple eigenvalue $\beta_1$ whose modulus is not exceeded by $|\beta_i|$, i = 2, $\cdots$, n, and which satisfies

$$\min_i \left( \sum_{j=1}^{n} s_{ij} + \sigma_o \right) \leq \beta_1 \leq \max_i \left( \sum_{j=1}^{n} s_{ij} + \sigma_o \right) . \qquad (2.66)$$

Hence, from (2.65) and Gersgorin's theorem, if S is irreducible, then it has a real, simple, least-negative eigenvalue, $\sigma_1$, which satisfies

$$\min_i \sum_{j=1}^{n} s_{ij} \leq \sigma_1 \leq \max_i \sum_{j=1}^{n} s_{ij} , \qquad (2.67)$$

where the left or right equality holds only if they both hold. This result means that, for irreducible S, if

$$\phi_{ia} + P_i > 0 , \qquad (2.68)$$

for <u>some</u> $i = 1, \cdots, n$, then S is nonsingular. Moreover, if

$$\phi_{ia} + P_i = 0 , \quad i = 1, \cdots, n , \qquad (2.69)$$

that is, if the system is closed and conservative, then zero is a simple eigenvalue of S. Also, the slowest transient response mode corresponds to a simple, real eigenvalue, and all the coefficients of this mode are positive. If zero is a multiple eigenvalue of S, then S is necessarily reducible.

Hearon, incidentally, shows that the particular solution of tracer system (1.18) associated with a multiple zero eigenvalue is always a constant vector [2.8, p. 46]. This result, along with the results from Gersgorin's theorem that all nonzero eigenvalues of S have strictly negative real parts,

confirms the intuitive belief that no physical compartmental system in steady state can result in unbounded tracer behavior.

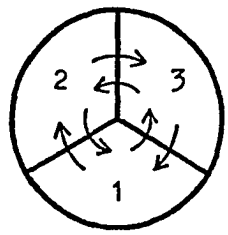


Fig. 2.7. The Closed, Conservative, Three-Compartment System.

It can be shown by example that the tracer system S matrix can, indeed, have complex eigenvalues. Consider the general closed, conservative, steady state three-compartment system shown in Fig. 2.7. The tracer S matrix associated with this system is

$$S = \begin{pmatrix} -\frac{1}{x_1}(\phi_{12}+\phi_{13}) & \frac{\phi_{12}}{x_1} & \frac{\phi_{13}}{x_1} \\ \frac{\phi_{21}}{x_2} & -\frac{1}{x_2}(\phi_{21}+\phi_{23}) & \frac{\phi_{23}}{x_2} \\ \frac{\phi_{31}}{x_3} & \frac{\phi_{32}}{x_3} & -\frac{1}{x_3}(\phi_{31}+\phi_{32}) \end{pmatrix}, \quad (2.70)$$

and S has the eigenvalues

$$\sigma_1 = 0$$

$$\sigma_{2,3} = -\frac{1}{2} Q \pm \frac{1}{2}\sqrt{R}\,, \quad Q \geq 0\,, \quad (2.71)$$

where Q and R are functions of the intercompartmental fluxes and substance amounts. Whether $\sigma_{2,3}$ are complex conjugates or real depends on the sign of R. Consider the case

$$x_1 = x_2 = x_3 = x$$

$$\phi_{12} = \phi_{23} = \phi_{31} = \phi_\ell \tag{2.72}$$

$$\phi_{21} = \phi_{32} = \phi_{13} = \phi_r \ .$$

It can be shown in this case that

$$R = -\frac{3}{x^2}(\phi_\ell - \phi_r)^2 \leq 0 \ , \tag{2.73}$$

so that $\sigma_{2,3}$ are, indeed, complex conjugates unless $\phi_\ell = \phi_r$. As another case, consider

$$x_2 = x_3 = x_{23}$$

$$\phi_{12} = \phi_{23} = \phi_{31} = 0 \tag{2.74}$$

$$\phi_{21} = \phi_{32} = \phi_{13} = \phi \ .$$

Then,

$$R = \frac{\phi^2}{x_1}\left(\frac{1}{x_1} - \frac{4}{x_{23}}\right) \ , \tag{2.75}$$

and $\sigma_{2,3}$ are distinct, negative real for $x_{23} > 4x_1$, are non-distinct negative real for $x_{23} = 4x_1$, and are complex conjugates with negative real parts for $x_{23} < 4x_1$.

### 2.3.2 Real Eigenvalues of Tracer Matrix S

Because S can have complex eigenvalues, conditions on the original compartmental system are now derived under which all the eigenvalues of S are real. Goldberg [2.9, p. 87] considers an n-square real matrix $A = (a_{ij})$, found in the theory of dielectric relaxation, whose elements satisfy

$$a_{ij} \leq 0$$

$$a_{ii} \leq 0 \ , \quad i, j = 1, \cdots, n \ , \quad i \neq j \ , \tag{2.76}$$

and

$$a_{i_1 i_2} a_{i_2 i_3} \cdots a_{i_k i_1} = a_{i_2 i_1} a_{i_3 i_2} \cdots a_{i_1 i_k} \ , \tag{2.77}$$

$$\text{for all } i_1, \cdots, i_k, \ k \leq n \ .$$

Though his proof is invalid as it stands, Goldberg intends to show that A has only real eigenvalues. His method of proof can be corrected and generalized to apply to a broad class of tracer matrices as follows:

Let the elements $s_{ij}$ of tracer matrix S satisfy the cyclic relationships of (2.77), and define the symmetric matrix $B = (b_{ij})$ by

$$b_{ij} = (s_{ij}s_{ji})^{1/2}$$

$$b_{ii} = s_{ii} = -(s_{ii}s_{ii})^{1/2} , \quad i, j = 1, \cdots, n, \quad i \neq j . \tag{2.78}$$

(This definition of B repairs Goldberg's proof.) Then,

$$\begin{aligned} b_{i_1i_2}b_{i_2i_3} \cdots b_{i_ki_1} &= (-1)^p \left| s_{i_1i_2}s_{i_2i_1}s_{i_2i_3}s_{i_3i_2} \cdots \right. \\ &\qquad \left. s_{i_ki_1}s_{i_1i_k} \right|^{1/2} \\ &= (-1)^p \left| s_{i_1i_2}s_{i_2i_3} \cdots s_{i_ki_1} \right| \\ &= s_{i_1i_2}s_{i_2i_3} \cdots s_{i_ki_1} , \qquad \text{for all } i_1, \cdots, i_k , \end{aligned} \tag{2.79}$$

where p is the number of diagonal elements in the product. Goldberg's proof goes on to show that the corresponding principal minors of S and B are equal, and, hence, S and B have the same eigenvalues [2.9, p. 87]. Since the eigenvalues of real symmetric matrix B are real, any tracer matrix, S, whose elements satisfy (2.77) has all real eigenvalues.

Condition (2.77) can be simplified. All expressions in (2.77) for k = 1, 2 are trivally satisfied. Also, for $k \geq 3$, any diagonal elements can be removed. Therefore, for a tracer matrix, (2.77) reduces to

$$\frac{\phi_{i_1 i_2}}{x_{i_1}} \cdots \frac{\phi_{i_k i_1}}{x_{i_k}} = \frac{\phi_{i_2 i_1}}{x_{i_2}} \cdots \frac{\phi_{i_1 i_k}}{x_{i_1}} , \qquad (2.80)$$

$$\text{for all } i_1, \cdots, i_k, \text{ distinct,}$$

$$k = 3, \cdots, n ,$$

which is equivalent to

$$\phi_{i_1 i_2}\phi_{i_2 i_3} \cdots \phi_{i_k i_1} = \phi_{i_2 i_1}\phi_{i_3 i_2} \cdots \phi_{i_1 i_k} , \qquad (2.81)$$

$$\text{for all } i_1, \cdots, i_k, \text{ distinct,}$$

$$k = 3, \cdots, n .$$

Hence, any tracer S matrix associated with a compartmental system whose intercompartmental fluxes satisfy (2.81) has only real eigenvalues. As an example, the criteria in (2.81) for a four-compartment system become

$$\begin{aligned}
&\phi_{12}\phi_{23}\phi_{31} = \phi_{21}\phi_{32}\phi_{13} \\
&\phi_{23}\phi_{34}\phi_{42} = \phi_{32}\phi_{43}\phi_{24} \\
&\phi_{34}\phi_{41}\phi_{13} = \phi_{43}\phi_{14}\phi_{31} \\
&\phi_{41}\phi_{12}\phi_{24} = \phi_{14}\phi_{21}\phi_{42} \qquad (2.82) \\
&\phi_{12}\phi_{23}\phi_{34}\phi_{41} = \phi_{21}\phi_{32}\phi_{43}\phi_{14} \\
&\phi_{13}\phi_{34}\phi_{42}\phi_{21} = \phi_{31}\phi_{43}\phi_{24}\phi_{12} \\
&\phi_{14}\phi_{42}\phi_{23}\phi_{31} = \phi_{41}\phi_{24}\phi_{32}\phi_{13} .
\end{aligned}$$

There are some noteworthy special cases of compartmental systems whose fluxes satisfy (2.81). For example, if $\phi_{ij} \neq 0$, $i, j = 1, \cdots, n$, $i \neq j$, then (2.81) is guaranteed by the <u>three-cycle equalities</u>,

$$\phi_{i_1 i_2}\phi_{i_2 i_3}\phi_{i_3 i_1} = \phi_{i_2 i_1}\phi_{i_3 i_2}\phi_{i_1 i_3}, \qquad (2.83)$$

$$i_1, i_2, i_3 = 1, \cdots, n, \text{ distinct}.$$

To show that (2.81) follows from (2.83), represent the compartmental structure by a graph, where each compartment becomes a node, and each intercompartmental flux is a directed arc connecting the appropriate nodes (see Fig. 2.8). Call $\phi_{i_1 i_2} \cdots \phi_{i_k i_1}$ and $\phi_{i_2 i_1} \cdots \phi_{i_1 i_k}$ ($i_1, \cdots, i_k$ distinct, $k \geq 3$) a <u>k-cycle</u> and the corresponding <u>reverse k-cycle</u>, respectively. The loop in a system graph corresponding to a particular k-cycle has associated with it a set T of 3-cycles constructed by addending the fluxes between appropriate nodes. For example, in Fig. 2.9, the 3-cycles $\phi_{12}\phi_{23}\phi_{31}$, $\phi_{34}\phi_{41}\phi_{13}$, and $\phi_{45}\phi_{51}\phi_{14}$ are associated with the 5-cycle $\phi_{12}\phi_{23}\phi_{34}\phi_{45}\phi_{51}$. Note that each time an addended flux, $\phi_{ij}$, is part of a 3-cycle in T, its reverse, $\phi_{ji}$, is also part of a 3-cycle in T. Similarly, the reverse k-cycle has associated with it the set T' of reverse 3-cycles which contain the same addended fluxes as the set of 3-cycles in T. By (2.83), the product of cycles in T equals the product of cycles in T'. But, all the addended fluxes cancel out of this equality, leaving only the

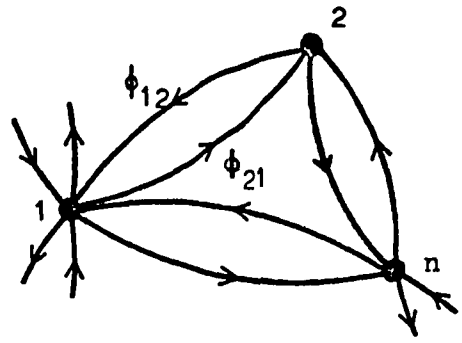


Fig. 2.8. A Graph Representation of an n-Compartment System.

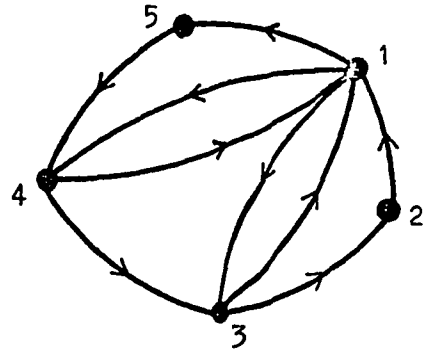


Fig. 2.9. A Set of 3-Cycles Associated with a 5-Cycle.

equality of the original k-cycle and its reverse. As an example, consider again the 5-cycle in Fig. 2.9. The relation between the products of 3-cycles in T and reverse 3-cycles in T',

$$(\phi_{12}\phi_{23}\phi_{31})(\phi_{34}\phi_{41}\phi_{13})(\phi_{45}\phi_{51}\phi_{14})$$

$$= (\phi_{21}\phi_{32}\phi_{13})(\phi_{43}\phi_{14}\phi_{31})(\phi_{54}\phi_{15}\phi_{41}) \ , \qquad (2.84)$$

becomes the desired equality of the 5-cycle and its reverse,

$$\phi_{12}\phi_{23}\phi_{34}\phi_{45}\phi_{51} = \phi_{21}\phi_{32}\phi_{43}\phi_{54}\phi_{15} , \tag{2.85}$$

when pairs $\phi_{31}\phi_{13}$ and $\phi_{41}\phi_{14}$ of addended fluxes are cancelled from (2.84).

As another special case, it is evident that (2.81) is satisfied if

$$\phi_{ij} = \phi_{ji} , \quad i, j = 1, \cdots, n, i \neq j . \tag{2.86}$$

A compartmental system whose fluxes satisfy (2.86) is said to be in a state of <u>detailed balance</u> [2.8, p. 53], a term borrowed from thermodynamics to describe chemical systems which have equal rate constants between each pair of chemical states. Clearly, the tracer S matrix associated with a system satisfying (2.86) always has only real eigenvalues.

Finally, (2.81) is satisfied for a system in which

$$\phi_{i_1 i_2} \cdots \phi_{i_k i_1} = 0 , \tag{2.87}$$

$$\text{for all } i_1, \cdots, i_k, \text{ distinct} ,$$

$$k = 3, \cdots, n ,$$

that is, for a compartmental system having no nonzero cycles. Two important examples of <u>cycle-free</u> compartmental systems are the <u>series</u> or <u>catenary</u> system and the <u>parallel</u> or <u>mammillary</u> system, both shown in Fig. 2.10. Under suitable compartment numbering, as in Fig. 2.10a, the tracer matrix for a

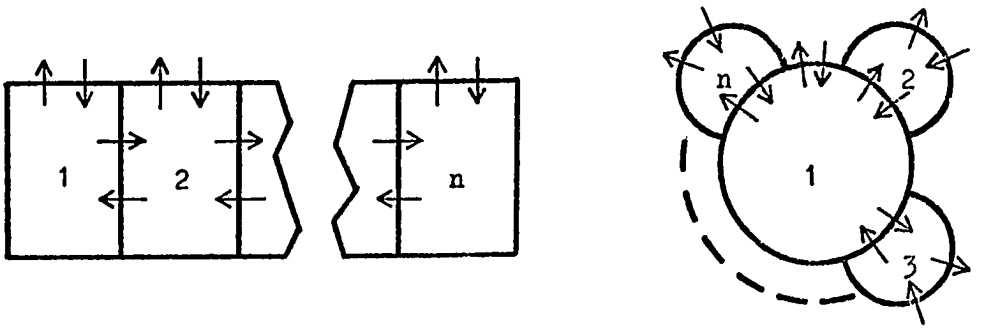


a. b.

Fig. 2.10. Two Special Cases of Cycle-Free Compartmental Systems: a. Series or Catenary; b. Parallel or Mammillary.

series system has the continuant form

$$S = \begin{pmatrix} s_{11} & s_{12} & & & & \\ s_{21} & s_{22} & s_{23} & & & 0 \\ & s_{32} & s_{33} & \cdot & & \\ & & \cdot & \cdot & \cdot & \\ & & & \cdot & \cdot & s_{n-1,n} \\ & 0 & & & s_{n,n-1} & s_{n,n} \end{pmatrix} . \qquad (2.88)$$

Similarly, a parallel system whose compartments are labeled as shown in Fig. 2.10 has a tracer matrix of the form

$$S = \begin{pmatrix} s_{11} & s_{12} & \cdots & s_{1n} \\ s_{21} & s_{22} & & \\ \vdots & & \ddots & 0 \\ \vdots & 0 & \ddots & \\ s_{n1} & & & s_{nn} \end{pmatrix} . \tag{2.89}$$

Of course, each compartment in each of these types of systems can still exchange with the environment and produce and destroy substance.

Hearon [2.8] describes more restrictive conditions on a compartmental system under which the associated tracer matrix has only real eigenvalues. He uses the properties that a real symmetric matrix has real eigenvalues and that, for any similarity transformation on a matrix A defined by

$$B = K^{-1}AK , \tag{2.90}$$

the eigenvalues are invariant. That is, to show that an S matrix has real eigenvalues, Hearon finds a nonsingular matrix K such that

$$B = K^{-1}SK = K^{*}S^{*}(K^{-1})^{*} = B^{*} . \tag{2.91}$$

The class of systems for which the tracer matrix satisfies Hearon's condition, (2.91), is a subclass of those systems satisfying condition (2.81). If it can be shown, however, that a tracer matrix satisfies (2.91), then it is known that S has n linearly independent eigenvectors. Therefore, in

this case, the particular solution associated with an eigenvalue $\sigma_r$ of S, even if $\sigma_r$ has multiplicity greater than one, always has the form

$$\bar{p}(t) = \bar{p}_o e^{\sigma_r t} , \tag{2.92}$$

where $\bar{p}_o$ is a constant [2.10, p. 170].

Hearon considers only similarity transformations of the form

$$K = \text{diag}(k_1, \cdots, k_n) . \tag{2.93}$$

For (2.93), symmetry condition (2.91) becomes

$$SK^2 = K^2 S^* , \tag{2.94}$$

or, by (1.19),

$$\frac{\phi_{ij}}{x_i} k_j^2 = \frac{\phi_{ji}}{x_j} k_i^2 , \quad i, j = 1, \cdots, n, i \neq j . \tag{2.95}$$

The elements of the resultant symmetric matrix $B = (b_{ij})$ are

$$\begin{aligned} b_{ij} &= \frac{k_j}{k_i} s_{ij} = (s_{ij} s_{ji})^{1/2} \\ b_{ii} &= s_{ii} , \quad i, j = 1, \cdots, n, i \neq j . \end{aligned} \tag{2.96}$$

Hearon then develops transforms of form (2.93) to show that the S matrices of some important compartmental systems are,

indeed, similar to symmetric matrices. For example, the S matrix of a system in a state of detailed balance (condition (2.86)) can be symmetrized by a K matrix having elements satisfying

$$\frac{k_i}{k_j} = \left(\frac{x_j}{x_i}\right)^{1/2} , \quad i, j = 1, \cdots, n , \tag{2.97}$$

where one $k_i$ is arbitrary.

Hearon also shows that a tracer matrix for a system having no cycles (condition (2.87)) and which is sign-symmetric can be similarly transformed by a diagonal transformation matrix to a symmetric matrix. A real n-square matrix A is sign-symmetric if $a_{ij}a_{ji} \geq 0$, i, j = 1, ···, n, and $a_{ij} = 0$ if and only if $a_{ji} = 0$ [2.8, p. 50]. Hence a tracer matrix is sign-symmetric if the system intercompartmental fluxes satisfy

$$\phi_{ij} = 0 \quad \text{if and only if } \phi_{ji} = 0 , \tag{2.98}$$
$$i, j = 1, \cdots, n, \; i \neq j .$$

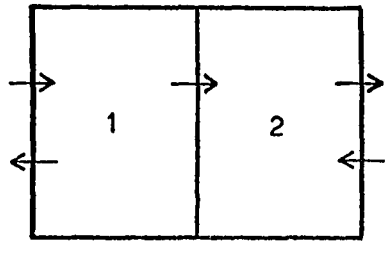


Fig. 2.11. A Compartmental System Violating Sign-Symmetry.

The following example shows that the sign-symmetry of S is essential in being able to find a nonsingular diagonal matrix K whose elements satisfy (2.95). Let n = 2 and let $\phi_{12} = 0$, $\phi_{21} \neq 0$ (see Fig. 2.11). Then, (2.95) requires that

$$\frac{\phi_{21}}{x_2} k_1^2 = 0 \ , \tag{2.99}$$

whose solution, $k_1 = 0$, violates the requirement that K be nonsingular.

Both the series (2.88) and parallel (2.89) systems are special cases of systems satisfying no cycles and sign-symmetry. Clearly, there are also sign-symmetric, cycle-free systems ($n \geq 5$) which are neither strictly series nor strictly parallel. Fig. 2.12 shows such a system.

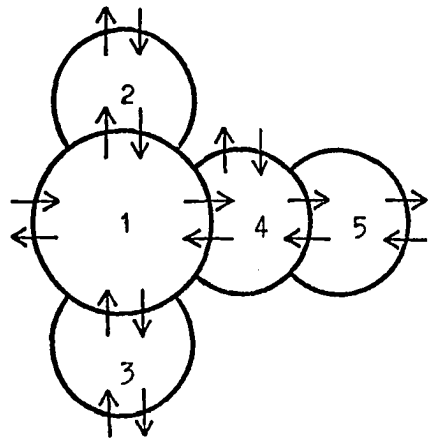


Fig. 2.12. A Sign-Symmetric, Cycle-Free Compartmental System.

The S matrices associated with detailed balance and sign-symmetric, cycle-free compartmental systems can be shown

similar to symmetric matrices by means of diagonal K matrices. Other tracer matrices, satisfying neither the detailed balance nor the sign-symmetry, no cycle criterion, may still be similar to symmetric matrices and hence have real eigenvalues and n linearly independent eigenvectors. Satisfaction of (2.91) for those S matrices may, however, require more general symmetric or even asymmetric K matrices. As an example, consider again the system in Fig. 2.11 in which $\phi_{12} = 0$, $\phi_{21} \neq 0$. Both detailed balance and sign-symmetry are violated. The eigenvalues of a general second-order S matrix are

$$\sigma_{1,2} = -\frac{1}{2} Q \pm \frac{1}{2}\sqrt{R} , \tag{2.100}$$

where Q is nonnegative real, and

$$R = \left[\frac{1}{x_1}(\phi_{12} + \phi_{1a} + P_1) - \frac{1}{x_2}(\phi_{21} + \phi_{2a} + P_2)\right]^2 + 4\,\frac{\phi_{12}\phi_{21}}{x_1 x_2} \geq 0 . \tag{2.101}$$

Hence, the eigenvalues for any 2 × 2 S matrix, including the tracer matrix associated with the system in Fig. 2.11, are always real. (That such eigenvalues must be real can also be seen from condition (2.87).) For this system, elements of symmetric matrix

$$K = \begin{pmatrix} k_{11} & k_{12} \\ k_{12} & k_{22} \end{pmatrix} \tag{2.102}$$

which satisfy (2.94) can be derived from the relation

$$\frac{k_{11}^2 + k_{12}^2}{k_{12}(k_{11} + k_{22})} = \frac{s_{11} - s_{22}}{s_{21}} , \quad s_{11} \neq s_{22} , \tag{2.103}$$

or, for $k_{11} = 0$, from

$$\frac{k_{12}}{k_{22}} = \frac{s_{11} - s_{22}}{s_{21}} , \quad s_{11} \neq s_{22} , \tag{2.104}$$

### 2.3.3 Distinct Real Eigenvalues of Tracer Matrix S

Once it is known that a tracer matrix has real eigenvalues, the next problem is to determine whether the eigenvalues are distinct. The application of a general theorem by Parter [2.11] to compartmental systems partially answers this question. Consider a real n-square matrix $A = (a_{ij})$ which is sign-symmetric and cycle-free; that is,

$$a_{ij}a_{ji} \geq 0$$

$$a_{ij} = 0 \quad \text{if and only if } a_{ji} = 0 , \tag{2.105}$$

$$i, j = 1, \cdots, n ,$$

and

$$a_{i_1 i_2} a_{i_2 i_3} \cdots a_{i_k i_1} = 0 , \tag{2.106}$$

$$i_1, \cdots, i_k, \text{ distinct},$$

$$k = 3, \cdots, n .$$

Then, using Parter's terminology, a necessary and sufficient condition that $\lambda$ be a multiple eigenvalue of A is that there exist a point p of order $\geq 3$ in the graph of A such that $\lambda$ is an eigenvalue of at least three of the branches of p.

Parter's theorem is now applied to the tracer S matrix associated with a compartmental system. Parter defines a branch of the graph G of matrix A as a new graph formed by eliminating the directed arcs between two adjacent points of G. A point in graph G corresponds to a compartment in the compartmental system. Hence, as the analog in a compartmental system to a branch in a graph, define compartmental system $C_{pq}$. System $C_{pq}$ is derived from the original compartmental system by eliminating the direct fluxes, $\phi_{pq}$ and $\phi_{qp}$, between compartments p and q. Now, analogous to conditions (2.105) and (2.106) for A, let the compartmental system satisfy the conditions of sign-symmetry (2.98) and no cycles (2.87). Then, by Parter's theorem, the following is a necessary and sufficient condition that $\sigma$ be a multiple eigenvalue of tracer matrix S: In the compartmental system, there exists a compartment p in direct exchange with the distinct compartments $q_1, \cdots, q_k$, $k \geq 3$, such that $\sigma$ is an eigenvalue of the tracer matrices associated with at least three of the systems $C_{pq_j}$, $j = 1, \cdots, k$. An immediate consequence of this condition is that no tracer matrix associated with a sign-symmetric, cycle-free compartmental system with less than four compartments can have repeated eigenvalues.

There are also other tools available for examining the existence of multiple eigenvalues in a tracer matrix. It is known, for example, that for any nested sequence of principal minors of symmetric matrix B, the eigenvalues of the minor of order m + 1 are separated by the eigenvalues of the minor of order m [2.12, p. 108]. Here, a principal minor of order m is obtained from B by deleting n - m rows and the same numbered n - m columns from B. An immediate result of this separation property is that the eigenvalues of B,

$$\beta_n \leq \cdots < \beta_1 \ , \tag{2.107}$$

satisfy

$$\beta_n \leq b_{ii} \leq \beta_1 \ , \quad i = 1, \cdots, n \ . \tag{2.108}$$

It can be seen, by reviewing the proof of Goldberg's theorem at the beginning of Section 2.3.2, that the results of (2.108) can be directly extended to any tracer matrix associated with a compartmental system whose fluxes satisfy the cyclic relations in (2.81). That is, for such a system, the eigenvalues of the tracer S matrix,

$$\sigma_n \leq \cdots \leq \sigma_1 \ , \tag{2.109}$$

satisfy

$$\sigma_n \leq s_{ii} \leq \sigma_1 \ , \quad i = 1, \cdots, n \ . \tag{2.110}$$

The bounds on the eigenvalues of S in (2.110) can also be combined with bounds provided by Gersgorin's and Frobenius' theorems. First, by Gersgorin's theorem, if S has real eigenvalues $\{\sigma_i\}$, then

$$-\max_j\left(\sum_{p=1}^{n} s_{jp} - 2s_{jj}\right) \leq \sigma_i \leq -\min_j\left(-\sum_{p=1}^{n} s_{jp}\right), \qquad (2.111)$$

$$i = 1, \cdots, n .$$

Hence, for S from a compartmental system satisfying (2.81), conditions (2.110) and (2.111) can be combined to yield

$$-\min_j(-s_{jj}) \leq \sigma_1 \leq -\min_j\left(-\sum_{p=1}^{n} s_{jp}\right) \qquad (2.112)$$

and

$$-\max_j\left(\sum_{p=1}^{n} s_{jp} - 2s_{jj}\right) \leq \sigma_n \leq -\max_j(-s_{jj}) . \qquad (2.113)$$

Moreover, if S is irreducible, then, by (2.67) of Frobenius' theorem,

$$-\max_j\left(-\sum_{p=1}^{n} s_{jp}\right) \leq \sigma_1 \leq -\min_j\left(-\sum_{p=1}^{n} s_{jp}\right) . \qquad (2.114)$$

Therefore, (2.112) and (2.114) can be combined into

$$-\min\left[\min_j(-s_{jj}),\ \max\left(-\sum_{p=1}^{n} s_{jp}\right)\right] \leq \sigma_1 \leq -\min_j\left(-\sum_{p=1}^{n} s_{jp}\right) . \qquad (2.115)$$

The above bounds on eigenvalues $\sigma_1$ and $\sigma_n$ are more specific than those developed by Hearon; that is [2.8, p. 56],

$$-\min_j(-s_{jj}) \leq \sigma_1 \leq 0 , \tag{2.116}$$

and

$$-2\max_j(-s_{jj}) \leq \sigma_n \leq -\max_j(-s_{jj}) . \tag{2.117}$$

For special classes of compartmental systems, more can be said about the existence of repeated eigenvalues for the tracer S matrix. Consider, for example, the general closed, conservative parallel system, for which S becomes, from (2.89),

$$S = \begin{pmatrix} -\frac{1}{x_1}\sum_{p=1}^{n}{}' \phi_{1p} & \frac{\phi_{12}}{x_1} & \cdots & \frac{\phi_{1n}}{x_1} \\ \frac{\phi_{21}}{x_2} & -\frac{\phi_{21}}{x_2} & & \\ \vdots & & \ddots & 0 \\ \frac{\phi_{n1}}{x_n} & 0 & & -\frac{\phi_{n1}}{x_n} \end{pmatrix} . \tag{2.118}$$

Assume that the peripheral compartments are numbered so that

$$\frac{\phi_{i+1,1}}{x_{i+1}} \geq \frac{\phi_{i1}}{x_i} , \quad i = 2, \cdots, n-1 . \tag{2.119}$$

Then the characteristic equation for S is

$$\sigma\left[1 + \frac{1}{x_1}\sum_{p=1}^{n}{}' \frac{\phi_{1p}}{\left(\sigma + \frac{\phi_{p1}}{x_p}\right)}\right]\prod_{q=1}^{n}{}'\left(\sigma + \frac{\phi_{q1}}{x_q}\right) = 0 \ , \qquad (2.120)$$

and the roots of (2.120) satisfy

$$\sigma_n < -\frac{\phi_{n1}}{x_n} < \sigma_{n-1} < -\frac{\phi_{n-1,1}}{x_{n-1}} < \cdots < \sigma_2 < -\frac{\phi_{21}}{x_2} < \sigma_1 = 0 \ , \qquad i = 1, \cdots, n-1 \ , \qquad (2.121)$$

for $\phi_{i1}/x_i \neq \phi_{i+1,1}/x_{i+1}$, $i = 1, \cdots, n-1$ [2.13, p. 514]. Hence S in (2.118) has a repeated eigenvalue if and only if

$$\frac{\phi_{i1}}{x_i} = \frac{\phi_{i+1,1}}{x_{i+1}} = \frac{\phi_{i+2,1}}{x_{i+2}} \ , \qquad (2.122)$$

for <u>some</u> $i = 2, \cdots, n-2$, and (2.122) also gives the value of the repeated root.

As another special case, consider the conservative series system, labeled as in Fig. 2.10a, in which a steady state unidirectional flux, $\phi$, enters from the environment into compartment 1 and exists from compartment n. That is,

$$\phi_{i,i+1} = 0$$

$$\phi_{i+1,i} = \phi_{1a} = \phi \ , \quad i = 1, \cdots, n-1 \ . \qquad (2.123)$$

Then, S becomes

$$S = \begin{pmatrix} -\frac{\phi}{x_1} & & & 0 \\ \frac{\phi}{x_2} & -\frac{\phi}{x_2} & & \\ & \ddots & \ddots & \\ 0 & & \frac{\phi}{x_n} & -\frac{\phi}{x_n} \end{pmatrix}, \tag{2.124}$$

with characteristic equation

$$\prod_{i=1}^{n} \left(\sigma + \frac{\phi}{x_i}\right) = 0 \ . \tag{2.125}$$

The eigenvalues of (2.124),

$$\sigma_i = -\frac{\phi}{x_i} \ , \quad i = 1, \cdots, n \ , \tag{2.126}$$

are distinct if and only if

$$x_i \neq x_j \ , \quad i, j = 1, \cdots, n, \ i \neq j \ . \tag{2.127}$$

# CHAPTER III

# ANALYSIS OF STEADY STATE AND DYNAMICAL BEHAVIOR

## 3.1 Introduction

Chapter II considers how tracer methods can assist in determining the order of a compartmental bilinear control model. The present chapter discusses how tracer techniques can aid in identifying and analyzing the steady state and dynamical behaviors of such systems.

First, bilinear structure (1.5) is assumed to be derived from theoretical, as opposed to experimental, considerations. That is, the pertinent physiological structures and mechanisms in the controlled process under study are postulated or given, and (1.5) is synthesized from these mechanisms using (1.9) and (1.12)-(1.15).

When analyzing the behavior of the physiological control system whose plant is modeled by (1.5) it is necessary to know the behavior of the state and control variables. Perhaps steady state values of $\bar{x}$ and $\bar{u}$ are of interest. On the other hand, when studying the dynamics of regulation during an experiment over time interval $I = [t_o, t_f]$, it is desirable to know $x(t)$ and $\bar{u}(t)$ over I. From such data, for

example, it may be possible to derive the overall feedback relations,

$$\bar{u} = \bar{h}(\bar{x}) \ , \tag{3.1}$$

in the system, or perhaps even the optimization criteria governing the operation of the regulatory system.

It may be difficult or impossible to measure directly the state and control variables of the physiological system associated with model (1.5). Therefore, in this chapter, methods are developed to obtain $\bar{x}$ and $\bar{u}$ based on the application of tracers to compartmental structure (1.1). When compartmental system (1.1) is not in steady state, general tracer system (2.49), encompassing both direct insertion and "natural" absorption of tracer, becomes

$$\begin{aligned} \dot{\bar{a}} &= S(t)\bar{a} + R(t)\bar{v} \\ \bar{w} &= Q\bar{a} \ . \end{aligned} \tag{3.2}$$

In (3.2) $n \times \tilde{p}$ matrix $R(t)$ is given by

$$R(t) = (X^{-1}(t)P \ X^{-1}(t)\Phi_{.a}(t)P') \ , \tag{3.3}$$

where $n \times p$ matrix $P$ and $n \times p'$ matrix $P'$ are defined in Sections 2.2.1 and 2.2.2, respectively, $\tilde{p} = p + p'$, and $X(t)$ and $\Phi_{.a}(t)$ are as given for (1.18).

The remaining quantities in (3.2) are the same as those defined for (1.18) (specific activity n-vector, $\bar{a}$, and n-

square state matrix, S(t)), and (2.49) (input $\tilde{p}$-vector $\bar{v}$, output $\bar{q}$-vector, $\bar{w}$, and q × n output matrix, Q). Starting with general tracer system (3.2), a three-part approach is suggested for determining the behaviors of the state and control variables of compartmental bilinear system (1.5). First, the elements of linear tracer system (3.2) are identified from specific activity measurements. As can be seen from (1.19)-(1.21) and (3.3), the elements of both matrices S(t) and R(t) provide information on the parameters of compartmental structure (1.1). Depending on the values of matrices P and P', it may be possible to obtain values for some of the state variables, $x_i(t)$, i = 1, ···, n, and some of the influxes, $\phi_{ia}(t)$, i = 1, ···, n, from R(t). The bulk of the information, however, is contained in matrix S(t), and the main effort is directed at evaluating S(t). Techniques for obtaining the elements of matrix S(t) from experimental data using (3.2) are presented in Section 3.2. Sections 3.2.1 and 3.2.2 apply the two common identification techniques of linear system synthesis and parameter estimation by error minimization, respectively. Then, a more straightforward "algebraic" method for obtaining S(t) is proposed and detailed in Section 3.2.3.

Secondly, in Section 3.3, relations (1.19)-(1.21) are used to derive the values of state variables $x_i(t)$, i = 1, ···, n, and the compartmental system parameters, $\phi_{ij}(t)$, $\phi_{ia}(t)$, $\phi_{ai}(t)$, $P_i(t)$, and $D_i(t)$, i, j = 1, ···, n, $i \neq j$, from the values of the elements of S(t). These compartmental

parameters are of great physiological interest in their own right. Here, however, they are used in Section 3.5, in conjunction with the bilinear forms of (1.9) for the compartmental parameters, to complete the third step of the analysis. That is, the compartmental parameters are used in Section 3.5 to provide information on control variable values.

The above procedure is based on observations of tracer specific activities. For purposes of comparison, an analogous development using total activities is presented briefly in Section 3.4, where total activity $\alpha_i(t)$ for compartment i is related to specific activity $a_i(t)$ by

$$\alpha_i(t) = x_i(t)\, a_i(t) \ . \tag{3.4}$$

## 3.2 Identification of Tracer Matrix S(t)

The first step in the above procedure for analyzing a compartmental bilinear system is the identification of tracer matrix S(t) in (3.2). Discussions of this problem in the literature [3.1, 3.2, 3.3] typically consider only closed, conservative compartmental systems in steady state. In this case, the associated tracer system takes the time-invariant form (2.49), with S defined by

$$\begin{aligned} s_{ij} &= \frac{\phi_{ij}}{x_i} \ , \quad i, j = 1, \cdots, n \ , \ i \neq j \ , \\ s_{ii} &= -\sum_{j=1}^{n}{}' \, s_{ij} \ , \quad i = 1, \cdots, n \ . \end{aligned} \tag{3.5}$$

Reference [3.2], for example, proposed the following identification technique for S, where S is assumed to have n nonpositive, real, distinct eigenvalues, and every compartment is accessible for observation ($Q = I_n$ so that $\bar{w} = \bar{a}$):

Perform a single transient response experiment on (2.49), recording $a_i(t)$ over interval $I = [t_o, t_f]$ in each of the n system compartments. Resolve each of these recordings into a sum of nonpositive real exponentials,

$$a_i(t) = \sum_{j=1}^{n} A_{ij} e^{\sigma_j t} , \quad i = 1, \cdots, n , \tag{3.6}$$

where some of the $A_{ij}$ may be zero. Define n-square matrices $\Lambda$ and E by

$$\Lambda = \mathrm{diag}(\sigma_1 \cdots \sigma_n) , \tag{3.7}$$

and

$$E = (\bar{e}^1 \cdots \bar{e}^n) , \tag{3.8}$$

respectively, where

$$e_i^j = A_{ij} , \quad i, j = 1, \cdots, n . \tag{3.9}$$

Then, if initial conditions on $\bar{a}$ are chosen so that every mode (every $\sigma_j$) is present in the transient response, E is nonsingular, and S is given by

$$S = E\Lambda E^{-1} . \tag{3.10}$$

The above technique of obtaining tracer matrix S is suitable only when the compartmental system is closed, conservative, and in steady state, and when S has n nonpositive, real, distinct eigenvalues. The remainder of this section develops more general methods of identifying matrix S(t) of tracer system (3.2). The first of these methods, presented in Section 3.2.1, applies the techniques of linear system synthesis to (3.2).

### 3.2.1 Synthesis of Linear Systems

Given the output responses of (3.2) to known inputs, there are techniques available [3.4, 3.5] for synthesizing a linear system having the same response characteristics. This generated system, however, is not unique. Therefore, in order to use these synthesis techniques to identify matrix S(t) of system (3.2), a procedure such as the following must be applied [3.5]: First, it is necessary to show that (3.2) is a minimal realization. That is, if nth-order system (3.2) is time-varying (time-invariant), it must be shown that the input-output relations observed for (3.2) cannot be reproduced by a linear time-varying (time-invariant) system of order $n_o < n$. Secondly, some minimal realization,

$$\begin{aligned} \dot{\bar{z}} &= A_o(t)\bar{z} + C_o(t)\bar{v} \\ \bar{w} &= D_o(t)\bar{z} \ , \end{aligned} \tag{3.11}$$

of the input-output relations observed for (3.2) must be obtained. Finally, a transformation, T, must be found which uniquely relates the desired state variables in $\bar{a}$ to those in $\bar{z}$ of minimal realization (3.11) according to

$$\bar{z} = T(t)\bar{a} \ . \tag{3.12}$$

The question of whether a time-invariant linear system is a minimal realization is considered in Section 2.1 of Chapter II. That is, from (2.4) and (2.5), (3.2) is a minimal realization for constant S and R if and only if

$$\rho(U_{n-r}(S, R)) = \rho(V_{n-s}(S, Q)) = n \ , \tag{3.13}$$

where $1 \leq r \leq \rho(R)$ and $1 \leq s \leq \rho(Q)$. If (3.2) is time-varying, the definitions of controllability matrix (2.2) and observability matrix (2.3) can be generalized, respectively, to

$$U_{n-1}(S(t), R(t)) = (R(t) \ \Delta_c R(t) \ \cdots \ \Delta_c^{n-1} R(t)) \ , \tag{3.14}$$

$$\Delta_c = -S(t) + \frac{d}{dt} \ ,$$

and

$$V_{n-1}(S(t), Q) = (Q^* \ \Delta_o Q^* \ \cdots \ \Delta_o^{n-1} Q^*)^* \ , \tag{3.15}$$

$$\Delta_o = S^*(t) + \frac{d}{dt} \ .$$

In (3.14) and (3.15), it is assumed that S(t) and R(t) are differentiable n - 2 and n - 1 times, respectively [3.5, pp. 103, 117]. With these new definitions, for time-varying (3.2) to be a minimal realization over $I = [t_o, t_f]$, it is sufficient[1] that [3.5, p. 134]

$$\rho(U_{n-1}(S(t), R(t)) = \rho(V_{n-1}(S(t), Q)) = n \quad \text{on } I \ . \quad (3.16)$$

Algorithms for synthesizing minimal realization (3.11) from input-output observations on a linear system exist for both time-varying and time-invariant linear systems. For example, methods for generating $A_o(t)$, $C_o(t)$, and $D_o(t)$ in (3.11) from the impulse response matrix, $H(t, \tau)$, of a time-varying system are presented in [3.5, p. 183]. Alternately, [3.4] contains methods of obtaining a linear time-invariant minimal realization from an experimentally determined transfer function matrix, H(s).

Once it is shown that the observed tracer system (3.2) is of minimal order, and a minimal realization (3.11) of the input-output data is generated, matrices S(t) and R(t) in (3.2) can be obtained from matrices $A_o(t)$, $C_o(t)$, and $D_o(t)$ of (3.11). In general, these matrices are related, through T(t) in (3.12), by [3.5, p. 147]

---

[1] More detailed conditions ensuring that a time-varying linear system is a minimal realization, i.e., CC and CO, are given in [3.5].

$$S(t) = -T^{-1}(t)\dot{T}(t) + T^{-1}(t)A_o(t)T(t) \ , \tag{3.17}$$

$$R(t) = T^{-1}(t)C_o(t) \ , \tag{3.18}$$

and

$$Q = D_o(t)T(t) \ . \tag{3.19}$$

In the time-invariant case, all the matrices in (3.17)-(3.19) are constant. The simplest way to define T(t) is to observe the tracer specific activity in every compartment. Then,

$$Q = I_n \ , \tag{3.20}$$

and, by (3.19),

$$T(t) = D_o^{-1}(t) \ . \tag{3.21}$$

Hence, tracer matrix S(t) is given by

$$S(t) = -D_o(t)\frac{d}{dt}(D_o^{-1}(t)) + D_o(t)A_o(t)D_o^{-1}(t) \ . \tag{3.22}$$

If (3.2) is time-invariant, (3.22) reduces to

$$S = D_o A_o D_o^{-1} \ . \tag{3.23}$$

These synthesis methods have the advantage of specifying exactly what experiments must be performed to obtain the desired realizations. The synthesis algorithms, however, may

be involved. In the referenced algorithms for time-varying systems, for example, it is necessary to obtain experimentally the impulse response matrix $H(t, \tau)$ which is a function of the two arguments t and $\tau$. Then, the first step of synthesis is the multiple differentiation of $H(t, \tau)$ with respect to both arguments [3.5, p. 182]. On the other hand, the algorithms mentioned for time-invariant systems utilize transfer function matrix H(s) [3.4], which must be generated from an experimentally obtained finite time approximation to the impulse response matrix, H(t).

An alternative to the above synthesis methods of finding tracer matrix S is the use of parameter estimation techniques which involve the minimization of an error criterion. The application of these methods to the tracer analysis problem is briefly reviewed in the next section.

### 3.2.2 Parameter Estimation by Error Minimization

The problem of estimating a set of time-invariant parameters, $\beta_i$, $i = 1, \cdots, r$, of a dynamical system,

$$\begin{aligned} \dot{\bar{x}} &= \bar{f}(\bar{x}, \bar{u}, \bar{\beta}, t) \\ \bar{y} &= \bar{g}(\bar{x}, \bar{u}, \bar{\beta}, t) \ , \end{aligned} \tag{3.24}$$

where $\bar{\beta}$ is the vector of parameters, can be formulated in many ways [3.6]. Assume, for example, that the forms of $\bar{f}$ and $\bar{g}$ in (3.24) are known except for the particular values of the parameters $\beta_i$, $i = 1, \cdots, r$. Let the input $\bar{u}$ be observed,

and assume there are M observations of the output, $\hat{\bar{y}}_j$, $j = 1, \cdots, M$. Then the parameters can be estimated by minimizing the expression

$$\sum_{j=1}^{M} \left[ (\bar{g}(\bar{x}^j, \bar{u}^j, \bar{\beta}, t_j) - \hat{\bar{y}}^j)^* W^j (\bar{g}(\bar{x}^j, \bar{u}^j, \bar{\beta}, t_j) - \hat{\bar{y}}^j) \right] , \tag{3.25}$$

where $W^j$, $j = 1, \cdots, M$ is a set of n-square positive definite weighting matrices. (See, for example, [3.7, pp. 442-443, 462-463].) This approach can be applied directly to the problem of estimating the elements of the S and R matrices of time-invariant linear tracer system (2.49). That is, let

$$\begin{aligned} \bar{f}(\bar{a}, \bar{v}, \bar{\beta}) &= S\bar{a} + R\bar{v} \\ \bar{g}(\bar{a}, \bar{v}, \bar{\beta}) &= \bar{w} = Q\bar{a} , \end{aligned} \tag{3.26}$$

and let $\bar{\beta}$ be comprised of the elements of S and R. Then, formulation (3.25) is still applicable.

Assume now that the parameters to be estimated in dynamical system (3.24) are time-varying. The above formulation still applies with suitable modification. Let the interval over which input-output observations are made be $I = [t_o, t_f]$, and assume that each parameter to be estimated, $\beta_i(t)$, can be represented over I by some finite sum of known functions of time, $h_{ik}(t)$; i.e.,

$$\beta_i(t) \approx \sum_{k=1}^{N} \beta_{ik} h_{ik}(t) , \quad i = 1, \cdots, r , \tag{3.27}$$

with constants $\beta_{ik}$, $i = 1, \cdots, r$; $k = 1, \cdots, N$. The time-varying parameters, $\beta_i(t)$, $i = 1, \cdots, r$, are then estimated by minimizing expression (3.25), where vector $\bar{\beta}$ now consists of the coefficients $\beta_{ik}$, $i = 1, \cdots, r$; $k = 1, \cdots, N$. The application of this minimization method to the estimation of tracer matrix $S(t)$ of system (3.2) is evident.

As with the synthesis methods, the matrix obtained by minimization is not known to be an estimate of tracer matrix $S(t)$ unless the proper state variables are assured. This problem is again resolved by requiring that the tracer system be CC and that all the specific activities be directly observed, so that (3.20) holds. Under (3.20), expression (3.25) for a tracer system with specific activities as state variables reduces to

$$\sum_{j=1}^{M} \left[ (\bar{a}^j(\bar{v}^j, \bar{\beta}, t_j) - \hat{\bar{a}}^j)^* W^j (\bar{a}^j(\bar{v}^j, \bar{\beta}, t_j) - \hat{\bar{a}}^j) \right] , \tag{3.28}$$

where $\hat{\bar{a}}^j$ is the state observed and $\bar{a}^j$ is the state calculated from tracer system (3.2).

In summary, the elements of the matrix $S(t)$ of tracer system (3.2) can be estimated by monitoring the input and making M observations on the state, $\bar{a}$. The unknown system matrices, $S(t)$ and $R(t)$, are then estimated by minimizing expression (3.28) with respect to $\bar{\beta}$. If the system is time-

invariant, $\bar{\beta}$ is made up of the elements of the unknown matrices. On the other hand, if S(t) and R(t) are time-varying, then the elements of $\bar{\beta}$ are the coefficients, $\beta_{ik}$, of approximating sums of known time functions for each of the elements of the unknown matrices.

Implementing the above estimation procedures requires the use of iterative computer algorithms, such as quasilinearization [3.7, 3.8], to solve the minimization problem formulated in (3.28). Moreover, the number of unknown parameters to be estimated is large. It is necessary to estimate not only the elements of S(t), but also those of R(t). Hence, for time-invariant nth-order systems with $\tilde{p}$ inputs, the number of parameters is $n^2 + n\tilde{p}$; for time-varying systems, this number increases to $N(n^2 + n\tilde{p})$. These procedures have the advantages of utilizing all the data and of generating estimates without the application of special test inputs, but the corresponding disadvantage that it is not known whether a particular set of observations results in adequate estimates of the unknown parameters.

Because of the potential complexities of both the parameter estimation methods suggested in this section and the synthesis techniques outlined in Section 3.2.1, a more straightforward "algebraic" method of obtaining tracer matrix S(t) of (3.2) is proposed and detailed in Section 3.2.3. This algebraic method has the advantages of the synthesis algorithms in that the necessary test conditions are specified,

and that matrix S(t) is directly synthesized with no iteration. It is not necessary, however, to obtain impulse responses. Moreover, no frequency transformation is necessary for time-invariant systems; also, only a single differentiation is required in the case of time-varying systems. Finally, only the single matrix S(t) need be synthesized in the process. As with the other methods, it is still necessary to assure complete controllability, at least to the extent defined later, and to observe specific activity in each compartment.

### 3.2.3 Algebraic Identification Technique

Consider, first, nth order time-varying tracer system (3.2), and let the experimental time interval of interest be $I = [t_o, t_f]$. Assume that $\bar{v}(t) \equiv \bar{0}$ over I and that $Q = I_n$, so that (3.2) becomes

$$\begin{aligned} \dot{\bar{a}} &= S(t)\ \bar{a} \\ \bar{w} &= \bar{a}\ , \quad t \in I\ . \end{aligned} \tag{3.29}$$

Perform n tracer experiments on the associated nonsteady state compartmental system (1.1) over interval I, observing the n specific activity vectors $\bar{a}^i(t)$, $i = 1, \cdots, n$, over I. If more than one tracer for substance X of the compartmental system is available, then some of these tracer experiments can be performed simultaneously. Otherwise, each tracer experiment is performed during a repetition of the nonsteady

state behavior of the compartmental system. Each of the vectors $\bar{a}^i(t)$, $i = 1, \cdots, n$, satisfies (3.29), and with the definition

$$A_a(t) = (\bar{a}^1(t) \cdots \bar{a}^n(t)) \ , \tag{3.30}$$

(3.29) implies

$$\dot{A}_a(t) = S(t)A_a(t) \ . \tag{3.31}$$

Hence, wherever $A_a(t)$ is nonsingular (vector set $\bar{a}^i(t)$, $i = 1, \cdots, n$, linearly independent), $S(t)$ can be obtained from (3.31) as

$$S(t) = \dot{A}_a(t)A_a^{-1}(t) \ . \tag{3.32}$$

It is known that any matrix $A_a(t)$ made up of solutions to (3.29) is nonsingular so long as $A_a(t_o)$ is nonsingular [3.9, p. 136]. Therefore, to assure that (3.32) can be used to find $S(t)$ over $I$, it is sufficient to apply the set $\bar{a}^i(t_o)$, $i = 1, \cdots, n$, of linearly independent initial conditions in the tracer experiments. Moreover, these necessary initial conditions can be obtained provided tracer system (3.2) is CC on interval $I_s = [t_s, t_o]$, where $t_s < t_o$; for (3.2) to be CC on $I_s$, it is sufficient that

$$\rho[U_{n-1}(S(t), R(t))] = n \quad \text{on } I_s \ , \tag{3.33}$$

where $U_{n-1}(S(t), R(t))$ is given by (3.14) [3.5, p. 103].

If, for tracer system (3.2), $\bar{v}(t) \not\equiv \bar{0}$ over I, then two sets of n experiments each must be performed to obtain S(t). Tracer input $\bar{v}(t)$ and the behavior of compartmental system (1.1) are repeated over I during each of the 2n experiments. The specific activity initial conditions, however, are chosen in the pairs $\bar{a}_1^i(t_o)$, $\bar{a}_2^i(t_o)$, $i = 1, \cdots, n$, such that the set of n vectors $\bar{a}^i(t_o)$, $i = 1, \cdots, n$, is linearly independent, where

$$\bar{a}^i(t) \equiv \bar{a}_2^i(t) - \bar{a}_1^i(t) , \quad i = 1, \cdots, n . \tag{3.34}$$

From (3.2) and (3.34),

$$\dot{\bar{a}}^i = S(t)\bar{a}^i , \quad i = 1, \cdots, n . \tag{3.35}$$

Hence, tracer matrix S(t) is again found from (3.32), with $A_a(t)$ defined in (3.30).

For a compartmental system in steady state, resulting in time-invariant tracer system (2.49), the above methods can be used to find constant matrix S. Alternately, as in the time-varying case above, assume that $\bar{v}(t) \equiv \bar{0}$ over experimental time interval $I = [t_o, t_f]$ and that $Q = I_n$, so that (2.49) becomes

$$\begin{aligned} \dot{\bar{a}} &= S\bar{a} \\ \bar{w} &= \bar{a} , \quad t \in I . \end{aligned} \tag{3.36}$$

Then, it is often possible to obtain S from a single tracer experiment. That is, start system (3.36) in initial condition $\bar{a}(t_o)$, and obtain the n constant vectors $\bar{a}(t_i)$, with derivatives $\dot{\bar{a}}(t_i)$, $i = 1, \cdots, n$, on I. With the definitions

$$A_a = (\bar{a}(t_1) \cdots \bar{a}(t_n)) \tag{3.37}$$

and

$$A_{at} = (\dot{\bar{a}}(t_1) \cdots \dot{\bar{a}}(t_n)) \ , \tag{3.38}$$

(3.36) implies

$$A_{at} = SA_a \ . \tag{3.39}$$

Therefore, whenever vector set $\bar{a}(t_i)$, $i = 1, \cdots, n$, is linearly independent, S is given by

$$S = A_{at}A_a^{-1} \ . \tag{3.40}$$

The linear independence of vector set $\bar{a}(t_i)$, $i = 1, \cdots, n$, for n distinct $t_i$ on I depends on the nature of matrix S. It is shown in Appendix A that any set $\bar{a}(t_i)$, $i = 1, \cdots, n$, with distinct but otherwise arbitrary $t_i$, from the same solution to (3.36) is linearly independent provided matrix S has n distinct real eigenvalues. (See Section 2.3 of Chapter II for a discussion of the relation between the eigenvalues of S and the structure of the original compartmental system.) Furthermore, for second-order systems, the linear independence

of two distinct vectors from the same solution is assured if matrix S has a repeated negative eigenvalue and only a single eigenvector. If S has two eigenvectors in this case, distinct vectors from the same solution are never independent. (See Appendix A.) Another condition which must be met for the linear independence of set $\bar{a}(t_i)$, $i = 1, \cdots, n$, is that all the transient response modes must appear in the solution. This condition depends on a proper choice of $\bar{a}(t_o)$. For example, in the case where S has n distinct real eigenvalues, Appendix A shows that the coefficients $c_j$, $j = 1, \cdots, n$, in (A.2) must all be nonzero to assure the linear independence of set $a(t_i)$, $i = 1, \cdots, n$. These coefficients, however, are related to initial condition $\bar{a}(t_o)$ by

$$\bar{c} = E_s^{-1}\bar{a}(t_o) \ , \tag{3.41}$$

where n-square matrix $E_s$ is the matrix of the eigenvectors of S. Hence, in order to set a suitable initial condition $\bar{a}(t_o)$ to find S for a tracer system time-invariant on $I = [t_o, t_f]$, it is again necessary that the system be CC.

Now assume for time-invariant tracer system (2.49) that the tracer input, $\bar{v}(t)$, is not identically zero over I. Then, to find S, two experiments must be performed with the same input, $\bar{v}(t)$, applied over I in each case. Define

$$\bar{a}(t) = \bar{a}_2(t) - \bar{a}_1(t) \tag{3.42}$$

from the two tracer responses $\bar{a}_2(t)$ and $\bar{a}_1(t)$. Then,

$$\dot{\bar{a}} = S\bar{a} \ , \tag{3.43}$$

and S is found using (3.40) as before.

In Sections 3.2.1-3.2.3, several methods of identifying tracer matrix S(t) given by (1.19)-(1.21), whether time-varying or time-invariant, are suggested. Throughout the remainder of this chapter, it is assumed that, in some way, S(t) is known during the experimental time $I = [t_o, t_f]$. The next section describes how to obtain values for the system state and compartmental parameters during I from S(t).

## 3.3 Identification of State and Compartmental Parameters

Once the elements of matrix S(t) are known, the important relations for obtaining the system state, $\bar{x}(t)$, and the compartmental parameters, $\phi_{ij}(t)$, $\phi_{ia}(t)$, $\phi_{ai}(t)$, $P_i(t)$, and $D_i(t)$, i, j = 1, $\cdots$, n, $i \neq j$, are given by (1.19)-(1.21). Expression (1.19) combined with (1.20) and (1.21) yields, respectively,

$$P_i(t) = -\left( \sum_{p=1}^{n} s_{ip}(t)x_i(t) + \phi_{ia}(t) \right) \ , \quad i = 1, \cdots, n \ , \tag{3.44}$$

and

$$\phi_{ai}(t) + D_i(t) = -\left( \sum_{q=1}^{n} s_{qi}(t)x_q(t) + \dot{x}_i(t) \right) \ , \quad i = 1, \cdots, n \ . \tag{3.45}$$

In matrix notation, (3.44) and (3.45) become

$$\bar{P}(t) = -X(t)S(t)\begin{pmatrix}1\\ \vdots\\ 1\end{pmatrix} - \bar{\phi}_{.a}(t) \ , \tag{3.46}$$

and

$$\bar{\phi}_{a.}(t) + \bar{D}(t) = -S^*(t)\bar{x}(t) - \dot{\bar{x}}(t) \ , \tag{3.47}$$

respectively, where $X(t)$ is given by (1.22). If the rates of production in $\bar{P}(t)$ and the influxes in $\bar{\phi}_{.a}(t)$ are known, then the state $\bar{x}$ of the compartmental system can be obtained by (3.44) as

$$x_i(t) = -\frac{\phi_{ia}(t) + P_i(t)}{\sum_{p=1}^{n} s_{ip}(t)} \ , \quad i = 1, \cdots, n \ . \tag{3.48}$$

Alternately, assume that the rates of destruction in $\bar{D}(t)$ and the effluxes in $\bar{\phi}_{a.}(t)$ are known. Then, if the compartmental system is not in steady state, $\bar{x}$ can be found from (3.47) as the solution to the dynamical equation

$$\dot{\bar{x}} = -S^*(t)\bar{x} - (\bar{\phi}_{a.}(t) + \bar{D}(t)), \ \bar{x}(t_*) = \bar{x}_*, \ t_* \in I \ , \tag{3.49}$$

where $\bar{x}_*$ is assumed known. Note that the homogeneous portion of (3.49) is the adjoint [3.4, p. 156] of the homogeneous part of tracer system (1.18). Moreover, if the compartmental system is in steady state, so that $\dot{\bar{x}} = \bar{0}$, then $\bar{x}$ can be obtained as the solution to the set of algebraic equations,

$$S^*\bar{x} = -(\bar{\phi}_{a.} + \bar{D}) \ . \tag{3.50}$$

Unless the model or data are incorrect, (3.50) has a solution for $\bar{x}$. This solution is unique if $\rho(S) = n$; otherwise, if $\rho(S) = r < n$, $\bar{x}$ has $n - r$ degrees of freedom [3.10, p. 21]. Once the state, $\bar{x}(t)$, is obtained, the set of intercompartmental fluxes $\{\phi_{ij}(t)\}$ can be found from the elements of $S(t)$ and (1.19) by

$$\phi_{ij}(t) = s_{ij}(t)x_j(t) , \quad i, j = 1, \cdots, n , i \neq j . \qquad (3.51)$$

Summarizing, when tracer matrix $S(t)$ is known, it is possible to find both the compartmental system state, $\bar{x}(t)$, and all the remaining compartmental parameters over experimental interval $I = [t_o, t_f]$, provided three of the four quantities $\bar{\phi}_{.a}(t)$, $\bar{\phi}_{a.}(t)$, $\bar{P}(t)$, and $\bar{D}(t)$ are known. If $\bar{x}(t)$ is calculated using (3.49), it is also necessary to know $\bar{x}(t_*)$, $t_* \in I$. Of course, depending on the known and unknown parameters, various combinations of the equations in (3.48) and (3.49) or (3.50) may need to be solved.

As a special example of a compartmental system, consider the closed, conservative system given by

$$\dot{x}_i(t) = \sum_{p=1}^{n}{}' \phi_{ip}(t) - \sum_{q=1}^{n}{}' \phi_{qi}(t) , \quad i = 1, \cdots, n. \qquad (3.52)$$

A conservative model can be used when the substance of interest can be assumed to be neither produced ($\bar{P} = \bar{0}$) nor destroyed ($\bar{D} = 0$) within the system. The water balance systems discussed later, for example, can be considered conservative

because, although water is created by cellular respiration, this water is usually assumed to be taken in via the animal's food. There is, of course, no such thing as a closed living system. Physiological systems, however, are often studied by placing them in a closed environment. In this case, an (n - 1)th order open physiological compartmental system becomes, in conjunction with its environment, an nth order closed compartmented system.

For compartmental system (3.52), the associated tracer system is

$$\dot{\bar{a}} = S(t)\bar{a} \ , \tag{3.53}$$

where matrix $S(t) = (s_{ij}(t))$ has the form

$$s_{ij}(t) = \frac{\phi_{ij}(t)}{x_i(t)}$$

$$s_{ii}(t) = -\frac{1}{x_i(t)} \sum_{p=1}^{n}{}' \phi_{ip}(t) \tag{3.54}$$

$$= -\frac{1}{x_i(t)}\left( \sum_{q=1}^{n}{}' \phi_{qi}(t) + \dot{x}_i(t) \right) \ ,$$

$$i, j = 1, \cdots, n \ .$$

Once the elements of matrix $S(t)$ are determined, state $\bar{x}(t)$ can be obtained from

$$\dot{\bar{x}} = -S^*(t)\bar{x} \ , \quad \bar{x}(t_*) = \bar{x}_*, \ t_* \in I \ , \tag{3.55}$$

if the compartmental system is not in steady state, or from

$$S^{*}\bar{x} = \bar{0} \ , \tag{3.56}$$

if the compartmental system is in steady state. The adjoint relation between tracer system (3.53) and system (3.55) for substance amounts, $x_i$, $i = 1, \cdots, n$, is now more evident. The S matrix in (3.56) is assured to be singular because, from (3.54),

$$\sum_{j=1}^{n} s_{ij} = 0 \ , \quad i = 1, \cdots, n \ . \tag{3.57}$$

Therefore, (3.56) always has a nontrivial solution for $\bar{x}$. If, for example, $\rho(S) = n - 1$, then (3.56) can be solved for $\bar{x}$ uniquely, given $x_i$ for one of the compartments.

## 3.4 Analysis Using Tracer Total Activities

In the above derivations in Sections 3.2 and 3.3, tracer specific activities $a_i$, $i = 1, \cdots, n$, were assumed measured. The specific activity of a tracer in a particular compartment can be determined, say, by finding the ratio of tracer amount to total substance amount in a sample removed from the compartment. In some situations, it may happen that total activities, given by (3.4), rather than specific activities have been or can only be measured. Total activity is measured, for example, by observing the emissions of a radioactive tracer from an entire compartment. In this section, then, methods for deriving the parameters of a compartmental

system from total activity measurements are developed for comparison with those based on specific activity.

Note that when relation (3.4) is substituted into tracer system (3.2), the resultant tracer dynamics in terms of total activity are

$$\begin{aligned} \dot{\bar{\alpha}} &= S'(t)\bar{\alpha} + R'(t)\bar{v} \\ \bar{\omega} &= Q\bar{\alpha} \ , \end{aligned} \tag{3.58}$$

where

$$S'(t) = X(t)S(t)X^{-1}(t) + \dot{X}(t)X^{-1}(t) \ , \tag{3.59}$$

and

$$\begin{aligned} R'(t) &= X(t)R(t) \\ &= (P\ \Phi_{.a}(t)P') \ . \end{aligned} \tag{3.60}$$

Hence, the elements, $s'_{ij}(t)$, of matrix $S'(t)$ are

$$s'_{ij}(t) = \frac{\phi_{ij}(t)}{x_j(t)} \ , \quad i, j = 1, \cdots, n \ , \ i \neq j \ , \tag{3.61}$$

and

$$s'_{ii}(t) = -\frac{1}{x_i(t)}\left( \sum_{q=1}^{n}{}' \phi_{qi}(t) + \phi_{ai}(t) + D_i(t) \right) \ , \tag{3.62}$$

$$i = 1, \cdots, n$$

$$= -\frac{1}{x_i(t)}\left(\sum_{p=1}^{n}{}' \phi_{ip}(t) + \phi_{ia}(t) + P_i(t) - \dot{x}_i(t)\right) , \quad (3.63)$$

$$i = 1, \cdots, n .$$

(Compare (3.61)-(3.63) with the elements of S(t) in (1.19)-(1.21).)

Matrix S'(t) can be obtained from (3.58) and observations on total activity $\bar{\alpha}$ in any of the ways suggested in Section 3.2 for finding S(t) from specific activity data. Alternately, assume that n linearly independent vectors, $\bar{\alpha}^i(t)$, i = 1, $\cdots$, n, are obtained over I, with the same input $\bar{v}(t)$ each time, and form an n-square, nonsingular matrix,

$$A_\alpha(t) = (\bar{\alpha}^1(t) \cdots \bar{\alpha}^n(t)) . \quad (3.64)$$

Then, S'(t) can be expressed, from (3.58), as

$$S'(t) = \dot{A}_\alpha(t)A_\alpha^{-1}(t) - R'(t)V(t)A_\alpha^{-1}(t) , \quad (3.65)$$

where $\tilde{p} \times n$ matrix V(t) is defined by

$$V(t) = (\bar{v}(t) \cdots \bar{v}(t)) . \quad (3.66)$$

Hence, if R'(t), defined in (3.60), as well as $A_\alpha(t)$ is known, (3.65) gives S'(t).

Once S'(t) is known, relations (3.61)-(3.63) can be combined to yield equations for the compartmental system state, $\bar{x}(t)$:

$$x_i(t) = -\frac{\phi_{ai}(t) + D_i(t)}{\sum_{q=1}^{n} s'_{qi}(t)}, \tag{3.67}$$

and

$$\dot{\bar{x}} = S'(t)\bar{x} + (\bar{\phi}_{.a}(t) + \bar{P}(t)), \ \bar{x}(t_*) = \bar{x}_*, \ t_* \in I . \tag{3.68}$$

(Compare (3.67) and (3.68) with (3.48) and (3.49) in the specific activity derivation.) If $\bar{\phi}_{.a}(t)$ and $\bar{D}(t)$ are known, $\bar{x}(t)$ is given by (3.67); alternately, if $\bar{\phi}_{.a}(t)$ and $\bar{P}(t)$, along with $\bar{x}(t_*)$, are known, (3.68) can be solved for $\bar{x}(t)$. As before, if the compartmental system is in steady state, then (3.68) reduces to the set of constant algebraic equations in $\bar{x}$,

$$S'\bar{x} = -(\bar{\phi}_{.a} + \bar{P}) . \tag{3.69}$$

In summary, when starting with tracer total activities, the relations available for obtaining the state, $\bar{x}(t)$, the fluxes, $\{\phi_{ij}(t)\}$, $\bar{\phi}_{.a}(t)$, and $\bar{\phi}_{a.}(t)$, the nonconservative terms, $\bar{D}(t)$ and $\bar{P}(t)$, are similar to but not identical with those developed earlier for specific activity observations. As before, state $\bar{x}$ and all the remaining compartmental parameters can be obtained from total activity tracer matrix $S'(t)$, provided three of the four vectors $\bar{\phi}_{.a}(t)$, $\bar{\phi}_{a.}(t)$, $\bar{D}(t)$, and $\bar{P}(t)$ are known. If (3.68) is used in finding $\bar{x}(t)$, it is also necessary to know boundary condition $\bar{x}(t_*)$.

Consider again the special case of the closed, conservative compartmental system in (3.52). In this case, the total activity kinetics are given by

$$\dot{\bar{\alpha}} = S'(t)\bar{\alpha} \ , \tag{3.70}$$

and (3.68) becomes

$$\dot{\bar{x}} = S'(t)\bar{x} \ . \tag{3.71}$$

Hence, given $S'(t)$ and $\bar{x}(t_*)$, the state, $\bar{x}(t)$, of the original compartmental system can be found as the solution to the same dynamical system as followed by the tracer total activity. If, furthermore, the compartmental system is in steady state, constant $\bar{x}$ must satisfy the algebraic equations

$$S'\bar{x} = \bar{0} \ . \tag{3.72}$$

As must hold in this case, $S'$ is singular, so (3.72) has a nontrivial solution for $\bar{x}$. Also, note that in this case, in fact, whenever $\dot{\bar{x}} = \bar{0}$, $S'$ and $S$ are related by

$$S' = XSX^{-1} \ . \tag{3.73}$$

From (3.73), it is seen that the eigenvalues of $S'$ and $S$ are identical.

## 3.5 Control Behavior

In the last three sections, tracer techniques are generalized and developed for evaluating the parameters of compartmental system (1.1), a system which may be open,

nonconservative, and nonsteady state. These techniques assume the measurement of tracer specific activities or total activities and perhaps some of the substance fluxes with the environment and some nonconservative terms; they yield compartmental substance amounts, $\bar{x}(t)$, intercompartmental fluxes, $\{\phi_{ij}(t)\}$, and the remaining elements of the fluxes with the environment, $\bar{\phi}_{.a}(t)$ and $\bar{\phi}_{a.}(t)$, and nonconservative terms, $\bar{P}(t)$ and $\bar{D}(t)$. In this section, it is assumed that these compartmental parameters are already known for the system of interest.

Recall that, by (1.12)-(1.16), the parameters of bilinear form (1.5) (and (1.6)) can be derived from the coefficients of the compartmental mechanisms of (1.9). Hence, given $\bar{x}(t)$, the state vector for the bilinear system, it is possible to obtain information on the behavior of control variable $\bar{u}(t)$ by using (1.6). That is, (1.6) can be rearranged into

$$\left(\sum_{j=1}^{n} x_j(t)E_j(t) + C(t)\right)\bar{u}(t) = (\dot{\bar{x}}(t) - A(t)\bar{x}(t) - \bar{g}(t)) , \tag{3.74}$$

which, for each time t, is a set of n algebraic equations, with known coefficients and nonhomogeneous terms, in the unknown variables $\bar{u}(t)$. Define

$$C'(t) = \sum_{j=1}^{n} x_j(t)E_j(t) + C(t) , \tag{3.75}$$

and

$$\bar{h}(t) = (\dot{\bar{x}}(t) - A(t)\bar{x}(t) - \bar{g}(t)) \ , \tag{3.76}$$

and form augmented matrix

$$C_h'(t) = (C'(t)\ \bar{h}(t)) \ . \tag{3.77}$$

Then, if there is no error in the assumed system structure or data,

$$\rho(C_h'(t)) = \rho(C'(t)) = r \leq m \ . \tag{3.78}$$

If equality holds in (3.78), (3.74) can be solved for $\bar{u}(t)$ uniquely. On the other hand, if $r < m$, the solution to (3.74) has $m - r$ degrees of freedom [3.10, p. 21]. A necessary condition, then, that (3.74) yield a unique solution is

$$n \geq m \ . \tag{3.79}$$

More information can generally be obtained on control variable behavior by also utilizing the known values of compartmental parameters $\phi_{ij}(t)$, $\phi_{ia}(t)$, $\phi_{ai}(t)$, $P_i(t)$, and $D_i(t)$, $i, j = 1, \cdots, n$, $i \neq j$, and the expressions in (1.9). For each time t, (1.9) is a set of $(n + 2)(n + 1) - 2 = n(n + 3)$ linear equations in $\bar{u}(t)$. In order to obtain $\bar{u}(t)$ uniquely by this method, it is necessary that

$$n(n + 3) \geq m \ . \tag{3.80}$$

Hence, by using the above compartmental parameters and (1.9), there are potentially $n^2 + 2n$ more equations to be used in

solving for the m unknown control variables than by using simply (1.6). Moreover, even if not all the coefficients in (1.9) are known beforehand, the above equations may still provide information on the behavior of $\bar{u}(t)$ and may even be used to evaluate some of the unknown coefficients. These remarks are illustrated in the physiological application in Chapter V.

This chapter concludes the theoretical development of tracer methods of analyzing compartmental bilinear biocontrol systems. In the remaining chapters, the physiological system associated with water acclimation in the wild house mouse is introduced, and the above methods are applied to its analysis.

# CHAPTER IV

# ACCLIMATION TO WATER DEPRIVATION IN THE WILD HOUSE MOUSE: PHYSIOLOGY

## 4.1 Introduction

### 4.1.1 Objectives

The primary aim in exploring the characteristics of compartmental models and bilinear control structures is to develop practical concepts and tools for use in biological research. For this reason, it was considered essential to work closely with a biological investigation in progress. As well as illustrating the application of a theory of compartmental bilinear systems, an actual problem would provide the opportunity to mold the theory to fit the special problems and demands of biological research. More generally, it would also test the feasibility of working constructively with an active life scientist.

The difficulties and challenges of working with biological systems stem from their complexity. Not only is each particular system, e.g., the water balance system, complex, but each system is intimately coupled with other systems. Many systems share the same components. As an extreme example of coupling, note the multitude of functions performed by the

blood. Also, because the systems in living organisms often compete for the same limited resources, there must be a ruling hierarchy of systems. For example, there must be a policy in the mouse (and man) for relegating water among the competing demands of adequate blood plasma volume, waste disposal, and evaporative cooling. Finally, there are factors, such as emotional stress and genetic variations, which influence the behavior of biological systems but which are difficult to assess and control.

A major consequence of the complexity of biological systems is the difficulty of obtaining data. Often a single experiment requires a long period of time. In the water regulation experiments presented later, for example, it took up to three months just to monitor a single group of animals. Some data are difficult to obtain because measurement techniques are complex. Also, it may not be possible to collect data as frequently as desired. Not only can a measurement require a relatively long time, but a measurement can seriously alter the system under study, causing even injury or death to the experimental animal. For example, experiments are discussed later in which blood plasma radioactivity in mice was monitored after an injection of tritiated water. The activity varied much faster initially than it was possible to follow, because of the time required to remove adequate samples of blood for analysis. Also, obviously, there is not much blood which can be removed from a mouse without affecting the

animal's behavior. Observing a changing parameter whose measurement involves sacrificing the animal, as in the determination of body water distribution, introduces the added complication of obtaining each data point from a different animal. Since animals are sacrificed to make measurements and because a "typical" animal does not exist, data on individual animals are not usually available. Instead, data from several animals are averaged with the hope of representing the entire species.

Because biological systems are so complex, it is impractical to wait to model and analyze the behavior of each system until all relevant structure and physiology are understood. In fact, system behavior is analyzed and modeled to provide clues on system structure. Also, even when a system has been thoroughly examined, it is very easy to lose sight of the basic system in the complex mass of detail. One criterion of the techniques developed in the previous chapters, then, is that, incorporating careful simplifications and assumptions, they should serve as useful tools in understanding the gross behavior of biological systems and in assimilating and organizing new data on these systems. Moreover, since data are so hard to obtain, it is essential to make the best possible use of those which are available and to plan experiments most carefully. Therefore, the techniques developed above for studying compartmental bilinear systems should be useful in relating desired parameters to available quantities

and for prescribing what must be measured to obtain desired information.

The discussion of the physiological problem presented below is divided into two sections: physiology and analysis. In the remaining portion of this chapter, the biological problem is introduced, and the essential physiology of the system is reviewed. Also, theoretical mathematical models are developed for the relevant water exchange processes, based on the physiology presented. Then, in Chapter V, specific experimental results, combined with the physiology of the present chapter, provide the basis for the analysis of structure and function of the physiological system.

### 4.1.2 Selection of the Biological Problem

A search was made at the University of Oklahoma for a suitable biological problem. The research by zoologist Dr. Howard Haines on acclimation to water deprivation in the wild house mouse seemed most appropriate, although there were risks in choosing this problem. Specifically, the pertinent physiology was not yet familiar to me, so it was not possible to know whether the system involved would be a satisfactory example of a compartmental bilinear system. Likewise, it was not possible to know fully what data were available or even what data would be needed. In addition, the experiments were virtually complete, and, because of their difficulty and the time required, there would be little opportunity to participate in planning experiments or to obtain new data.

On the other hand, there were several factors favorable to working with Dr. Haines' problem. For one thing, acclimation to water deprivation in the mouse involves structural changes suggestive of bilinear control modes. Furthermore, compartmented models of water distribution in the body are widely used, as are tracer techniques to determine compartment sizes and intercompartmental fluxes. Finally, fresh data were available from acclimation experiments in progress, and there was the opportunity to work directly with Dr. Haines in becoming familiar with the pertinent physiology of the mouse.

The goal of Dr. Haines' research was to improve the understanding of the structures and processes in the wild house mouse (Mus musculus) involved in acclimation to water deprivation. For this purpose, animals were subjected to water deprivation, and their responses were observed. Control values of water contents and water fluxes were obtained for normally hydrated animals, and the same quantities were then observed during acclimation to reduced drinking water. Structural and physiological parameters, such as skin tissue composition and metabolic rate, were also monitored. The results of these experiments are ultimately to provide insight both into the specific structures of the organs involved in water transport and regulation and into each one's contribution to the total response. Indirectly, the research will aid in understanding the general process of adaptation to environmental

changes in organisms and in extending the knowledge of water regulation in land mammals. It will also make a contribution to the still incomplete understanding of human water physiology, perhaps elucidating, for instance, the importance of the skin in water balance. This particular knowledge would be valuable, because not only is water loss through the skin critical when there is inadequate drinking water, but also in cases of increased importance in skin permeability, such as adult cardiac patients, infants in congestive failure, and burn patients [4.1, p. 323].

## 4.2 The Problem of Water Balance

The problem of water balance in the wild house mouse is now introduced. After the animal's overall water regulatory system is reviewed in Section 4.2.1, those aspects of water physiology necessary for the later systems analyses are discussed in more detail in Section 4.2.2. Adequate mathematical models of the relevant water exchange processes are not available in the literature. Hence, after each process is described physiologically, a mathematical model, based on the physiology, is also proposed. The structure and physiology of the water regulatory system of the wild house mouse is not completely known. Fortunately, however, this water system is basically the same as that of many other land mammals. Therefore, as is common in the literature, references to other land mammals, including man, are included in the following discussions of water balance in the wild house mouse.

Water, a basic component of living organisms, accounts for about 70% of a normal mouse's fat free body weight [4.2]. Besides providing a medium for the body's cellular activities, water is also essential for chemical transport in the form of blood and other extracellular fluids, for the removal of urinary and fecal wastes, and for evaporative heat removal. Excess body water disturbs cellular metabolism to produce water intoxication, including coma and convulsions, gastrointestinal dysfunction, muscular weakness, and cardiac arrhythmias [4.3, p. 891]. Dehydration, on the other hand, raises body fluid osmolality and impedes circulation by reducing blood volume and increasing blood viscosity. Death ultimately results from circulatory failure or cellular dehydration [4.4, p. 136].

An animal regulates and maintains its volume of water by adjusting its intake and loss of water. Animals have solved many variations of this problem, ranging from those living in fresh water which must keep excess water out to desert animals which must obtain most of their water from metabolic oxidation of food. The house mouse, like other land mammals, faces the problem of water conservation, since it is continually losing water to its environment and must actively take in fresh water. A descendant of a wild subspecies having unusual water conservation abilities, the house mouse lives successfully in man's dry food storehouses and also thrives in the wild in grasslands, savannas, deserts, arid islands,

coastal beaches, and salt marshes. They can survive for months at a time without drinking water if they have access to seeds or grain and can establish a den developing a high relative humidity. Also, water-deprived mice can tolerate up to a 40 percent loss of body weight, which they can restore within a few days when given adequate water [4.5, p. 103].

### 4.2.1 The Water Regulatory System

#### 4.2.1.1 Complete system

The major water compartments and influxes and effluxes for the mouse, as well as many other land mammals, are summarized in Figs. 4.1 and 4.2, respectively. The largest compartment in Fig. 4.1 (modified from [4.3, p. 879]) is the intracellular water (ICW) compartment, consisting of the water within the muscle cells, connective tissue cells, bone cells, skin cells, etc. The small transcellular water (TCW) compartment within the ICW compartment is composed of fluids, such as brain, spinal, and intraocular fluids, which are formed from water within special epithelial cells. The cells of each tissue mentioned above are bathed in interstitial fluid, which comprises the second largest, interstitial water (ISW), compartment. Blood, consisting of plasma and red blood cells, makes up the final compartment in Fig. 4.1. The compartmental configuration shown in Fig. 4.1 assumes that the blood compartment is the most accessible; relative compartmental sizes are for man. This compartmentation of body

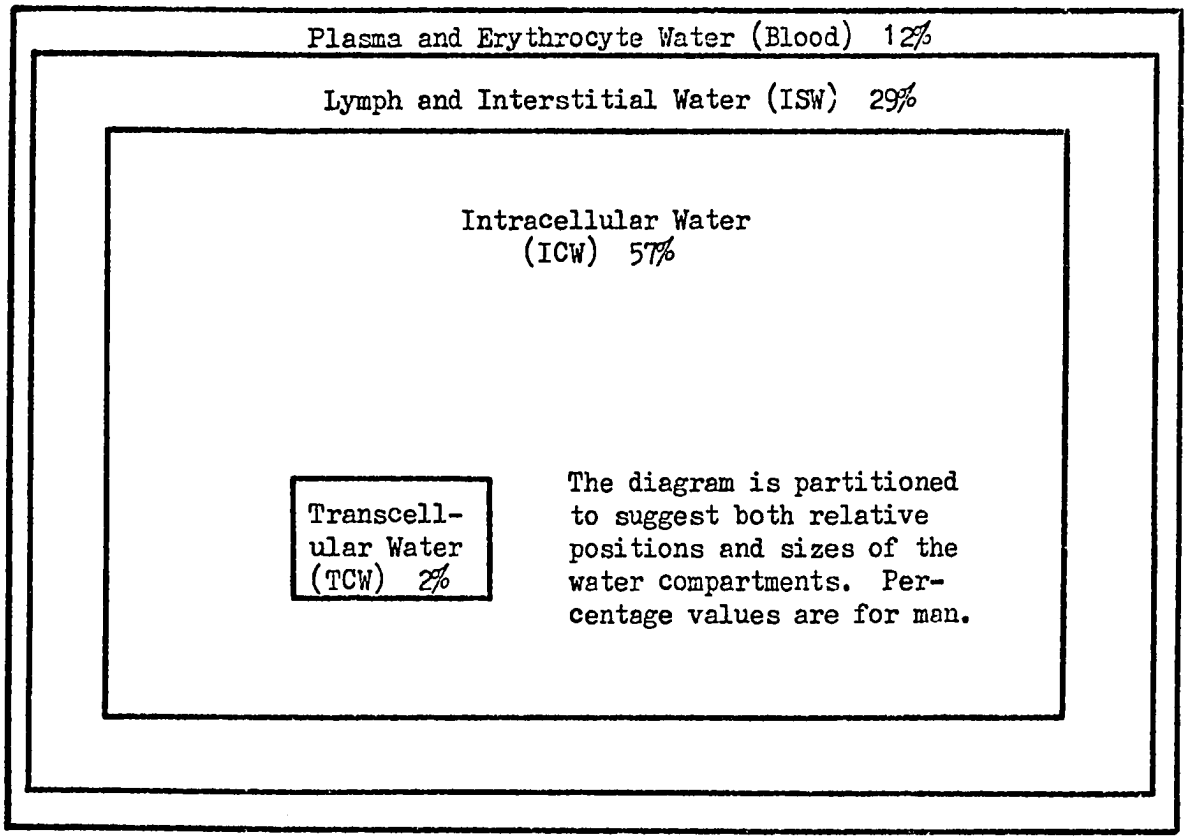


Fig. 4.1. Major Water Compartments in Mammals.

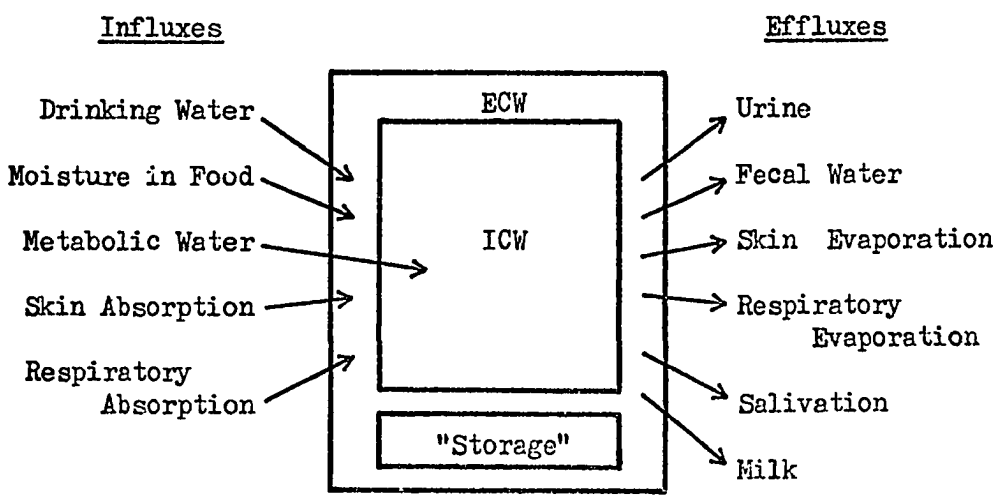


Fig. 4.2. A Summary of Water Exchange in the Wild House Mouse.

water is not unique; the choice depends on its application. Commonly, in fact, blood and ISW compartments are lumped into the single extracellular water (ECW) compartment, and the TCW compartment is neglected.

Fig. 4.2 (modified from [4.4, p. 45]) uses this abbreviated compartmentation scheme and includes a "storage" compartment to represent that water not readily exchangeable because it is bound in the formation of chemicals such as estrogen and progesterone [4.4, p. 45] and constituents of the connective tissues [4.3, p. 641]. Otherwise, water exchange within the body occurs very rapidly. In man, for example, an amount of water equal to 66 percent of the blood volume is exchanged between the blood and the extravascular fluid each minute, while labeled water is entirely equilibrated with the total body water in just a few hours [4.3, p. 627]. The contents of the gut are also rapidly made isotonic with body water by the passage of solutes from the intestinal wall. "There is no evidence that the rate of water absorption (from the gut) is ever a limiting factor in water balance." [4.4, p. 76].

Water is taken up by the mouse via drinking and eating of free water, metabolic oxidation, and water vapor absorption. In the wild, a mouse can obtain free water from dew, rain, surface water, and as a constituent of its food. Oxidative water, a metabolic end product, varies with the animal's diet and metabolic rate. Both the skin and the lungs

absorb water from the air, even though this absorption has often been erroneously overlooked.

A mouse may lose water by urination, fecal loss, evaporation, salivation, and lactation. A minimum urinary water flux is essential to the excretion of metabolic wastes; above this level, however, the loss rate can be adjusted to aid in water balance. The mouse cannot sweat, but insensible evaporation, dependent on ambient temperature and relative humidity and physiological factors, continually takes place from the skin and lungs. A thermally stressed animal spreads saliva on its fur to enhance evaporative cooling, and a female provides milk for her young.

#### 4.2.1.2 System observed in the laboratory

The physiological system observed in the laboratory was not the complete water regulatory system operating in the animal in its natural habitat. In this regard, the biologist distinguishes between acclimation and acclimatization. Acclimatization is an animal's response to several environmental changes at once, as it would experience in its natural habitat; acclimation is a response to a change in only one environmental factor, e.g., reduced drinking water [4.6, pp. 24-25]. The researcher wants to observe and understand acclimatization, but research "in the field" is so difficult that he confines his attention to acclimation studies in the laboratory, hoping that the latter will illuminate the former.

Hence, the laboratory environment is abnormally constant, as the researcher tries to quantify the relations among a few experimental parameters by holding constant as many others as possible. To this end, during the water acclimation experiments, the animals had minimal control over their water influxes. Their restricted drinking water was provided in weighed portions of purified 1% agar gel. Although the mice were given unlimited access to food (fixed composition, 2% hygroscopic water content), it was found that dehydration affected neither metabolic rate nor, therefore, the rate of formation (per unit body mass) of oxidative water [4.2]. Also, variations in water vapor absorption by the skin and lungs were constrained by keeping the animals in a constant temperature, constant humidity environment.

Routes of water efflux were also constrained. None of the animals was suckling young, so there was no milk loss. Also, there was no salivation, because the animals were not subjected to heat stress. Fecal water loss, though it varied with dehydration, was a negligible fraction of total water loss [4.2]. (For bookkeeping purposes, fecal loss is lumped with urinary loss in the later analysis.)

In summary, then, the animals could not adjust their drinking water intake, their diet, which would determine the metabolic water intake, or their environment, which would affect evaporative water exchange. Therefore, the mice could

regulate their body water only by controlling urinary and evaporative exchange.

Although the laboratory environment enables the biological researcher to control many experimental parameters, it also can influence the system under study in undesirable ways. An unusual diet causes changes in eating habits. Animals unaccustomed to free drinking water, for example, must learn to incorporate it into their diet. Stress from handling and their strange environment also affects the animals, resulting, for instance, in diuresis, that is, excessive excretion of urine.

### 4.2.2 Water Exchange Organs

Because urination and evaporation were so important in water regulation in the laboratory animals, the water physiology of the kidneys, the skin, and the lungs are now discussed in more detail. In each instance, following a presentation of the known physiology, a mathematical model is developed relating the water exchange via these organs to the regulated and regulating parameters of the organs. These three mathematical models are then used in Chapter V to synthesize a water regulatory system model. The mathematical models presented here are incomplete, perhaps erroneous, approximations of reality; they will need modification and correction as more physiological data become available.

4.2.2.1 Kidneys

Physiology

The following discussion of kidney physiology is based on[4.3], [4.4], and [4.7]. The kidneys, which process blood plasma to form urine, are each made up of thousands of distinct functional units, called nephrons, shown schematically in Fig. 4.3 (from [4.7, p. 23]). A nephron consists of the glomerulus, a renal capillary nodule within a Bowman's capsule; and the renal tubule, which can be segmented into the proximal convoluted tubule, the loop of Henle, and the distal convoluted tubule. The distal convoluted tubule drains into the collecting duct, which in turn empties formed urine into the ureter and thence into the bladder. The glomerulus and the proximal and distal convoluted tubules are located in the cortex, the outer layer of the kidney; the loop of Henle loops down into the medulla, the inner kidney tissue, and back up into the cortex;[1] and the collecting duct passes from the cortex down through the medulla. The blood vessels which enter the glomeruli in the cortex also follow the renal tubules, forming the vasa recta as they loop into the medulla and back into the cortex again.

An ultrafiltrate of the blood plasma passes into the proximal convoluted tubule at the glomerulus. (Net filtration

[1]Some tubules, especially these emanating from glomeruli near the outer surface of the cortex, turn upward again before reaching the medulla.

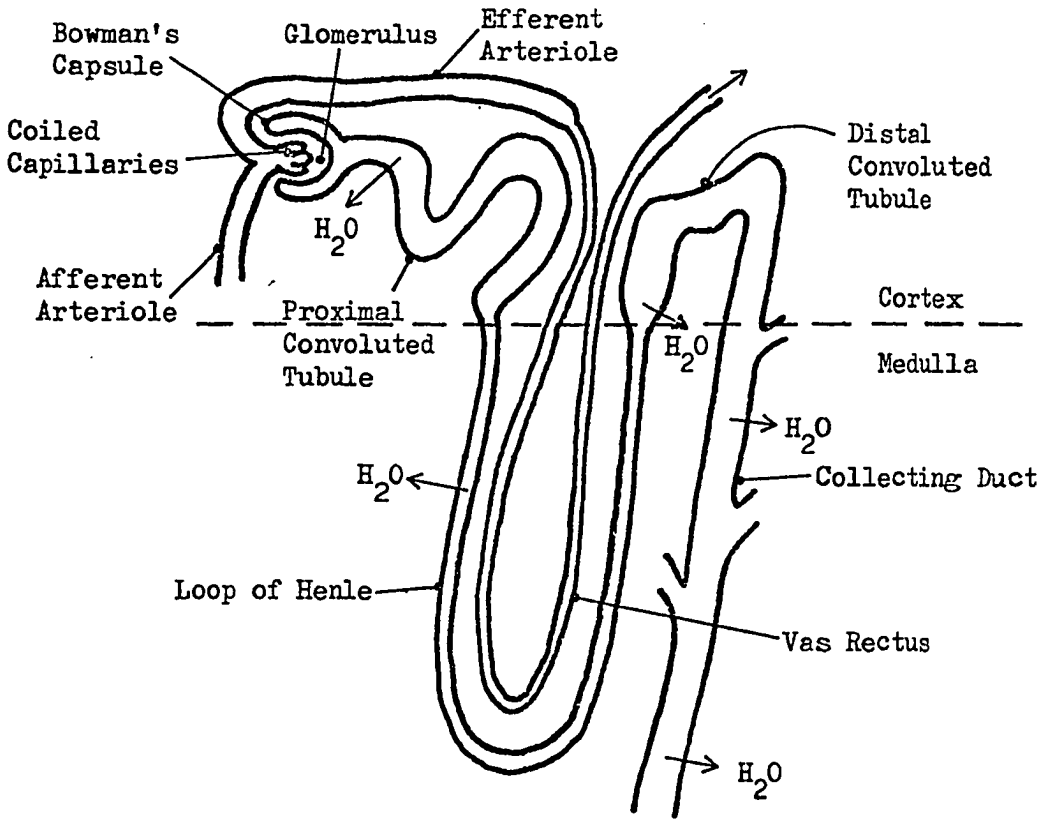


Fig. 4.3. Schematic Drawing of a Nephron.

pressure in the rat kidney is on the order of 40 mm. Hg [4.3, p. 626].) The glomerular filtrate normally contains no erythrocytes and little plasma protein, but all major ions, glucose, amino acids, and urea appear at about the same concentrations as exist in the plasma. In the tubule, both solute and water transport take place. The high rate of passive reabsorption of water and solutes in the proximal convoluted tubule causes more than 80 percent of the filtrated load of water to leave the tubule before reaching the loop of Henle. The osmolality (a measure of solute concentration) of the medullary tissue through which the loop of Henle passes

progressively increases inward from the cortex. Hence, the osmotic pressure of the fluid in the descending limb of the loop of Henle increases as water is passively reabsorbed, while that of the fluid in the ascending limb progressively decreases. The osmotic gradient in the medulla exists because active transport removes solutes in the ascending limb.

Water reabsorption along an osmotic gradient continues in the distal convoluted tubule and in the collecting duct, but the permeability of the tubule to water is regulated by antidiuretic hormone (ADH). During diuresis (low ADH level), the water permeability of the walls of the distal tubule and collecting duct is low, so that the urine has the same low osmolality as the hypotonic fluid entering the distal system. With antidiuresis (high ADH level), the high permeability of the distal and collecting duct system allows water reabsorption, so that the osmolality of the urine can become much greater than that of the plasma. Only a small fraction (1-2 percent in man) of the amount of water filtered at the glomeruli is normally excreted in the urine.

As mentioned above, urinary water loss can be regulated by the action of ADH on tubule and collecting duct permeability. Other factors also influence water loss. Both glomerular filtration rate (GFR) and renal plasma flow (RPF) may be varied widely by both extrarenal and intrarenal factors. Renal blood flow depends on arterial blood pressure and on the arteriolar resistance in the kidney, which is controlled

by an abundant network of constrictor muscles. The relations between arterial pressure and capillary and intracapsular pressures at the glomerulus are not completely known, but Fig. 4.4 shows how glomerular filtration rate is related to arterial pressure in man (from [4.3, p. 849]). Plasma osmotic pressure also affects glomerular filtration rate as well as tubular reabsorption. The hormones of the adrenal cortex (aldosterone, etc.) are necessary for the maintenance of normal glomerular filtration, and they inhibit the renal tubular reabsorption of water. Finally, the osmotic gradient maintained in the medulla depends on the amounts of various chemicals in the plasma (e.g., urea) and on the metabolically governed rate of active transport of solutes in the ascending limb of the loop of Henle.

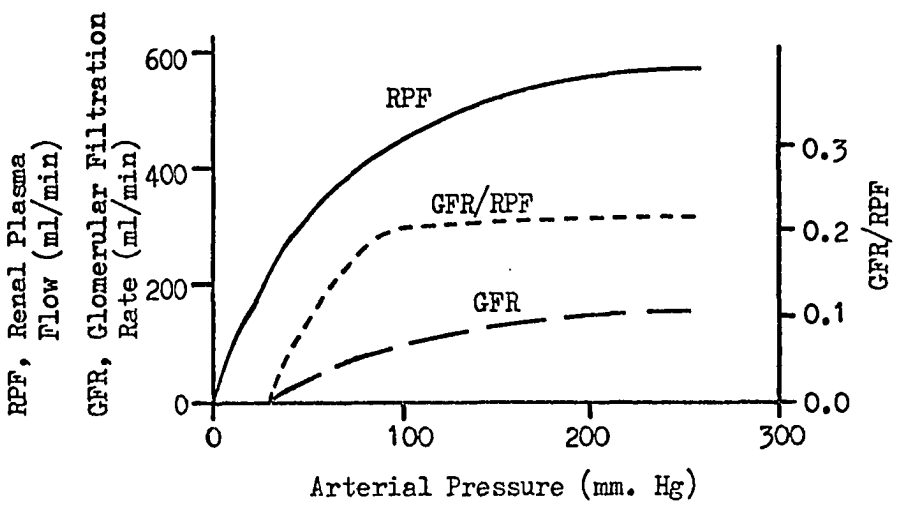


Fig. 4.4. Renal Plasma Flow and Glomerular Filtration Rate Versus Arterial Pressure in Man.

Water flux model

Water loss via the kidneys has been studied more extensively than that through the skin and lungs. No mathematical model, however, could be found in the literature which accounts for the above physiological influences on renal water loss. Therefore, the following model is proposed for water loss through the kidneys:

The net urinary water efflux, $\phi_u$, is the difference between the rate of water filtration into the tubules at the glomerulus and the rate of water reabsorption by the renal tubules. That is,[1]

$$\phi_u = (\text{GFR}) - (\text{Water Reabsorption Rate}) . \tag{4.1}$$

Glomerular filtration rate, GFR, is assumed to depend on the net filtration pressure, $p_{gnet}$, and the effective permeability of the glomerular membranes, $\rho_g$, so that

$$\text{GFR} = \rho_g p_{gnet} . \tag{4.2}$$

The permeability $\rho_g$ depends on, among other things, the amount of adrenocortical hormone present. According to the Starling Hypothesis [4.3, p. 625], $p_{gnet}$ is the difference between the glomerular capillary and proximal convoluted tubule hydrostatic

[1] To improve clarity, the time dependence of parameters in this model and those for the skin and kidneys is indicated only in the final equations ((4.9), (4.24), (4.33), and (4.37)).

pressures, $p_{gc}$ and $p_t$, less the difference between the corresponding osmotic pressures, $\pi_{gc}$ and $\pi_t$. That is,

$$p_{gnet} = (p_{gc} - p_t) - (\pi_{gc} - \pi_t) \ . \tag{4.3}$$

Since the filtrate is considered isosmotic with the plasma, the osmotic contribution will be neglected. Furthermore, the hydrostatic pressure, $p_t$ (~10 mm. Hg in rat kidney [4.3, p. 626]), is considerably less than the glomerular capillary hydrostatic pressure, $p_{gc}$ (~60-65 mm. Hg in rat kidney [4.3, p. 626]), so that (4.3) is approximated by

$$p_{gnet} = p_{gc} \ . \tag{4.4}$$

Now, assume that the glomerular capillary pressure, $p_{gc}$, is some fraction, $f_k$, of the kidney arterial pressure, $p_{ka}$, this fraction being determined by the vasomotor controlled arteriolar resistance of the kidney circulation; that is,

$$p_{gc} = f_k p_{ka} \ . \tag{4.5}$$

Furthermore, assume that $p_{ka}$ depends on the amount of body water, $W_B$, according to

$$p_{ka} = (k_{k1} + k_{k2} W_B) \ , \tag{4.6}$$

where $k_{k1}$ and $k_{k2}$ are constants, and $k_{k2}$ is positive. The relation in (4.6) is proposed because the amount of extracellular water, of which the blood is a part, is directly

related to the total water volume. Also, a change in blood volume results in a change, in the same direction, in arterial blood pressure. Such changes in blood pressure are partially compensated by feedback regulation, but this compensation involves the adjustment of peripheral blood flow to maintain pressure in the heart and brain at the expense of other organs [4.3, pp. 660-661]. Therefore, a change in $W_B$ would cause a change in kidney blood pressure, $p_{ka}$, as approximated by (4.6). Combining (4.2), (4.4), (4.5), and (4.6), the glomerular filtration rate becomes

$$GFR = \rho_g f_k (k_{k1} + k_{k2} W_B) \ . \tag{4.7}$$

The fraction of filtrate water which is reabsorbed from the renal tubules depends on the osmotic gradients in the kidney and on the permeability to water of the membranes of the collecting duct. Assume, then, that the rate of water reabsorption in the kidney is approximated by

$$\text{Water Reabsorption Rate} = k_{k3} \rho_{ADH} \pi_k (GFR) < GFR \ , \tag{4.8}$$

where $\rho_{ADH}$ is an effective tubule permeability governed by the presence of ADH (and perhaps other hormones such as those from the adrenocortex), $\pi_k$ is an average osmotic pressure driving water out of the renal tubules, and $k_{k3}$ is a constant. Combining (4.7) and (4.8), net water loss in the kidney, $\phi_u$, is, then,

$$\phi_u(t) = \rho_g(t) f_k(t) (k_{k1} + k_{k2} W_B(t)) [1 - k_{k3} \rho_{ADH}(t) \pi_k(t)] \ . \tag{4.9}$$

In summary, a number of factors in (4.9) can be used by the animal to control $\phi_u$. The permeability at the glomeruli, $\rho_g$, can be varied by hormones, such as those from the adrenocortex. The fraction $f_k$ denotes the influence of vasomotor variations in kidney arteriolar circulation. Water reabsorption is driven by an effective osmotic pressure, $\pi_k$, which varies with the chemical constituency of the blood and the rate of active transport (or, essentially, the metabolic rate). Finally, the amount of ADH affects reabsorption by controlling the permeability, represented by $\rho_{ADH}$, of the renal tubules to water. On the other hand, the amount of body water, $W_B$, affects $\phi_u$ as shown in (4.9) by influencing the arterial pressure at the kidney.

#### 4.2.2.2 Skin

Physiology

The following discussion of skin physiology is based primarily on [4.3], [4.4], [4.8], and [4.9]. Much still needs to be learned about the structure and function of mammalian skin with regard to water exchange and regulation. Not long ago, some biologists believed water could not pass through the epidermis [4.1, p. 323]. Some still believe that there is little participation by the skin in water regulation or conservation [4.4, p. 81]. The skin, however, has been

demonstrated to be an important and controllable two-way avenue of water transfer. For instance, the net insensible water loss from the skin alone accounts for about 1/5 of the water turnover in the wild house mouse under normal conditions [4.2]. When these animals are subject to water deprivation, skin water loss can be reduced by 1/3 [4.2].

Skin is defined as "a surface covering easily separable from the underlying muscular layer of the body wall" [4.8]. Land mammal skin consists of a thin outer epidermis of epithelial cells and a thicker underlying dermis of connective tissue. The inner cells of the epidermis are "live" structures, but, as the surface is approached, the cells become flatter, lifeless, and filled with keratin. This dry, relatively impervious outer layer is a testimony to the importance of reducing water loss in land mammals. A distinct layer, composed of the granular stratum granulosum and the transparent stratum lucidum, separates the lower, living stratum germinativum and the external stratum corneum. The under surface of the stratum germinativum is scalloped by dermal projections called papillae, which carry blood vessels to the epidermis. Its basal layer, consisting of tall columnar cells, continuously proliferates the epithelial cells which are pushed towards the surface and shed.

The dermis is made up of connective tissue interlaced with abundant capillaries and lymphatics. Connective tissue consists of a gelatinous ground substance containing a network

of long, slender collagenous fibers, flexible but inelastic, which are formed by fibroblasts. Dermis connective tissue is compact, with dense masses of fibers forming a feltlike structure. (Leather is tanned dermis.) Fatty or adipose tissue, a modified connective tissue, commonly develops beneath the dermis. Also, striated muscle tissues derived from underlying body muscles may attach to the under surface of the skin.

Water transport in the skin can be separated into three domains: exchange between the blood and the dermal connective tissue, exchange between the dermis and the stratum corneum of the epidermis, and exchange between the stratum corneum and the surrounding air. Water is exchanged between the blood and the dermis by means of capillaries. A capillary wall is a sheet of endothelial cells in contact with blood on one side and with the complex colloidal matrix of connective tissue on the other. Exchange takes place by filtration and diffusion. The force inducing capillary filtration is described by the Starling Hypothesis, which states that the net force p driving water out of a capillary is [4.3, p. 625]

$$p = (P_i - P_o) - (\pi_i - \pi_o) ,$$

where

$P_i$ = blood hydrostatic pressure

$P_o$ = tissue hydrostatic pressure

$\pi_i$ = blood osmotic pressure

$\pi_o$ = tissue osmotic pressure.

Capillary hydrostatic pressure depends on the arteriolar pressure and on the amount and distribution of vasomotor constriction within the capillary bed. In rat mesentery, this pressure averages 22.1 mm. Hg in the arteriolar ends of the capillaries and 12.5 mm. Hg in the venous ends of the capillaries [4.3, p. 626]. The capillary osmotic pressure results from the concentration of large molecules in the plasma, which do not easily pass through the capillary walls, and, in rat mesentery, ranges from 16 to 21 mm. Hg [4.3, p. 626]. Tissue hydrostatic pressure arises from the natural elasticity of tissue and is relieved by lymphatic drainage. In human subcutaneous tissue, this pressure is not above 6.5 mm.Hg [4.3, p. 626]. Osmotic pressure in the extracapillary tissue is difficult to assess because the tissue is a colloidal matrix, which is partially soluble and partially insoluble, and whose structure is continually changing. Also, there are small fluxes of plasma protein through the region. This pressure is generally taken to be on the order of 5 mm. Hg [4.3, p. 625]. When all these hydrostatic and osmotic pressures are considered, it is found that there is a net outward force in the capillaries at the arteriolar end of the bed and a net inward force at the venous end.

Superimposed on the bulk transport of filtration, diffusion is another major process of water exchange across the capillary walls. It is not certain whether the diffusion occurs through intercellular pores or across some continuous

membrane, but it is described by an effective permeability. This permeability depends both on the properties of the capillary wall structure and on the properties of the surrounding colloidal matrix.

Water is transported between the dermis and outer layers of the epidermis by diffusion. Diffusion in the epidermis occurs through duct openings and through a layer of tightly bound keratin fibers and lipid material; there is a distinct water barrier layer located between the granulosum and corneum strata. The permeability of excised human trunk skin is .5 mg $H_2O/cm^2/hr$, and would be greater with hair follicles and sweat glands. Surface oil films, however, play no part in human skin permeability [4.4, p. 88].

Insensible water exchanges between the skin and the surrounding air by evaporation and condensation. Some sources feel that water loss is described by [4.4, p. 86]

$$\text{Net Insensible Water Loss} = k(VP_s - VP_a) \ . \qquad (4.10)$$

where

$VP_s$ = saturated vapor pressure at skin temperature

$VP_a$ = vapor pressure of the air.

The results of some recent experiments on human skin, however, are in disagreement with (4.10) if k is constant. These experiments indicate a nonlinear relationship between the rate of cutaneous insensible water loss and ambient vapor pressure, but they do not test the effect of changes in skin temperature

[4.10]. Others have found, however, that increased temperature results in an increased resistance to the passage of water vapor through the skin, which may indicate that the assumption that $VP_s$ is the vapor pressure of saturated air at skin temperature is faulty [4.4, p. 87].

Water is stored in the skin. The process of keratinization in the skin can generate water, and the corneum absorbs and releases water with changes in atmospheric humidity. The dermal connective tissue also holds variable amounts of water in a colloidal gel. This water is not normally visible but is part of the colloidal structure, being bound by electrostatic van der Waal forces [4.3, p. 641]. A considerable amount of water can be stored in the skin. Rabbits, for instance, have been found to store half of experimentally given excess water in their skins [4.4, p. 134]. The skin's water binding capacity varies with changes in the condition and quantity of constituent acid mucopolysaccharides. Keratinization normally produces no more than about 2% of the insensible water lost, but insensible water loss may increase two to five times in diseases in which keratinization is increased [4.4, p. 88].

When an animal is subjected to a lack of water with no heat stress, there is a gradual decline in extracellular and intracellular water volumes. Intracellular loss is greater than extracellular loss because circulation volume is preferentially maintained. In many animals tested, the skin loses

relatively and absolutely more water than other tissues [4.4, p. 132]. This depletion of water from the skin may have the further effect of diminishing skin permeability, so that both the smaller supply of water in the skin and the lower permeability contribute to reducing water loss by insensible evaporation.

The skin's permeability to water can also be influenced by hormones. A chemically-induced reduction in the permeability of the capillary walls, of the surrounding connective tissue, or of the epidermal barrier layer can each reduce insensible water loss. Furthermore, vasomotor constriction can shunt the blood from external to internal circulatory networks and can reduce blood flow through skin capillaries. This reduction in blood flow to the skin has two effects. First, the reduced capillary hydrostatic pressure results in less water transfer into the skin ahd thus in less water available for evaporation. Also, less heat is transferred to the skin, and skin temperature drops, reducing evaporation.

Water flux model

A formula frequently appearing in the literature to describe net insensible evaporation from the skin, $(\phi_e - \phi_a)_s$, is given, from (4.10), by

$$(\phi_e - \phi_a)_s = k_{sl}(p_e - p_a) \ , \tag{4.11}$$

where $p_e$ and $p_a$ are water vapor pressures in the skin and surrounding air, respectively, and $k_{sl}$ is a constant. Vapor pressure $p_e$ is assumed to equal saturated vapor pressure, $p_{se}$, at skin temperature $T_s$. In the air, vapor pressure $p_a$ is related to saturated vapor pressure, $p_{sa}$, at air temperature $T_a$ by

$$p_a = rp_{sa} ,$$

where r is the relative humidity. The relation between saturated vapor pressure and temperature is given in Fig. 4.5 (from [4.11, p. 327]); for the skin, this relation can be approximated about a given quiescent point by

$$p_{se} = c_{s1} + c_{s2}T_s . \tag{4.12}$$

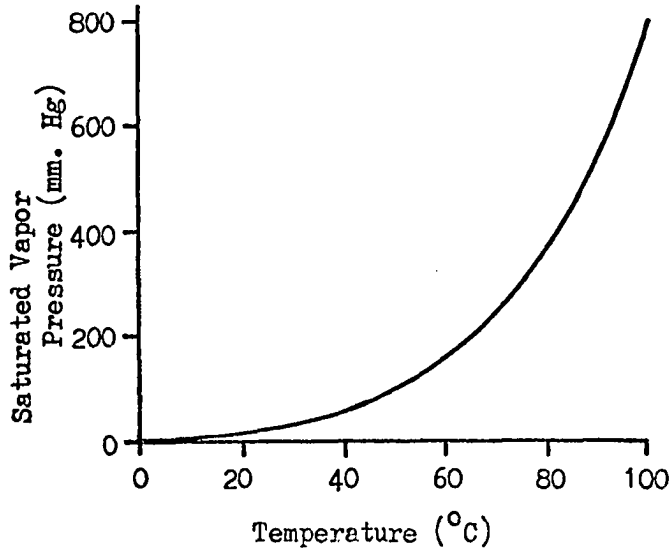


Fig. 4.5. Relation Between Saturated Vapor Pressure and Temperature.

With this approximation, (4.11) becomes

$$(\phi_e - \phi_a)_s = k_{s1}(c_{s1} + c_{s2}T_s - rp_{sa}) \ . \qquad (4.13)$$

Hence, for a fixed environment, evaporative loss through the skin is entirely dependent on skin temperature, $T_s$, according to (4.13). It is therefore desirable to relate $T_s$ to W, the amount of water in the animal. To this end, assume a two-compartment thermal model for the animal, as shown in Fig. 4.6 [4.12, pp. 530-531]. The "core" and "skin" compartments are enclosed by effective thermal conductivities $G_c$ and $G_a$ and are at temperatures $T_c$ and $T_s$, respectively. In thermal steady state,

$$G_c(T_s - T_c) + M_c = 0 \ , \qquad (4.14)$$

where $M_c$ is the metabolic rate of heat production in the "core" compartment. Therefore, the variable skin temperature, $T_s$, is related to the assumed fixed core temperature, $T_c$, by

$$T_s = T_c - \frac{M_c}{G_c} \ . \qquad (4.15)$$

It is mentioned earlier that during the water acclimation experiments, the metabolic rate per unit body mass remained constant. Moreover, the fraction of body mass made up of water was constant at the different levels of water deprivation. Therefore, assume that $M_c$ and the amount of water in the animal, $W_B$, are related by

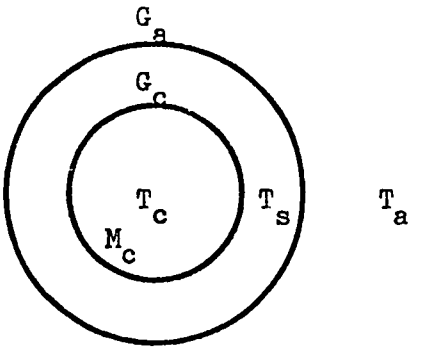


Fig. 4.6. A Two-Compartment Thermal Model for the Wild House Mouse.

$$M_c = k_{s2}W_B \ , \tag{4.16}$$

with positive constant of proportionality, $k_{s2}$. Also, assume that the effective thermal conductivity, $G_c$, is proportional to the total blood flow, B, and to the fraction, $f_s$, of blood flow to the skin; that is,

$$G_c = k_{s3}f_sB \ . \tag{4.17}$$

Blood flow, B, varies with the amount of water in the body, but the amount of fluid in the circulatory system may be preferentially regulated over other body fluids [4.3, p. 660]. Therefore, assume that the blood flow, B, is related to $W_B$ by

$$B = k_{s4} + k_{s5}W_B \ , \tag{4.18}$$

with positive constants $k_{s4}$ and $k_{s5}$.

Let

$$k_{s6} \equiv \frac{k_{s2}}{k_{s3}k_{s4}} \ ,$$

and

$$k_{s7} \equiv \frac{k_{s5}}{k_{s4}} .$$

Then, with (4.16), (4.17), and (4.18), (4.15) becomes

$$T_s = T_c - \frac{k_{s6}}{\left(\frac{1}{W_B} + k_{s7}\right) f_s} . \tag{4.19}$$

Using (4.19) in (4.12), the skin saturated vapor pressure becomes

$$p_{se} = c_1 + c_2 T_c - \frac{c_2 k_{s6}}{\left(\frac{1}{W_B} + k_{s7}\right) f_s} . \tag{4.20}$$

Finally, with the definitions

$$k_{s8} \equiv c_1 + c_2 T_c , \tag{4.21}$$

and

$$k_{s9} \equiv c_2 k_{s6} , \tag{4.22}$$

(4.20) becomes

$$p_{se} = k_{s8} - \frac{k_{s9}}{\left(\frac{1}{W_B} + k_{s7}\right) f_s} . \tag{4.23}$$

Hence, with approximation (4.23), the net water loss through the skin becomes, from (4.13),

$$(\phi_e(t) - \phi_a(t))_s = k_{s1}\left[k_{s8} - \frac{k_{s9}}{\left(\frac{1}{W_B(t)} + k_{s7}\right)f_s(t)} - rp_{sa}\right] . \tag{4.24}$$

Equation (4.24), then, is the final approximation of (4.11) for the net water loss through the skin of the wild house mouse by insensible evaporation. The model implies that the only control the experimental animals had over this water loss is the regulation of skin temperature by the vasomotor adjustment of $f_s$, the fraction of blood flow into the skin. Also, the model indicates the effect on flux of changes in $W_B$.

Formula (4.11), however, may not be adequate to account for some experimental findings on water exchange through the skin [4.4, p. 87], [4.10, p. 205]. The skin does not lose water as though it were a water surface at temperature $T_e$, because diffusion, as well as evaporation and condensation, is involved in the water exchange. Based on this fact, and the above physiology of the skin, an original modified model is now proposed for water exchange through the skin, if model (4.24) proves inadequate. This model, represented in Fig. 4.7, assumes that water loss via the skin involves two mechanisms. First, water diffuses, with net flux $\phi_{\rho_s}$, through a barrier layer of effective permeability $\rho_s$ from a relatively

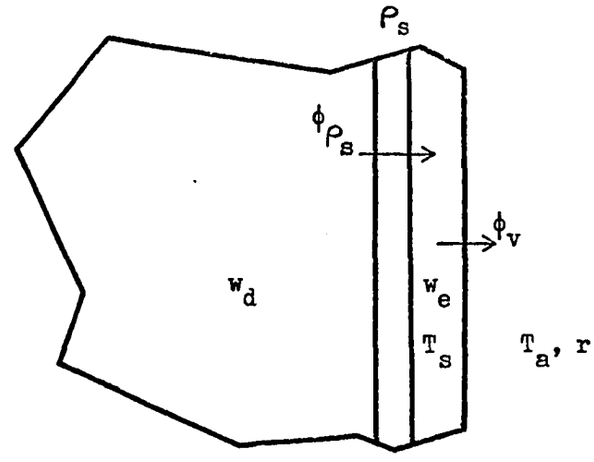


Fig. 4.7. A Modified Model of Water Exchange Through the Skin.

homogeneous region in the dermis with water concentration $w_d$ to an external layer in the outer epidermis with water concentration $w_e$. Then, the water evaporates, with net efflux $\phi_v$, from the epidermal surface layers into the air. Of course, these fluxes include water moving inward from the air into the body, as well. The net diffusion flux is described by

$$\phi_{\rho_s} = \rho_s(w_d - w_e) \ , \tag{4.25}$$

and the net evaporative flux, $\phi_v$, is assumed to obey

$$\phi_v = k_{sl}(p_e - p_a) \ . \tag{4.26}$$

As before, $p_a = rp_{sa}$, but, now, it is assumed that

$$p_e = w_e p_{se} \ , \tag{4.27}$$

so that (4.26) becomes

$$\phi_v = k_{s1}(w_e p_{se} - r p_{sa}) \ . \tag{4.28}$$

Assume the steady state condition that

$$(\phi_e - \phi_a)_s = \phi_{\rho_s} = \phi_v \ , \tag{4.29}$$

which, with (4.25) and (4.26), implies

$$w_e = \frac{\rho_s w_d + k_{s1} r p_{sa}}{\rho_s + k_{s1} p_{se}} \ . \tag{4.30}$$

Hence, the net flux through the skin becomes

$$(\phi_e - \phi_a)_s = k_{s1}\left[\frac{\rho_s w_d + k_{s1} r p_{sa}}{\rho_s + k_{s1} p_{se}} p_{se} - r p_{sa}\right] . \tag{4.31}$$

Finally, using approximation (4.23) for $p_{se}$ and assuming that the concentration of water in the dermis is proportional to the amount of water in the body, that is,

$$w_d = \gamma_d W_B \ , \tag{4.32}$$

(4.31) takes the form

$$(\phi_e - \phi_a)_s = k_{s1}\left[\frac{\rho_s(t)\gamma_d(t)W_B(t) + k_{s1} r p_{sa}}{\rho_s(t)} - r p_{sa}\right] \cdot \frac{1}{\left(k_{s8} - \frac{k_{s9}}{\left(\frac{1}{W_B(t)} + k_{s7}\right) f_s(t)}\right)} + k_{s1} \tag{4.33}$$

This more complex model for water loss through the skin includes more control possibilities than that in (4.24). Not only is the animal's ability to adjust $f_s$, the blood flow to the skin, included, but also its capability to vary the water diffusion permeability, $\rho_s$, of the skin and the water storage characteristics of the dermis, through $\gamma_d$. As before, the effects of changes in $W_B$ on the flux are included in (4.33), as well.

#### 4.2.2.3 Lungs

Physiology

When the mouse breathes, it takes in air at ambient temperature and relative humidity. This air is rapidly brought to saturation at body temperature upon exposure to the moist air passages and alveolar surfaces. Saturated air is expired, and if this air were at body temperature, considerable water would be lost through breathing. The wild house mouse, along with many other animals living in dry environments, recovers much of this potentially wasted water by means of what Jackson and Schmidt-Nielsen call an alternating flow countercurrent heat exchanger in the respiratory passages [4.13, p. 1196].

The alternating flow countercurrent exchanger operates as follows: Water evaporating from the nasal mucosa to saturate the incoming air cools these surfaces. When the saturated air at body temperature is exhaled, the cool nasal surfaces remove heat from the exiting air and condense out some

of the water vapor. Small mammals have such narrow breathing passages that virtually complete temperature and vapor pressure equilibrium can occur between the air and mucosa. The exchanger can work well enough in these animals to lower the temperature of the expired air not only below body core temperature, but also several degrees below that of the surrounding air [4.13, p. 1193].

Cooling of the expired air depends both on the temperature $T_r$ of the surfaces of the upper respiratory tract and the effectiveness of heat transfer between those surfaces and the air flowing over them. Temperature $T_r$ is determined by ambient temperature $T_a$ and relative humidity r and by the blood circulation into those regions. The efficiency of heat exchange depends on the rate and type of airflow, the temperature gradient between air and surface, and the geometry of the respiratory passage [4.13, p. 1196].

Another factor affecting respiratory water loss is the depth of breathing. Deeper breathing permits the animal to reduce its ventilation rate and hence its respiratory water loss because more of each breath is available for supplying oxygen. The ratio of respiratory water loss to oxygen exchange can change by as much as a factor of 10 between panting and "summit" metabolism deep breathing [4.4, p. 89].

Water flux model

No mathematical model of water exchange via the lungs could be found in the literature. Therefore, the following

model is proposed, based on the above physiological review. The net water flux lost from the lungs is the difference between the water content of the expired air and that of the inspired air times the lung ventilation rate, $\dot{V}$. A graph of the water content of saturated air versus temperature, T, is given in Fig. 4.8 (from [4.4, p. 92]). Approximate this relation about a given quiescent point by the first two terms of a Taylor series expansion, i.e., Water Content = $c_{\ell 1}$ + $c_{\ell 2}T$, and the net water efflux from the lungs becomes

$$(\phi_e - \phi_a)_\ell = \dot{V}[(c_{\ell 1} + c_{\ell 2}T_e) - rw_{sa}] \ . \tag{4.34}$$

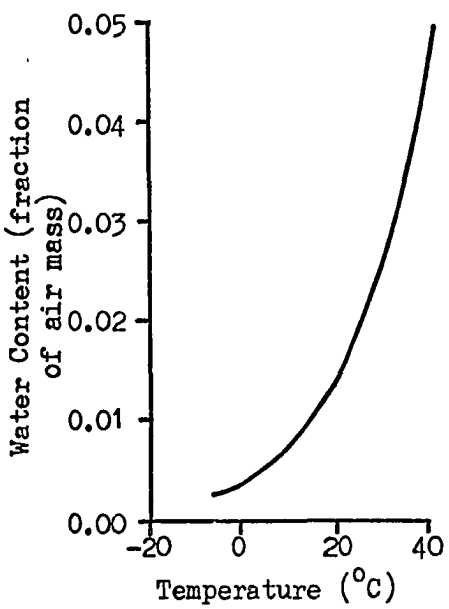


Fig. 4.8. The Water Content of Saturated Air as a Function of Temperature.

In (4.34), the expired air is saturated at temperature $T_e$, and the ambient air is at relative humidity r and temperature $T_a$, corresponding to saturated water content, $w_{sa}$. Now,

assume that the efficiency of thermal exchange between the nasal mucosa at temperature $T_r$ and the expired air at temperature $T_e$ can be expressed by

$$T_e = \beta_\ell T_r \ . \tag{4.35}$$

Also, analogous to (4.19) for the skin, assume that, for constant r and $T_a$, the relation between $T_r$ and blood flow to the upper respiratory surfaces can be approximated by

$$T_r = T_c - \frac{k_{\ell 1}}{\left(\frac{1}{W_B} + k_{\ell 2}\right) f_\ell} \ , \tag{4.36}$$

where $f_\ell$ is the fraction of blood flow to the respiratory surfaces. Then, with (4.35) and (4.36), the net water efflux from the lungs in (4.34) becomes

$$(\phi_e(t) - \phi_a(t))_\ell = \dot{V}(t)\left\{\left[c_{\ell 1} + c_{\ell 2}\beta_\ell(t)\left(T_c - \frac{k_{\ell 1}}{\left(\frac{1}{W_B(t)} + k_{\ell 2}\right) f_\ell(t)}\right)\right] - rw_{sa}\right\} . \tag{4.37}$$

In a fixed environment, therefore, (4.37) summarizes that a mouse can vary water loss from the lungs by varying ventilation rate, $\dot{V}$, which, as was mentioned in the physiology review, can be changed without affecting oxygen exchange. Also, the animal can alter $(\phi_e - \phi_a)_\ell$ by varying the rate of air flow through and the geometry of the respiratory passages,

thus influencing the efficiency of heat exchange, represented by $\beta_{\ell}$, between the respiratory passage surfaces and the expired air. Finally, by vasodilation or constriction of upper respiratory blood vessels, the animal can control water loss via the lungs by changing the fraction of blood, $f_{\ell}$, flowing to the respiratory surface area. The amount of body water, $W_B$, also affects water loss through the lungs, as shown in (4.37), by influencing the total blood flow rate.

# CHAPTER V

# ACCLIMATION TO WATER DEPRIVATION IN THE WILD HOUSE MOUSE: ANALYSIS

## 5.1 Introduction

### 5.1.1 Objectives

Chapters II and III present techniques to aid in applying compartmental bilinear models to the study of physiological systems. Tracer methods are developed in Chapter II for estimating the orders of such models. In Chapter III, tracer techniques are developed for determining the dynamical behavior of the compartmental system and, by means of the given compartmental structure and mechanisms, the behavior of the bilinear system.

This compartmental approach is now applied to the analysis of water acclimation in the wild house mouse. First, in Section 5.2 a compartmental structure for the water acclimation system is derived. This compartmental model is intended to be the simplest such structure consistent with the known physiology and the raw numerical data obtained from Dr. Haines. Then, in Section 5.3, the dynamics of water acclimation are investigated. First, in Section 5.3.1, more raw tracer data collected by Dr. Haines during the process of

water acclimation are presented. In Section 5.3.2, the water flux mechanisms developed in Chapter IV are incorporated into a one-compartment structure to generate the total control model for the water acclimation plant. This model is then represented as a bilinear control system. Finally, in Section 5.3.3, the experimental data of Section 5.3.1 are used to study the dynamical behavior of the control system of Section 5.3.2 during water acclimation.

Before Dr. Haines' experimental data on water acclimation are presented and utilized, Section 5.1.2 briefly introduces the experimental animals and their laboratory environment.

### 5.1.2 Experimental Animals

The animals used were drawn from a colony of wild house mice stocked originally from two Oklahoma sites: Norman in Cleveland County and Clinton in Washita County. Occasionally, the colony was outbred with freshly trapped animals. The colony was kept at a temperature of about 25° C with a 12 hour light-12 hour dark photoperiod. The animals, ranging in age from 3 to 6 months, were fed Purina Lab Chow and water ad libitum. (Ad libitum means the animals were allowed unrestricted access.)

Experimental animals were caged individually at 20° C, 50 percent relative humidity with an unregulated photoperiod, and they were allowed a two week adjustment period before any experiment was begun. Their commercially prepared food (GBI

Hicarbohydrate Test Diet or GBI Synthetic Stock Diet) consisted of 22% protein, 66% carbohydrate, 8% lipid, and 4% salt, and their drinking water was weighed portions of 1% purified agar (Difco No. 0560-01) [5.1].

## 5.2 Compartmental Structure

In this section, a compartmental structure for the water acclimation system of the wild house mouse is developed which is as simple as possible, yet consistent with known physiology and Dr. Haines' experimental data. Section 5.2.1 graphs the steady state values of body water content and water fluxes with the environment at different levels of water deprivation. Then, in Section 5.2.2, tracer data on steady state water exchange are analyzed to determine a suitable internal compartmentation for the water system.

### 5.2.1 Steady State Water Content and External Fluxes

The first experimental results presented summarize the different steady state conditions of animals acclimated to drinking water supplies ranging from ad libitum to 1/8 ad libitum. The body masses, expressed as a percentage of ad libitum body mass, for these acclimation states are shown in Fig. 5.1 (from [5.1][1]). From other experiments, Dr. Haines

[1]The descriptions of these and later experimental data on the wild house mouse are relatively brief. The data are meant, however, not as a treatise on water balance in the mouse but to illustrate the kinds of data available and how such data can be utilized. The expression "from [5.1]" means that the raw data on which Fig. 5.1 is based were obtained from [5.1].

concluded that the mass of body water, $W_B$, maintains the constant ratio, .69, to the total body mass [5.1]. Hence, Fig. 5.1 also describes the decline of steady state body water mass in the mouse as it is subjected to increasingly restricted drinking water levels. The body mass of an experimental animal at ad libitum water conditions was usually in the vicinity of 20g.

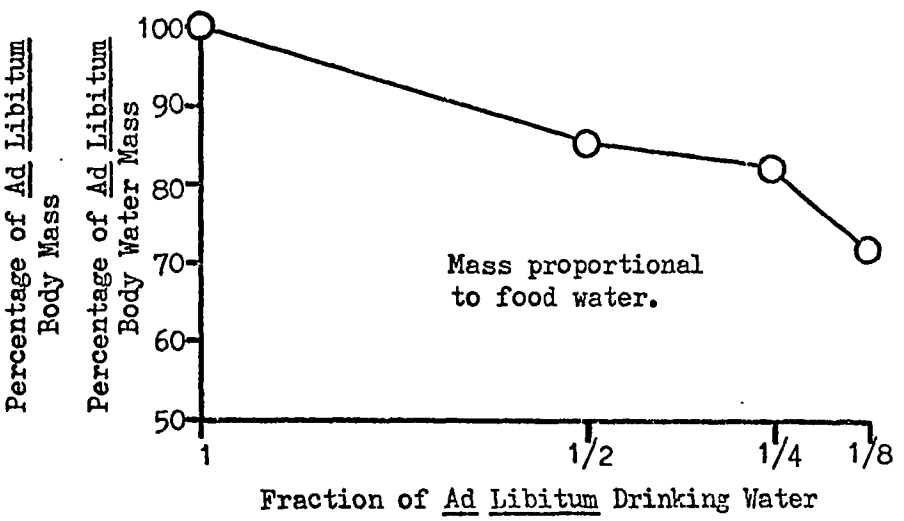


Fig. 5.1. Steady State Body Mass and Body Water Mass (Percentage of Ad Libitum) Versus Water Deprivation in the Wild House Mouse.

In presenting steady state acclimation data on external water fluxes in the mouse, the water exchange model is simplified over that shown in Fig. 4.2. A nonexchanging "storage" compartment is not considered. Moreover, the water influxes due to moisture in the food and metabolic water are combined into a single water influx from food. Also, because fecal water loss is relatively small, this efflux is combined with

urinary water loss. Finally, there is no water loss due to salivation or lactation. This simpler water exchange model is summarized in Fig. 5.2.

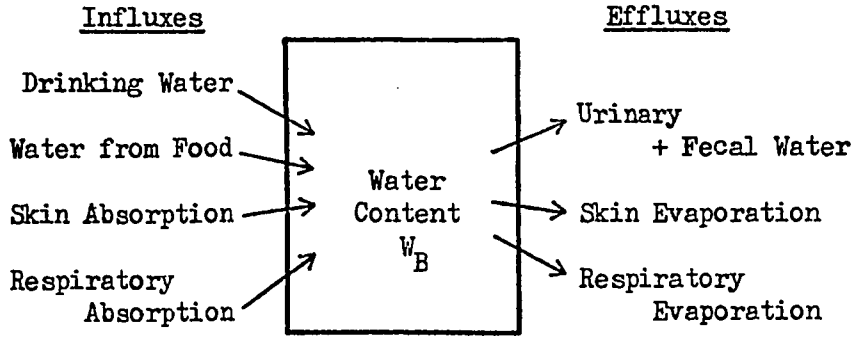


Fig. 5.2. A Simplified Water Exchange Model for the Experimental Wild House Mouse.

In these steady state acclimation experiments, drinking water was supplied by measured quantities of 1% purified agar. Water influx from food, the sum of oxidative and hygroscopic water, was calculated using an experimentally determined constant of proportionality relating food water influx and body mass [5.1]. Urinary and fecal water fluxes were measured directly from daily collections under paraffin oil; fecal loss was small and relatively insensitive to water deprivation. Net evaporative water was estimated as the difference between the above influxes and effluxes. Evaporation measurements performed in dry air at 29° C on ad libitum animals and animals acclimated to 1/4 and 1/8 ad libitum provided ratios of pulmonary to cutaneous contributions to evaporative water loss.

Steady state acclimation graphs averaged over several animals of drinking influx, food water influx (including oxidative and hygroscopic), urine efflux, and net exchange via the skin and lungs are presented in Fig. 5.3 (from [5.1]). Fig. 5.3a describes the reduction in water influxes under increased water deprivation. The solid curve connects the values of drinking water influxes given to the experimental animals at the various levels of water deprivation. The dashed curve connects the calculated values of water influx from food. As mentioned above, this influx is proportional to the body mass graphed in Fig. 5.1. Water effluxes are shown in Fig. 5.3b. Urinary and fecal daily water losses at the different levels of acclimation are indicated by the dash-dot curve. The solid curve joins net evaporative water effluxes at different drinking water levels. Observe that, as drinking water was reduced, both urinary-fecal and evaporative losses decreased. The change in net evaporative loss, however, was both relatively and absolutely greater than the corresponding change in urinary-fecal loss. Fig. 5.3b also indicates the breakdown of net evaporative loss into net skin evaporation and net respiratory evaporation, shown, respectively, by the points on the short dash curve and those on the long dash curve.

### 5.2.2 Compartmentation

In this section, steady state tracer data obtained by Dr. Haines are analyzed to develop a model of the internal

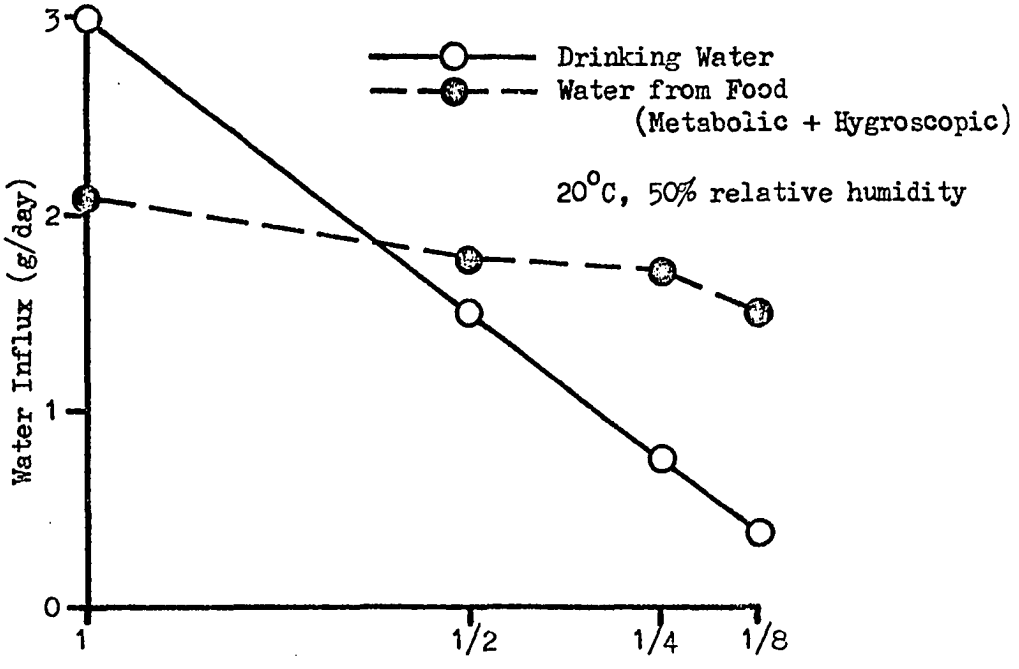


a. Influxes

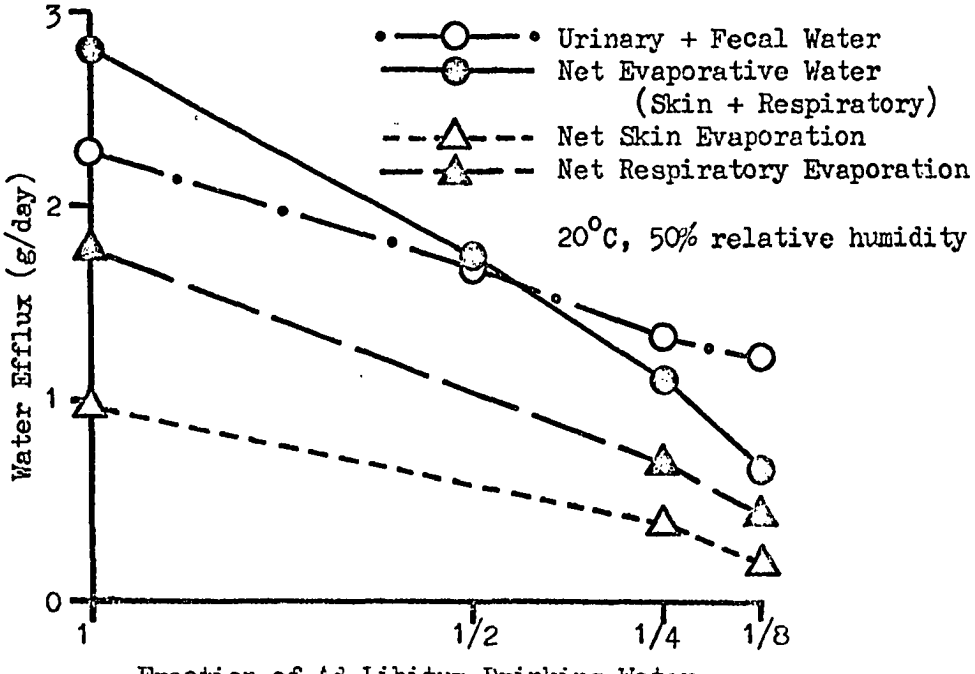


b. Effluxes

Fig. 5.3. Steady State Water Fluxes Versus Water Deprivation in the Wild House Mouse: a. Influxes; b. Effluxes.

compartmentation of the mouse's water content. A one-compartment model seems consistent with the first tracer washout data presented. This model, however, cannot account for observed differences in the tracer specific activities of plasma and evaporate samples taken separately. Both nonideal tracer effects and a multi-compartment structure are considered as possible explanations for the difference in specific activities. A survey of the literature on tritiated water (THO), the radioactive tracer used, shows that tracer effects may, indeed, exist in the mouse. The nonideal tracer behavior of THO, however, cannot alone account for the experimental observations. A two-compartment structure is then developed which is consistent with the experimental data, both neglecting and including the effects of a nonideal tracer.

#### 5.2.2.1 One-compartment model

Ideal tracer

A typical long-term record of tracer washout in a steady state animal (ad libitum) is shown by the open circles on the semilog graph in Fig. 5.4 (from [5.1]). After intraperitoneal THO injection, periodic samples of body water were analyzed for radioactivity. These samples, consisting of both excreted and evaporated water, were removed to collecting tubes by dry air passing through the animal's chamber. The observed decline in radioactivity within the experimental animal was not due to radioactive decay (tritium has a half life of 12.5 years) but rather to the continuous replacement with ordinary

water of the tritiated water lost by excretion and evaporation. As can be seen by the straight line in Fig. 5.4, this decline can be closely fitted by a single negative exponential curve over the time interval shown.

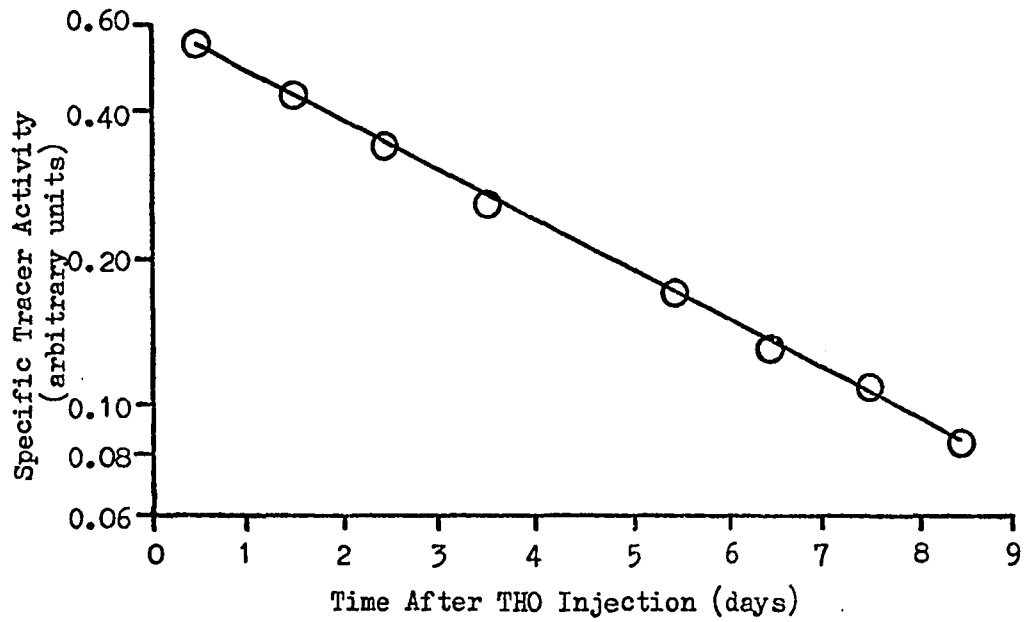


Fig. 5.4. Specific Activity Versus Time After THO Injection in an Ad Libitum Wild House Mouse (Semilog Grid).

Experiments to determine the initial mixing of the injected THO with the animal's body water were also performed. Fig. 5.5 graphs the rise of tracer specific activity immediately after injection (from [5.1]). In Fig. 5.5a, values of tracer activity in samples of plasma are plotted during the first few hours after injection for two animals. Observe that activity in the plasma attained its maximum value virtually before the first sample could be taken. (Plasma

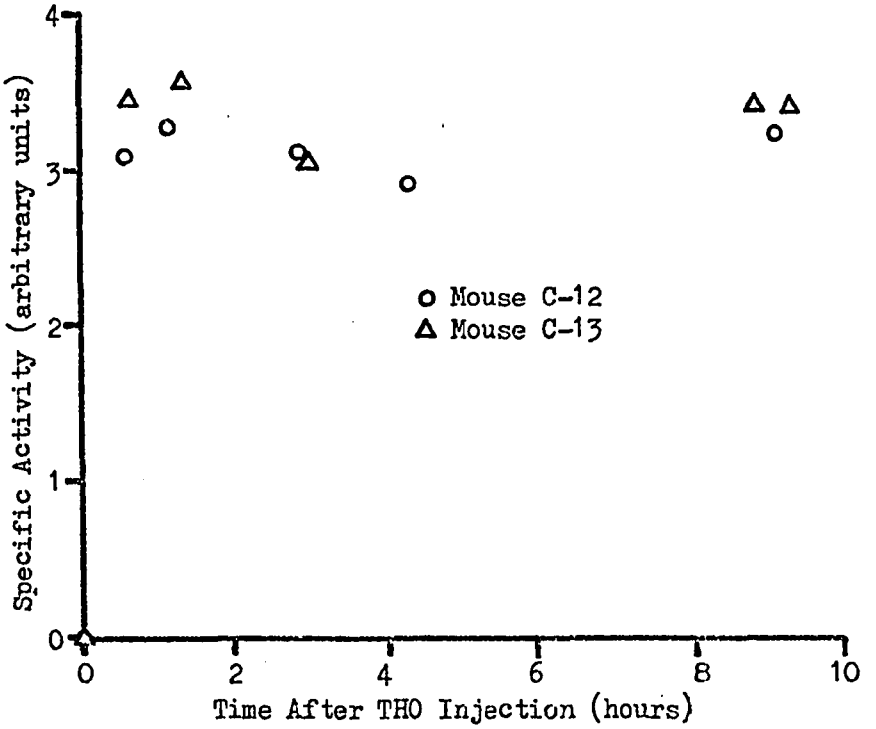


a. Plasma

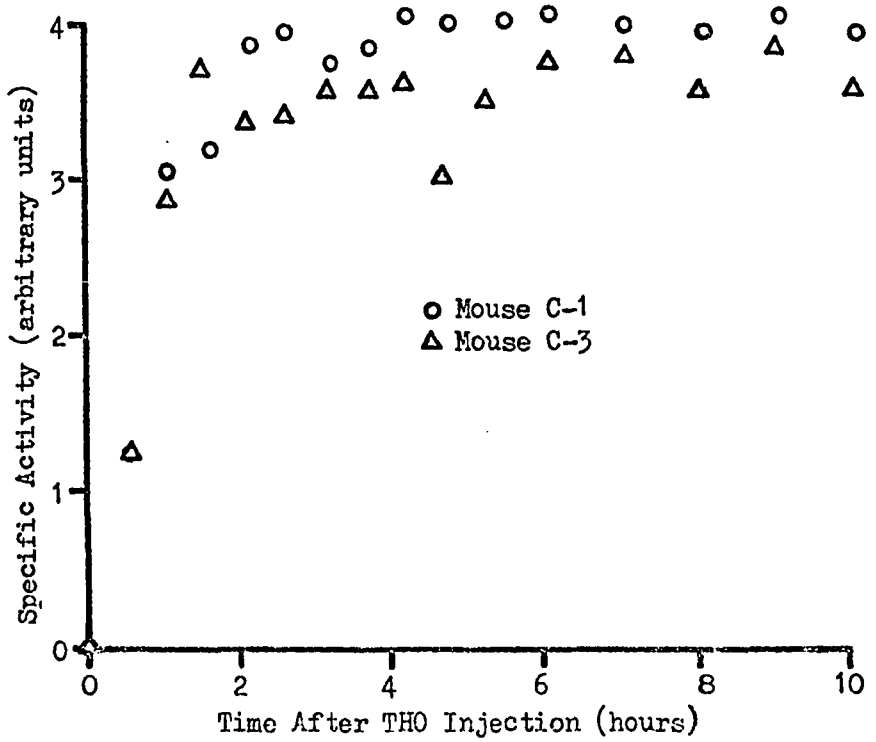


b. Evaporate

Fig. 5.5. Specific Activity Versus Time After Intraperitoneal THO Injection in the Ad Libitum Wild House Mouse: a. Plasma, b. Evaporate.

samples were obtained by repeated amputation of the tail.) Tracer activity in the evaporate, recorded for two other animals in Fig. 5.5b, also rose rapidly, reaching a maximum within a few hours after injection. Evaporate samples were collected in the same apparatus described above, except it was assured that there was no urinary-fecal excretion during the collecting interval.

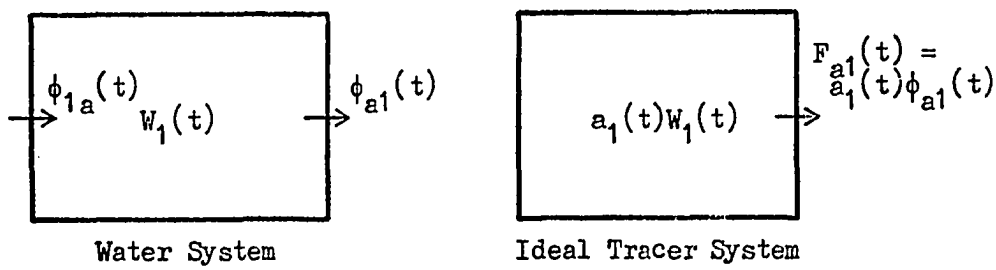


Fig. 5.6. A One-Compartment Water Model and Associated Ideal Tracer System.

Based on the single exponential decline of tracer activity shown in Fig. 5.4 and the rapid tracer mixing with body water shown in Fig. 5.5, it seems reasonable to represent the water structure of the mouse by the single-compartment model shown in Fig. 5.6. With reference to Fig. 5.2, define the following fluxes:

$\phi_{gd}(t)$ = water influx from drinking

$\phi_{gf}(t)$ = water influx from food

$\phi_{as}(t)$ = water influx through skin

$\phi_{a\ell}(t)$ = water influx via ventilation

$\phi_{u}(t)$ = water efflux in urine and fecal loss

$\phi_{es}(t)$ = water efflux through skin

$\phi_{e\ell}(t)$ = water efflux via ventilation.

Then, total water influx, $\phi_{1a}(t)$, and total efflux, $\phi_{a1}(t)$, are given, respectively, by

$$\phi_{1a}(t) = \phi_{gd}(t) + \phi_{gf}(t) + \phi_{as}(t) + \phi_{a\ell}(t) \tag{5.1}$$

and

$$\phi_{a1}(t) = \phi_{u}(t) + \phi_{es}(t) + \phi_{e\ell}(t) \ . \tag{5.2}$$

In the one-compartment model, influx $\phi_{1a}$ and efflux $\phi_{a1}$ are related to the amount of body water, $W_1(t) = W_B(t)$, by

$$\dot{W}_1 = \phi_{1a}(t) - \phi_{a1}(t) \ . \tag{5.3}$$

The associated tracer system is also represented in Fig. 5.6, where the notation $F_z$ denotes the tracer flux associated with water flux $\phi_z$. In terms of specific activity $a_1$, this system is described by

$$\dot{a}_1 = -\left(\frac{\phi_{1a}(t)}{W_1(t)}\right)a_1 \ . \tag{5.4}$$

(In this and the following tracer systems, the environmental specific activity is assumed zero.) When compartmental system (5.3) is in steady state, tracer system (5.4) has the solution

$$a_1(t) = a_{10} e^{-\left(\frac{\phi_{1a}}{W_1}\right)t} . \qquad (5.5)$$

The above one-compartment model predicts that the specific activity of an ideal tracer at a given time should be the same in the animal's body water as that for every efflux from the animal. Indeed, plasma and urine tracer specific activities were shown experimentally to be identical. Dr. Haines found, however, that plasma and evaporate tracer specific activities were consistently different. Animals were acclimated to various levels of water deprivation and injected intraperitioneally with THO. Daily measurements were then made on each animal of plasma and evaporate specific activity. Typical results for a mouse at ad libitum drinking water and another at 1/2 ad libitum are given in Figs. 5.7a and 5.7b, respectively (from [5.1]). Observe that, in a particular state of hydration, plasma and evaporate specific activities differ in magnitude, although they both decline at the same exponential rate. Note, furthermore, that the difference in activity magnitudes increases with water deprivation.

In the next section, it is found that THO may exhibit nonideal tracer behavior in the mouse's water system. These tracer effects are then incorporated into the above one-compartment model to see whether they account for the experimental results shown in Fig. 5.7.

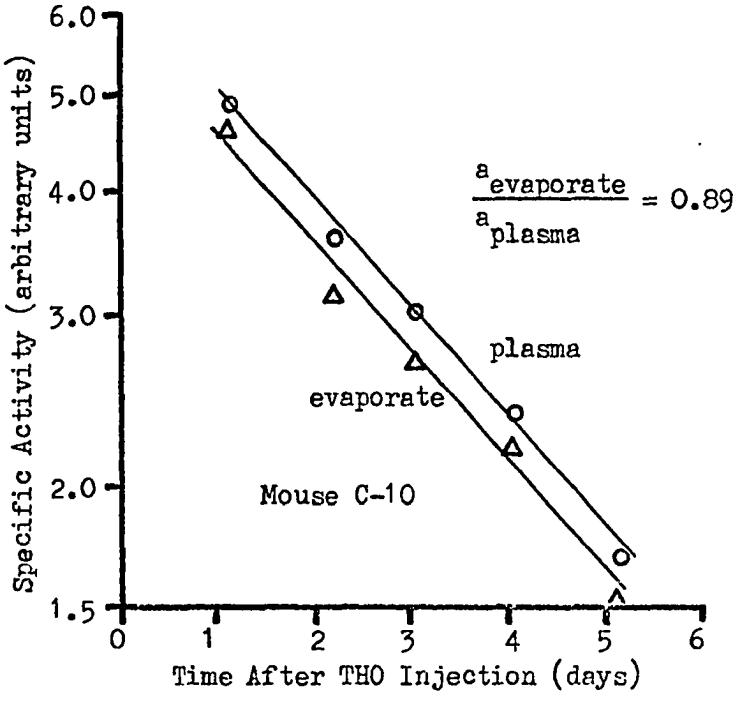


a. Ad Libitum

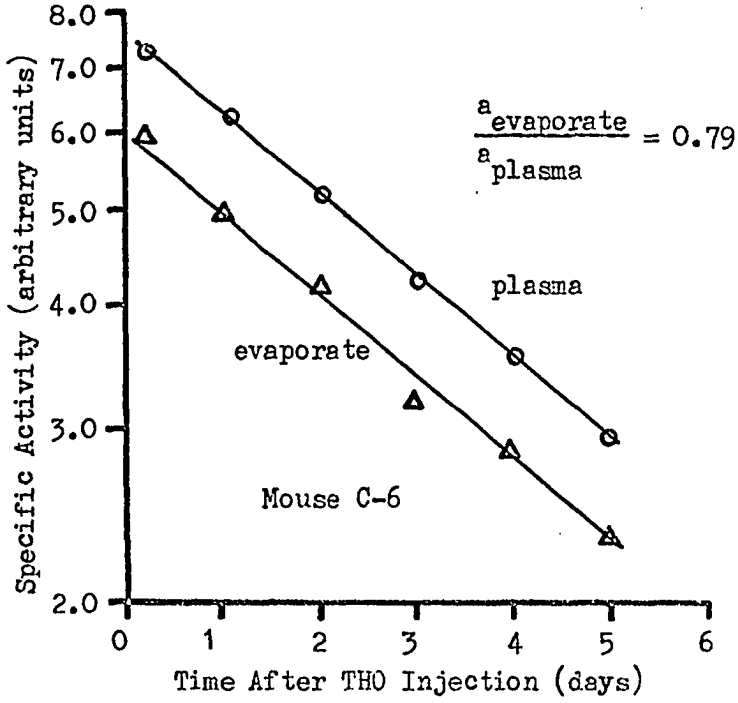


b. 1/2 Ad Libitum

Fig. 5.7. Steady State Plasma and Evaporate Specific Activities Versus Time After THO Injection in the Wild House Mouse: a. Ad Libitum; b. 1/2 Ad Libitum.

Nonideal tracer

It is usually assumed that THO acts as an ideal tracer of water in biological systems. (Recall from Chapter I that an ideal tracer does not affect the behavior of the biological system under study and behaves identically with the unlabeled substance in the system.) In fact, Pinson [5.2, pp. 128-129] states the following:

> ...the HTO [THO] concentration of water of urine, sputum, sweat, feces and insensible perspiration of man is the same, within the measuring sensitivity, as that existing in the water of the blood at the time of collection of these excreta. The same has been found for HDO [deuteriated water, DHO] in the urine and gastric juice of man and in the milk of cows. If a rate difference exists for transfer of $H_2O$, HDO, or HTO across membranes involved in the formation and excretion of these fluids the time periods involved in the net transfer are sufficiently long to permit isotopic equilibrium to be established. Thus either HDO or HTO at equilibrium in body fluids serve as excellent tracers for $H_2O$ in these transfers so far as can be ascertained from data available.

A survey of the literature on the possible nonideal behavior of THO in living systems is presented in Appendix B. In agreement with Pinson's statement, it is concluded in Appendix B that the proper use of THO as a tracer does not disturb the system under study. Moreover, it is found that hydrogen isotopes (THO and deuteriated water) may safely be used to measure water transfer across internal biological membranes. Contrary to Pinson's conclusions, however, THO does not behave like $H_2O$ in evaporation. In particular, in a mixture of THO and $H_2O$, evaporation tends to leave the tritium behind in the liquid phase. Hence, in the above experiments on the

mouse, the tracer specific activity of the skin evaporate could be on the order of 90% of that in the body. (See Table B.1.)

The above one-compartment model is now modified to include this nonideal behavior of the tracer THO upon evaporation. Water influx, $\phi_{1a}$, into the system is kept the same, but efflux $\phi_{a1}$ is separated into the urinary flux $\phi_u$ and the evaporative flux

$$\phi_e = \phi_{es} + \phi_{e\ell} \ . \tag{5.6}$$

To model the tracer effect, the tracer specific activity of evaporative efflux $\phi_e$ is defined as some fraction, r, $0 < r < 1$, of that of the body water and of urinary efflux $\phi_u$. The resultant model is shown in Fig. 5.8. As in (5.3), the fluxes are related to the amount of body water, $W_1(t) = W_B(t)$, by

$$\dot{W}_1 = \phi_{1a}(t) - (\phi_u(t) + \phi_e(t)) \ , \tag{5.7}$$

but the associated tracer system becomes

$$\dot{a}_1 = -\frac{1}{W_1(t)}(\phi_u(t) + r\phi_e(t))a_1 \ . \tag{5.8}$$

The solution to (5.8) when compartmental system (5.7) is in steady state is

$$a_1(t) = a_{10}e^{-\frac{1}{W_1}(\phi_u+r\phi_e)t} \ . \tag{5.9}$$

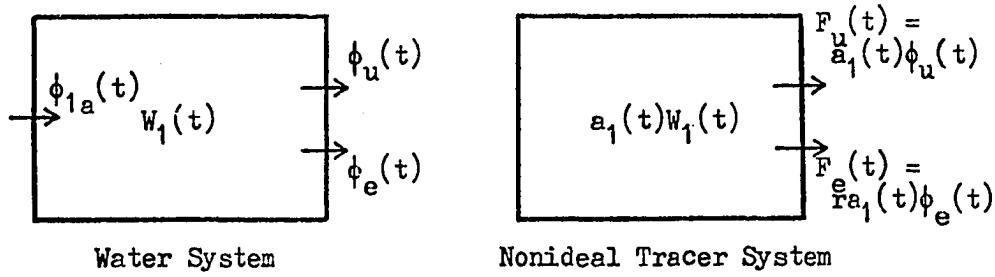


Fig. 5.8. A One-Compartment Water Model and Associated Nonideal Tracer System.

On the other hand, the specific activity of evaporate collected from the animal in this case is

$$\frac{F_e(t)}{\phi_e} = ra_1(t) \ , \tag{5.10}$$

with $a_1(t)$ given by (5.9). Note that the nonideal behavior of THO as a tracer alters the exponents of both the internal (5.9) and evaporate (5.10) specific activity washout curves. Observe, also, that (5.9) and (5.10) have the same exponents and that their magnitudes are in the constant ratio, r, regardless of the sizes of the steady state fluxes $\phi_{1a}$, $\phi_u$, and $\phi_e$.

The above model, assuming a single water compartment and a nonideal tracer, can account for the fact that the semilog plots of plasma and evaporate specific activities in Fig. 5.7 are straight lines of constant ratio (constant vertical spacing). The model cannot, however, account for the increase in the ratio of plasma to evaporate specific activity, seen by comparing Figs. 5.7b and 5.7a, as the animal is more severely

deprived of water. Recall again that specific activities (5.9) and (5.10) have the constant ratio, r, regardless of the steady state water flux values. Also, note from Table B.1 that, even if the skin temperature changes with water deprivation, this change is not enough to account for the change in specific activity ratios from about .9 at ad libitum to about .8 at 1/2 ad libitum.

Because of the deficiency of the above one-compartment model, even considering nonideal tracer behavior, more complex water storage structures are examined in the next section as models to explain the experimental results of Fig. 5.7.

5.2.2.2 Two-compartment model

In the graphs of initial tracer mixing in Fig. 5.5, the rise in evaporate specific activity in Fig. 5.5b is noticeably slower than that of plasma specific activity in Fig. 5.5a. Hence, perhaps mammalian skin contains extravascular fluids which are not in a state of rapid exchange with the bulk of body fluid. This supposition is supported in experiments involving skin exposure to THO in man. With warmed skin, urinary THO concentration reaches a constant value within an hour. On the other hand, if the skin is cooled after exposure to THO, thus reducing its circulatory exchange, the urinary concentration is still increasing after 5 hours [5.2, p. 128]. Therefore, this section analytically tests the hypothesis of a water model consisting of an internal

water compartment in equilibrium with the plasma and a skin and lung extravascular fluid compartment affected by evaporative exchange.

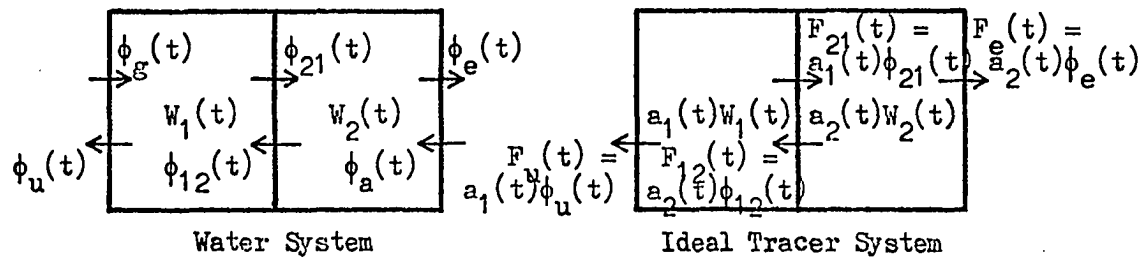


Fig. 5.9. A Two-Compartment Water Model and Associated Ideal Tracer System.

Ideal tracer

The proposed two-compartment model is shown in Fig. 5.9. In this model, compartment 1, to be called the plasma compartment, contains all the body water, $W_1(t)$, in equilibrium with the blood plasma. Similarly, compartment 2, the "evaporate" compartment, contains the body water, $W_2(t)$, in equilibrium with insensible evaporation from the animal ($W_1(t) + W_2(t) = W_B(t)$). The plasma compartment receives water from the environment, $\phi_g(t)$, via the gastrointestinal tract in the form of drinking water, as well as hygroscopic and metabolic water from the animal's food. Water is lost to the environment from the plasma compartment in the urine, $\phi_u(t)$. The evaporate compartment exchanges water with the environment via efflux $\phi_e(t)$ and influx $\phi_a(t)$. The two compartments, of course,

exchange water inside the animal, with flux $\phi_{ij}(t)$ to compartment i from compartment j.

By inspection, the water conservation equations for this model are

$$\begin{aligned} \dot{W}_1 &= -\phi_{21}(t) + \phi_{12}(t) - \phi_u(t) + \phi_g(t) \\ \dot{W}_2 &= \phi_{21}(t) - \phi_{12}(t) - \phi_e(t) + \phi_a(t) \ , \end{aligned} \tag{5.11}$$

and in water balance ($\dot{W}_1 = \dot{W}_2 = 0$),

$$\phi_{21}(t) - \phi_{12}(t) = \phi_g(t) - \phi_u(t) = \phi_e(t) - \phi_a(t) \ . \tag{5.12}$$

The associated specific activity kinetics for an ideal tracer applied to system (5.11) are given by

$$\dot{\bar{a}} = S(t)\bar{a} \ , \tag{5.13}$$

where

$$S(t) = \begin{pmatrix} -\dfrac{(\phi_{12}(t)+\phi_g(t))}{W_1(t)} & \dfrac{\phi_{12}(t)}{W_1(t)} \\ \dfrac{\phi_{21}(t)}{W_2(t)} & -\dfrac{(\phi_{21}(t)+\phi_a(t))}{W_2(t)} \end{pmatrix} \ , \tag{5.14}$$

and

$$\bar{a} \equiv \begin{pmatrix} a_1 \\ a_2 \end{pmatrix} \ . \tag{5.15}$$

This ideal tracer system is also illustrated in Fig. 5.9, where, again, $F_z$ represents the tracer flux associated with water flux $\phi_z$.

In order to compare the behavior of tracer in steady state compartmental model (5.11) with that depicted for the experimental system in Fig. 5.7, it is necessary to examine the ratio of specific activities, $a_2(t)/a_1(t)$, after a large time. This ratio is simply the slope of the slow eigenvector of matrix S, now constant, in (5.14).

The eigenvalues of the tracer system matrix are

$$\sigma_{1,2} = -\frac{\phi_{21}(W_1+W_2)+\phi_u W_2+\phi_a W_1}{2W_1W_2}$$

$$\pm \frac{1}{2W_1W_2}\Big([\phi_{21}(W_1+W_2)+\phi_u W_2+\phi_2 W_1]^2$$

$$-4W_1W_2[\phi_{21}(\phi_e+\phi_u)+\phi_u\phi_a]\Big)^{1/2} . \qquad (5.16)$$

The corresponding eigenvector slopes, $m_{1,2}$, are

$$m_i = \frac{a^i_{2e}}{a^i_{1e}} = \frac{\phi_{21}}{\phi_{21} + \phi_a + W_2\sigma_i} , \quad i = 1, 2 . \qquad (5.17)$$

From Section 2.3.2, it is known that eigenvalues $\sigma_1$ and $\sigma_2$ are real. Moreover, $\sigma_1$ and $\sigma_2$ are distinct if

$$[(\phi_{21}+\phi_u)W_2+(\phi_{21}+\phi_a)W_1]^2 > 4W_1W_2[\phi_{21}\phi_e+\phi_{21}\phi_u+\phi_u\phi_a] . \qquad (5.18)$$

But, the left side of (5.18) always satisfies

$$[(\phi_{21}+\phi_u)W_2+(\phi_{21}+\phi_a)W_1]^2 \geq 4W_1W_2(\phi_{21}+\phi_u)(\phi_{21}+\phi_a) \ . \qquad (5.19)$$

Furthermore, the inequality

$$4W_1W_2(\phi_{21}+\phi_u)(\phi_{21}+\phi_a) > 4W_1W_2[\phi_{21}\phi_e+\phi_{21}\phi_u+\phi_u\phi_a] \qquad (5.20)$$

holds if

$$\phi_{21} + \phi_a > \phi_e \ . \qquad (5.21)$$

By (5.12), and the fact that $\phi_{12} > 0$, (5.21) is true, and hence, combining (5.18)-(5.20), the eigenvalues $\sigma_1$ and $\sigma_2$ are shown to be distinct. That $\sigma_1$ and $\sigma_2$ are distinct can also be shown by using the application of Parter's theorem to compartmental systems derived in Section 2.3.3.

Also, it can be shown that the eigenvector slopes satisfy $m_1 > 0$ and $m_2 < 0$. The eigenvector slopes in (5.17) take on the signs of their denominators, or, equivalently, the signs of the expressions

$$2W_1(\phi_{21}+\phi_a) - [\phi_{21}(W_1+W_2)+\phi_uW_2+\phi_aW_1]$$

$$\pm \left([\phi_{21}(W_1+W_2)+\phi_uW_2+\phi_aW_1]^2-4W_1W_2[\phi_{21}(\phi_e+\phi_u)+\phi_u\phi_a]\right)^{1/2} \ . \qquad (5.22)$$

But, the left side of (5.18) always satisfies

$$[(\phi_{21}+\phi_u)W_2+(\phi_{21}+\phi_a)W_1]^2 \geq 4W_1W_2(\phi_{21}+\phi_u)(\phi_{21}+\phi_a) \ . \qquad (5.19)$$

Furthermore, the inequality

$$4W_1W_2(\phi_{21}+\phi_u)(\phi_{21}+\phi_a) > 4W_1W_2[\phi_{21}\phi_e+\phi_{21}\phi_u+\phi_u\phi_a] \qquad (5.20)$$

holds if

$$\phi_{21} + \phi_a > \phi_e \ . \qquad (5.21)$$

By (5.12), and the fact that $\phi_{12} > 0$, (5.21) is true, and hence, combining (5.18)-(5.20), the eigenvalues $\sigma_1$ and $\sigma_2$ are shown to be distinct. That $\sigma_1$ and $\sigma_2$ are distinct can also be shown by using the application of Parter's theorem to compartmental systems derived in Section 2.3.3.

Also, it can be shown that the eigenvector slopes satisfy $m_1 > 0$ and $m_2 < 0$. The eigenvector slopes in (5.17) take on the signs of their denominators, or, equivalently, the signs of the expressions

$$2W_1(\phi_{21}+\phi_a) - [\phi_{21}(W_1+W_2)+\phi_uW_2+\phi_aW_1]$$

$$\pm \left([\phi_{21}(W_1+W_2)+\phi_uW_2+\phi_aW_1]^2-4W_1W_2[\phi_{21}(\phi_e+\phi_u)+\phi_u\phi_a]\right)^{1/2} \ . \qquad (5.22)$$

But, the magnitude of the square root term in (5.22) is greater than the magnitude of the remaining portion of (5.22). The proof of this again depends on (5.20), which is equivalent to

$$\left([\phi_{21}+\phi_a)W_1+(\phi_{21}+\phi_u)W_2]^2-4W_1W_2[\phi_{21}(\phi_e+\phi_u)+\phi_u\phi_a]\right)^{1/2}$$

$$> |(\phi_{21}+\phi_a)W_1-(\phi_{21}+\phi_u)W_2| \ . \qquad (5.23)$$

Hence, using $\sigma_1$ with the positive square root sign, $m_1 > 0$, and, similarly, $m_2 < 0$. The phase portrait for tracer system (5.13) is shown in Fig. 5.10.

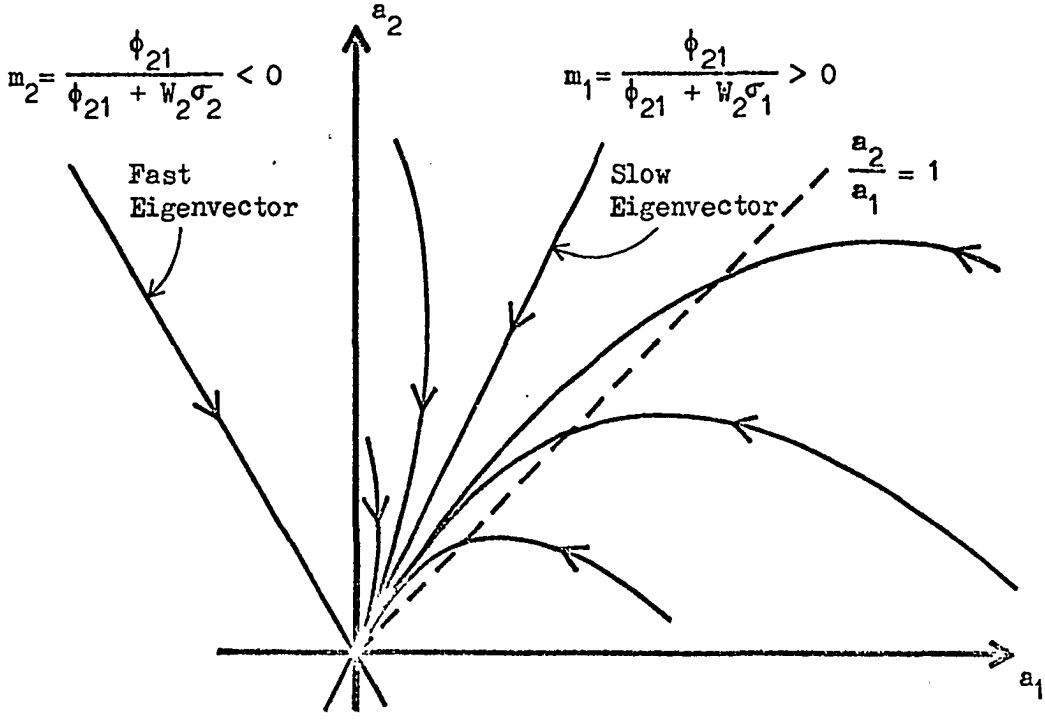


Fig. 5.10. Phase Portrait for Two-Compartment Tracer Kinetics.

The suitability of this model, however, depends on whether the slow eigenvector slope, $m_1$, the value which the ratio of $a_2(t)$ to $a_1(t)$ approaches for large time, can satisfy the inequality

$$\lim_{t\to\infty} \frac{a_2(t)}{a_1(t)} = m_1 = \frac{\phi_{21}}{\phi_{21} + \phi_a + W_2\sigma_1} < 1 , \tag{5.24}$$

for $\phi_a < \phi_e$. Inequality (5.24) is satisfied if

$$\phi_a + W_2\sigma_1 > 0 , \tag{5.25}$$

or, substituting for $\sigma_1$, if

$$\left([\phi_{21}(W_1+W_2)+\phi_u W_2+\phi_a W_1]^2-4W_1W_2[\phi_{21}(\phi_e+\phi_u)+\phi_u\phi_a]\right)^{1/2}$$

$$> \phi_{21}(W_1+W_2)+\phi_u W_2+\phi_a W_1-2\phi_a W_1 , \tag{5.26}$$

or if

$$4\phi_a W_1[\phi_{21}(W_1+W_2)+\phi_u W_2] > 4W_1W_2[\phi_{21}(\phi_e+\phi_u)+\phi_u\phi_a] . \tag{5.27}$$

Inequality (5.27) reduces, using (5.12), to the condition

$$\phi_a(W_1 + W_2) > (\phi_a + \phi_g)W_2 , \tag{5.28}$$

or

$$\phi_a W_1 > \phi_g W_2 , \tag{5.29}$$

or,

$$\phi_e > \phi_a > \frac{W_2}{W_1}\,\phi_g \,. \tag{5.30}$$

Thus, the two-compartment water model shown in Fig. 5.9 is consistent with the experimental results shown in Fig. 5.7, provided the absorbed water flux into the evaporative compartment, $\phi_a$, is greater than the external flux into the plasma compartment, $\phi_g$, times the ratio of evaporate compartment to plasma compartment water masses, $W_2/W_1$.

It is noteworthy that the above two-compartment model is inadequate when $\phi_a = 0$, that is, when there is no provision for water absorption from the air via the skin and lungs. This conclusion can be most easily seen from (5.29), which becomes an impossible inequality when $\phi_a = 0$. Hence, for $\phi_a = 0$, inequality (5.24) can never be satisfied. This result supports the importance of water influx from the air in the water regulation in the wild house mouse.

Nonideal tracer

If desired, the nonideal tracer behavior of THO mentioned above can also be included in the two-compartment model. The resultant tracer system is shown in Fig. 5.11. When two-compartment water system (5.11) is in steady state, the matrix, S, of the associated nonideal tracer system becomes

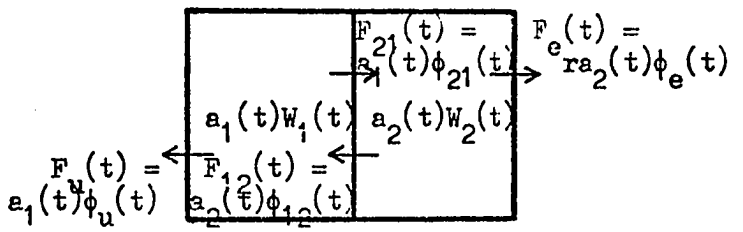


Nonideal Tracer System

Fig. 5.11. Nonideal Tracer System Associated with the Two-Compartment Water Model.

$$S = \begin{pmatrix} -\dfrac{(\phi_{21}+\phi_u)}{W_1} & \dfrac{\phi_{12}}{W_1} \\ \dfrac{\phi_{21}}{W_2} & -\dfrac{(\phi_{12}+r\phi_e)}{W_2} \end{pmatrix} . \tag{5.31}$$

Eigenvalues $\sigma_{1,2}$ and corresponding eigenvector slopes $m_{1,2}$ for the S matrix in (5.31) are given in (5.32) and (5.33) respectively.

$$\sigma_1, \sigma_2 = -\frac{[(\phi_{12}+r\phi_e)W_1+(\phi_{21}+\phi_u)W_2]}{2W_1W_2}$$

$$\pm \frac{1}{2W_1W_2}\Big([(\phi_{12}+r\phi_e)W_1+(\phi_{21}+\phi_u)W_2]^2$$

$$-4W_1W_2[\phi_u\phi_{12}+r\phi_e(\phi_{21}+\phi_u)]\Big)^{1/2} . \tag{5.32}$$

$$m_i = \frac{a_{2e}^i}{a_{1e}^i} = \frac{\phi_{21}}{\phi_{12} + r\phi_e + W_2\sigma_i} , \quad i = 1, 2 . \tag{5.33}$$

The specific activity of the evaporate efflux in this model is given by

$$\frac{F_e(t)}{\phi_e} = \frac{ra_2(t)\phi_e}{\phi_e} = ra_2(t) \ , \tag{5.34}$$

so that the ratio of evaporate to plasma specific activity no longer approaches the slow eigenvector slope for the system, but rather approaches

$$rm_1 = \frac{r\phi_{21}}{\phi_{12} + r\phi_e + W_2\sigma_1} \ . \tag{5.35}$$

It can be seen from (5.35) that it is not necessary, when assuming the above nonideal behavior of THO as a tracer in evaporation, that influx $\phi_a > 0$ in order to have $rm_1 < 1$.

Evaluation of steady state compartmental parameters

No experimental data were taken for the expressed purpose of evaluating the steady state parameters of the two-compartment water model in (5.11). The application, however, of the tracer analysis techniques developed in Chapter III to such a model can be illustrated. Note that when the parameter r denoting the nonideal tracer effect of THO is known, the tracer analysis of compartmental model (5.11) is essentially the same, whether the tracer is ideal (S matrix (5.14)) or not (S matrix (5.31)). For convenience, an ideal tracer is assumed.

The first task in evaluating the compartmental parameters of model (5.11) according to the method of Chapter III is to find the elements of matrix $S = (s_{ij})$ from specific

activity measurements. In particular, 2 × 2 constant matrix S can be calculated, say, from (3.40), where the columns of 2 × 2 matrix $A_a$ consist of two linearly independent specific activity vectors, $\bar{a}(t_1)$ and $\bar{a}(t_2)$, as in (3.37), and $A_{at}$ is given by (3.38). Tracer system (5.13) is homogeneous, and it is shown earlier in this section that the eigenvalues, $\sigma_1$ and $\sigma_2$, of matrix S are real and distinct. Therefore, the results of Section 3.2.3 and Appendix A guarantee that vectors $\bar{a}(t_1)$ and $\bar{a}(t_2)$, $t_1 \neq t_2$, from the same tracer transient response are linearly independent, provided both modes of the tracer system are excited.

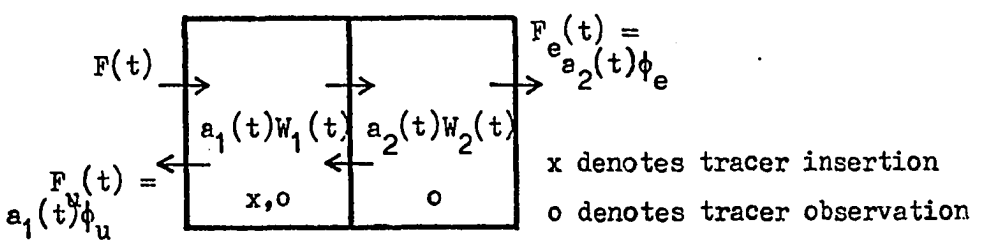


Fig. 5.12. Total Ideal Tracer System Used in Steady State Experiments.

The total tracer system used by Dr. Haines in the above steady state experiments is illustrated in Fig. 5.12. This system has the dynamical equations

$$\dot{\bar{a}} = S\bar{a} + X^{-1}PF$$
$$\bar{w} = I_2\bar{a} \quad . \tag{5.36}$$

In (5.36), S is given by (5.14),

$$X = \text{diag}(W_1, W_2) \ , \tag{5.37}$$

$$P = \begin{pmatrix} 1 \\ 0 \end{pmatrix} , \tag{5.38}$$

and scalar F is the influx of injected tracer. The intraperitoneal injection of tracer corresponds to insertion into compartment 1, denoted by the x in Fig. 5.12 and the value for P in (5.38). Both specific activities $a_1(t)$ and $a_2(t)$ can be observed directly, accounting for the o in each compartment in Fig. 5.12 and for the identity matrix, $I_2$, in (5.36). Specific activity $a_1(t)$ can be obtained either from the plasma or the urine; $a_2(t)$ is measured in the skin-lung evaporate. Hence, the experimental system satisfies the observation criterion of Chapter III. Moreover, the controllability matrix for (5.36) is, by (2.9),

$$U_1(S, P) = \begin{pmatrix} 1 & s_{11} \\ 0 & s_{21} \end{pmatrix} , \tag{5.39}$$

which, by (5.14), has rank 2. Therefore, system (5.36) is CC, and initial values, $a_1(0)$ and $a_2(0)$, can be chosen such that $\bar{a}(t_1)$ and $\bar{a}(t_2)$, $t_1 \neq t_2$, are linearly independent. In fact, it can be seen from the phase portrait of Fig. 5.10 that the initial condition

$$\bar{a}(0) = \begin{pmatrix} a_{10} \\ 0 \end{pmatrix} \tag{5.40}$$

generated by intraperitoneal injection always assures the linear independence of $\bar{a}(t_1)$ and $\bar{a}(t_2)$, $t_1 \neq t_2$, in the transient response.

The experimental data presented in Fig. 5.7 provide $\bar{a}(t_2)$ of the necessary pair of vectors. For example, choose the ad libitum case in Fig. 5.7a, and let $t_2$ = 3 days. Then, with the arbitrary units for specific activity shown,

$$\bar{a}(t_2) = \begin{pmatrix} 3 \\ 2.67 \end{pmatrix} . \tag{5.41}$$

Moreover,

$$\dot{\bar{a}}(t_2) \approx \sigma_1 \bar{a}(t_2)$$

$$\approx \begin{pmatrix} -0.75 \\ -0.667 \end{pmatrix} . \tag{5.42}$$

In practice, a vector $\bar{a}(t_1)$ linearly independent of $\bar{a}(t_2)$ in (5.41) must be obtained early in the tracer response. Unfortunately, however, no such measurements of plasma and evaporate specific activities are available for the experimental animal of Fig. 5.7a. Short-time specific activity data are given in Fig. 5.5, but plasma and evaporate measurements are not available for the same animal. If such data had been taken, then, with

$$A_a = \begin{pmatrix} a_1(t_1) & a_1(t_2) \\ a_2(t_1) & a_2(t_2) \end{pmatrix} , \tag{5.43}$$

and

$$A_{at} = \begin{pmatrix} \dot{a}_1(t_1) & \dot{a}_1(t_2) \\ \dot{a}_2(t_1) & \dot{a}_2(t_2) \end{pmatrix} , \tag{5.44}$$

tracer matrix $S = (s_{ij})$ is given, from (3.40), by

$$\begin{pmatrix} s_{11} & s_{12} \\ s_{21} & s_{22} \end{pmatrix} = \begin{pmatrix} \dot{a}_1(t_1) & \dot{a}_1(t_2) \\ \dot{a}_2(t_1) & \dot{a}_2(t_2) \end{pmatrix} \begin{pmatrix} a_1(t_1) & a_1(t_2) \\ a_2(t_1) & a_2(t_2) \end{pmatrix}^{-1} . \tag{5.45}$$

Once the elements of tracer matrix S are known, the parameters of compartmental system (5.11) can be evaluated. The equations in (3.44) provide the two relations,

$$s_{11}W_1 + s_{12}W_1 = -\phi_g , \tag{5.46}$$

and

$$s_{21}W_2 + s_{22}W_2 = -\phi_a . \tag{5.47}$$

Moreover, (3.50) yields

$$s_{11}W_1 + s_{21}W_2 = -\phi_u , \tag{5.48}$$

and

$$s_{12}W_1 + s_{22}W_2 = -\phi_e \ . \tag{5.49}$$

Finally, (3.51) implies

$$s_{12}W_1 = \phi_{12} \ , \tag{5.50}$$

and

$$s_{21}W_2 = \phi_{21} \ . \tag{5.51}$$

Equations (5.46)-(5.51) are six linear equations with the four known quantities, $s_{11}$, $s_{12}$, $s_{21}$, and $s_{22}$, and the eight unknowns, $W_1$, $W_2$, $\phi_g$, $\phi_a$, $\phi_u$, $\phi_e$, $\phi_{12}$, and $\phi_{21}$. These equations can be solved uniquely, provided two of the unknowns are measured. For example, two parameters which are readily accessible experimentally are water intake from food and drinking, $\phi_g$, and urinary-fecal water loss, $\phi_u$. Alternately, it is also possible to relate state variables $W_1$ and $W_2$ by

$$W_1 + W_2 = W_B \ . \tag{5.52}$$

Then, only $W_B$ and one unknown flux in the above 6 equations need be measured.

Quite by accident, Dr. Haines has recorded enough data during his steady state tracer washout experiments to provide at least rough estimates of the parameters of compartmental water model (5.11) for a "composite" mouse. That is, parameters can be estimated by combining data on different animals as follows: First, the slopes of the lines in Fig. 5.7 give

estimates of the slow eigenvalue, $\sigma_1$, of matrix S in (5.14). Also, the data in Fig. 5.5 can be used to estimate the fast eigenvalue, $\sigma_2$. The two-compartment model implies that, for initial condition $a_2(0) = 0$, the evaporate specific activity is of the form

$$a_2(t) = A_2\left(e^{\sigma_1 t} - e^{\sigma_2 t}\right) . \tag{5.53}$$

Hence, the relation

$$|\sigma_2| = \frac{\dot{a}_2(0)}{A_2} + |\sigma_1| \tag{5.54}$$

can be used with the indicated experimental data to estimate $\sigma_2$.

Other experimentally estimated model parameters include the slow eigenvector slope, $m_1$, which is the ratio of the evaporate to the plasma specific activity curves in Fig. 5.7. Also, the total amount of water in the experimental animal, $W_B = W_1 + W_2$, is estimated from the measured body mass multiplied by the experimentally determined fraction, .69, of body mass that is water. Finally, water fluxes $\phi_g$ and $\phi_u$ are known from Fig. 5.3. The measured and unknown quantities for the two-compartment, steady state water model are summarized in Table 5.1. The unknown parameters, however, are related to the measured quantities by the following set of equations:

Table 5.1: A Summary of Measured and Unknown Parameters for the Two-Compartment Water Model.

| Measured | Unknown |
|---|---|
| $\phi_g$ | $\phi_{21}$ |
| $\phi_u$ | $\phi_{12}$ |
| $W_B$ | $\phi_e$ |
| $\sigma_1$ | $\phi_a$ |
| $\sigma_2$ | $W_1$ |
| $m_1$ | $W_2$ |

$$\phi_{21} - \phi_{12} = \phi_g - \phi_u \tag{5.55}$$

$$\phi_e - \phi_a = \phi_g - \phi_u \tag{5.56}$$

$$W_B = W_1 + W_2 \tag{5.57}$$

$$W_1 W_2 \sigma_i^2 + [(\phi_{21}+\phi_a)W_1+(\phi_{21}+\phi_u)W_2]\sigma_i + \phi_{21}\phi_a+\phi_{21}\phi_g+\phi_u\phi_a = 0 , \quad i = 1, 2 \tag{5.58}$$

$$m_1 = \frac{\phi_{21}}{\phi_{21} + \phi_a + W_2\sigma_1} . \tag{5.59}$$

That is, given a set of values for the "measured" quantities in Table 5.1, the six relations in (5.55)-(5.59) can be used to solve for the set of "unknown" parameters in Table 5.1. Of course (5.16) could be used in place of (5.58).

As previously mentioned, the data available for evaluating the parameters of this two-compartment model are sketchy and come from a variety of experiments on different groups of animals. Consequently, an algorithm is not implemented to solve (5.55)-(5.59) for the unknowns given the measured quantities. Instead, the two-compartment tracer kinetics (5.13)-(5.14) are simulated on an analog computer. The initial conditions $a_1(0) = a_{10}$, $a_2(0) = 0$ simulate the experimental intraperitoneal THO injection initiating the tracer washout. Known fluxes for two steady state water conditions are first inserted. Then, keeping in mind relations (5.55)-(5.57), the unknown fluxes and water amounts are adjusted until the computer analogs for $a_1(t)$ and $a_2(t)$ satisfy the eigenvalues $\sigma_1$ and $\sigma_2$ and the slow eigenvector slope $m_1$. Because the data are inadequate--in fact, only an ad libitum value for $\sigma_2$ is available, and even that is very crude--the particular parameter values which "work" in this simulation should not be given much credence. The simulation, however, does verify that the above two-compartment system can be used to model tracer washout in the mouse at various steady state levels of water deprivation. Changes in the model parameters for different water states can account both for changes in the biological half-life of water[1] and in the ratio of evaporate to plasma specific activity.

[1]The biological half-life of water is the length of time for half the exchangeable water molecules in a steady state animal to be replaced from the environment.

Two steady state water conditions, ad libitum drinking water and 1/8 ad libitum drinking water, are simulated, and the values of the given parameters for each water state are shown in Table 5.2. Washout simulations for an ideal water tracer are given for these two water states in Fig. 5.13, and portions of these curves are replotted on semilog grids in Fig. 5.14. The associated derived fluxes and water amounts are shown in Table 5.3. The eigenvalues and slow eigenvector slopes from the simulations are also presented in Table 5.3 for comparison with those experimental values in Table 5.2. The $\sigma_2$ eigenvalues of the simulations were obtained by substituting the water fluxes and amounts into (5.16); the slow eigenvalues, $\sigma_1$, were estimated directly from the washout simulation curves.

Table 5.2. Measured Parameters for Ad Libitum and 1/8 Ad Libitum Drinking Water Conditions.

| | Ad Libitum | 1/8 Ad Libitum |
|---|---|---|
| $\phi_g$ (g/day) | 5.0 | 1.9 |
| $\phi_u$ (g/day) | 2.3 | 1.2 |
| $W_B$ (g) | 14.5 | 11.6 |
| $\sigma_1$ (·/day) | -0.3 | -0.2 |
| $\sigma_2$ (·/day) | -13 | -- |
| $m_1$ | 0.9 | 0.7 |

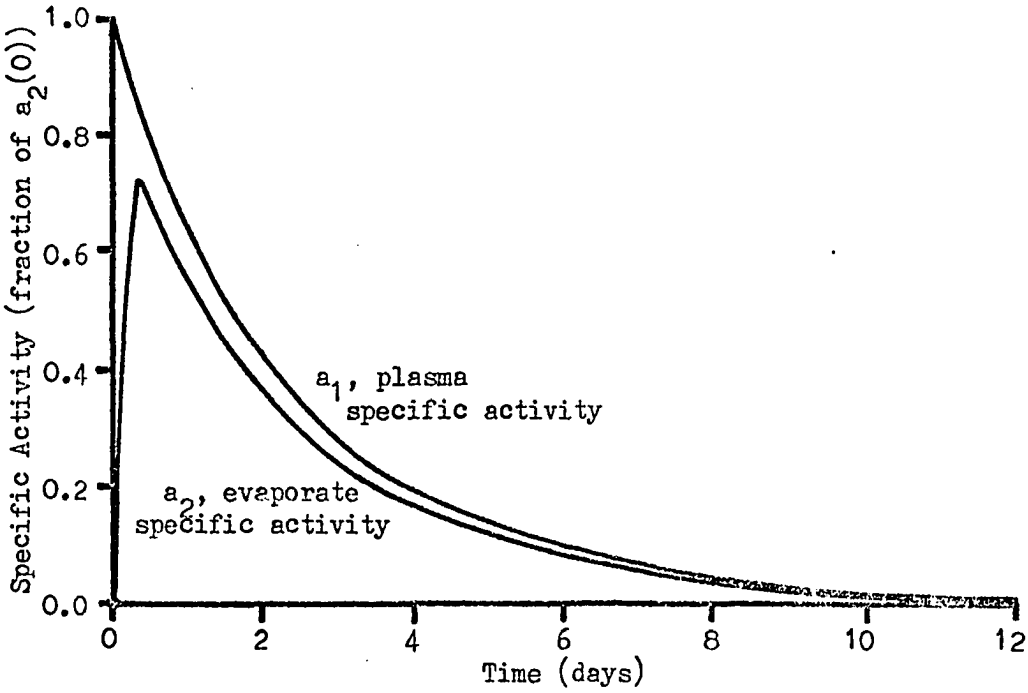


a. Ad Libitum

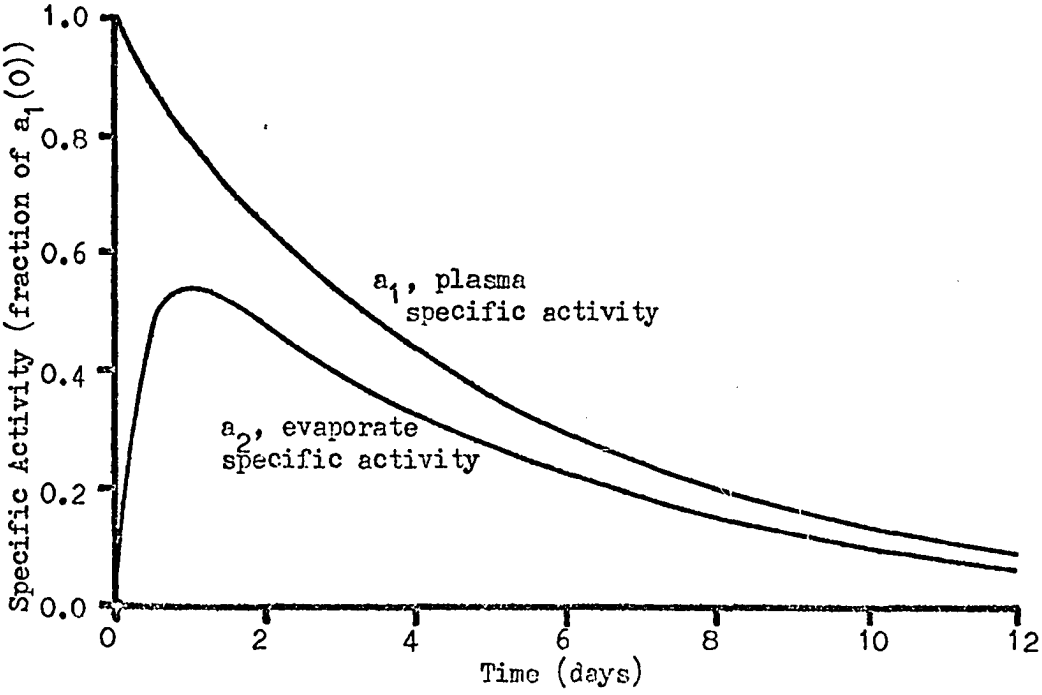


b. 1/8 Ad libitum

Fig. 5.13. Two-Compartment Analog Simulations of Steady State Tracer Experiments in the Wild House Mouse: a. Ad Libitum; b. 1/8 Ad Libitum.

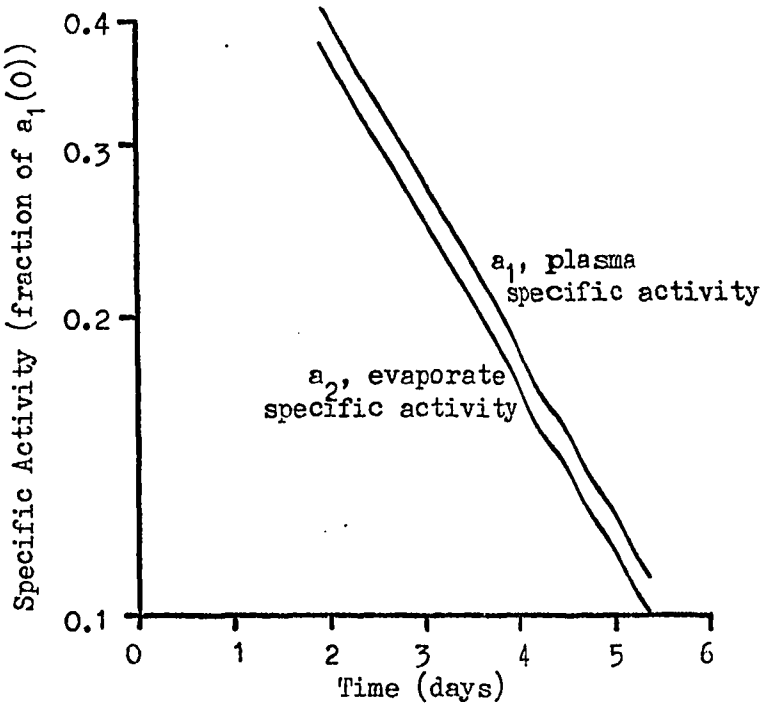


a. Ad Libitum

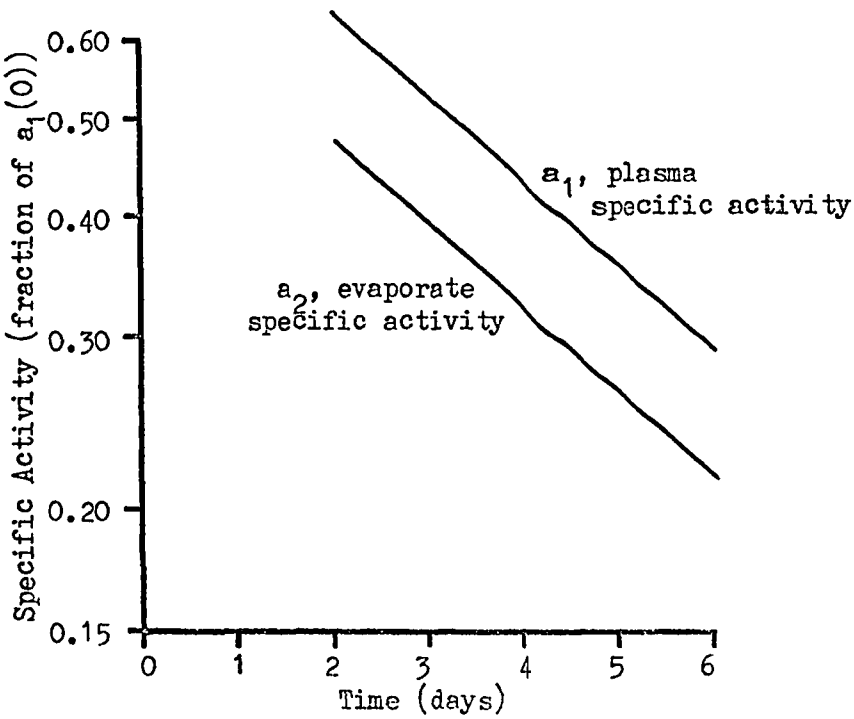


b. 1/8 Ad Libitum

Fig. 5.14. Portions of Analog Simulations Shown in Fig. 5.13 Replotted on Semilog Grids: a. Ad Libitum; b. 1/8 Ad Libitum.

Table 5.3. Parameters for Simulations of Ad Libitum and 1/8 Ad Libitum Drinking Water Conditions.

| | Ad Libitum | 1/8 Ad Libitum |
|---|---|---|
| $\phi_{21}$ (g/day) | 10.0 | 2.0 |
| $\phi_{12}$ (g/day) | 7.3 | 1.3 |
| $\phi_e$ (g/day) | 4.0 | 1.5 |
| $\phi_a$ (g/day) | 1.3 | 0.8 |
| $W_1$ (g) | 13.2 | 10.5 |
| $W_2$ (g) | 1.3 | 1.1 |
| $\sigma_1$ (·/day) | -0.35 | -0.19 |
| $\sigma_2$ (·/day) | -9.2 | -2.7 |
| $m_1$ | 0.91 | 0.73 |

In conclusion, Section 5.2 shows that a one-compartment, ideal tracer model is inadequate to explain all the steady state experimental data collected by Dr. Haines on water regulation in the wild house mouse. Certain properties of THO, the radioisotopic tracer for water used in these experiments, suggest that its nonideal behavior might account for the discrepancy between evaporate and plasma THO specific activity during steady state washout. The change in the ratio of these two specific activities with water deprivation implies, however, that the nonideal behavior of THO is not the only factor involved. A two-compartment model with an ideal tracer is then shown to be capable of explaining both the non-unity ratio of evaporate to plasma specific activities and the change of this ratio with water deprivation. This model is

also adequate when a nonideal tracer is used. The application of the tracer methods developed in Chapter III for obtaining compartmental parameters is illustrated with this model. Insufficient data are available to justify a refined analysis, but rough estimates of compartmental parameters are obtained by analog computer simulation.

Next, in Section 5.3, an analysis of the dynamical behavior of the water acclimation system of the wild house mouse is presented. Experimental data obtained by Dr. Haines on the dynamics of acclimation are shown in Section 5.3.1. Then, Section 5.3.2 develops a complete water acclimation model, based on the water exchange processes described in Chapter IV. Finally, in Section 5.3.3, the experimental data of Section 5.3.1 are applied to the analysis of the water model of Section 5.3.2.

## 5.3 Dynamical Behavior of Compartmental Bilinear System

There are limited data available on the dynamical process of water acclimation in the wild house mouse. It is shown in Section 5.3.1 that these data are applicable only to a one-compartment water model. Therefore, in Section 5.3.2, a one-compartment model is synthesized from the water exchange mechanisms developed in Section 4.2.2 of Chapter IV. For simplicity and consistency, this water model is approximated by a bilinear control model. Section 5.3.3 attempts to derive the dynamical variations of the control variables of this bilinear water model from the experimental data presented

in Section 5.3.1. It is shown that very little can be said about control behavior given only the time course of state $W_1(t) = W_B(t)$. A one-compartment tracer analysis provides more information, but, because of the large number of control variables, does not permit a complete analysis. The section concludes by showing that tracer data for two, and especially three, compartment models would be more useful in identifying the dynamics of control behavior during water acclimation.

### 5.3.1 Experimental Data on Acclimation Dynamics

The dynamics of water regulation in the mouse were observed during the process of acclimation from one level of drinking water to another. In a typical experiment, a mouse was kept at the same drinking water level, say ad libitum, for several days. Then, the animal was injected intraperitioneally with THO tracer, and daily recordings were taken of body mass and tracer specific activity. As discussed earlier, THO specific activity within the animal was estimated daily by counting the activity of a water sample obtained by passing dry air through a chamber containing the animal. Water collected in this way was mostly insensible evaporation from the animal, but would also include urinary or fecal water if present in the chamber. When these records of body mass and specific activity assured that the animal was indeed in steady state, the drinking water supply was suddenly changed to another constant level, say 1/2 ad libitum. The time course of body mass and tracer activity as the animal acclimated to this

new water supply was then observed until the animal attained a new steady state.

Raw data from Dr. Haines describing the time courses of body mass and tracer specific activity during a typical experiment are graphed, respectively, in Figs. 5.15 and 5.16 (from [5.1]). This particular animal was started in a 1/2 ad libitum condition, was then subjected to 1/4 ad libitum for about 26 days, and then finally switched to ad libitum drinking water. As can be seen in Fig. 5.15, the reduction in drinking water at 5 days caused an initial drop in body mass lasting about 10 days, but, as the animal acclimated, the body mass rose again to its original range. Also, the increase to ad libitum drinking water on the 31st day resulted in a gain in body mass, reaching a peak in about 9 days, and then a decrease in body mass again. Fig. 5.15 also describes the variation of body water, $W_B$, during acclimation, since it is assumed that $W_B$ equals .69 of body mass. Because of the long duration of the experiment relative to the biological half life of water, THO boosters had to be injected at intervals during the experiment. These repeated injections account for the sawtooth appearance of the graph of tracer specific activity in Fig. 5.16. The specific activity data of Fig. 5.16 are adjusted in Fig. 5.17 to compensate for the repeated injections. To obtain Fig. 5.17, each group of data points between booster injections in Fig. 5.16 was replotted on a semi-log grid. Then, the magnitude of each succeeding group of

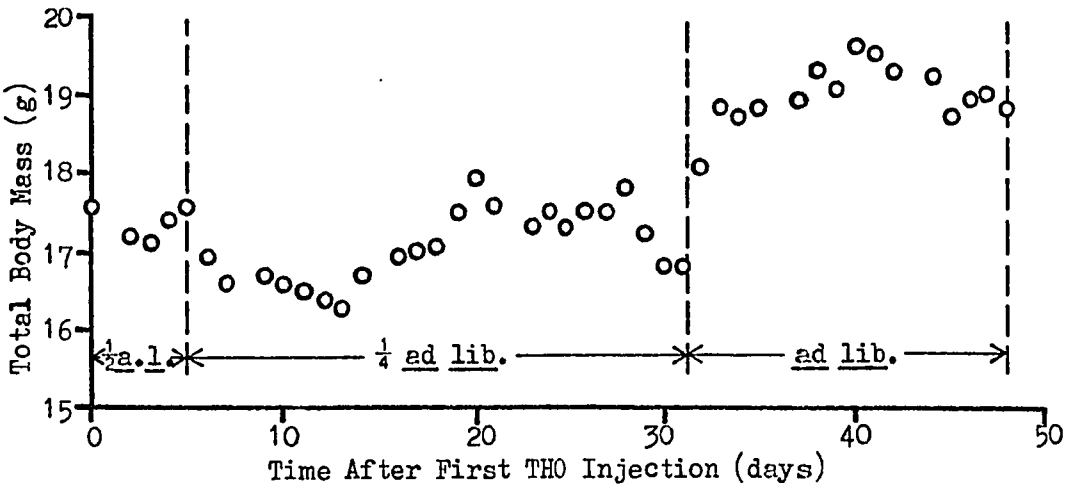


Fig. 5.15. Body Mass Versus Time During Water Acclimation Experiment in the Wild House Mouse.

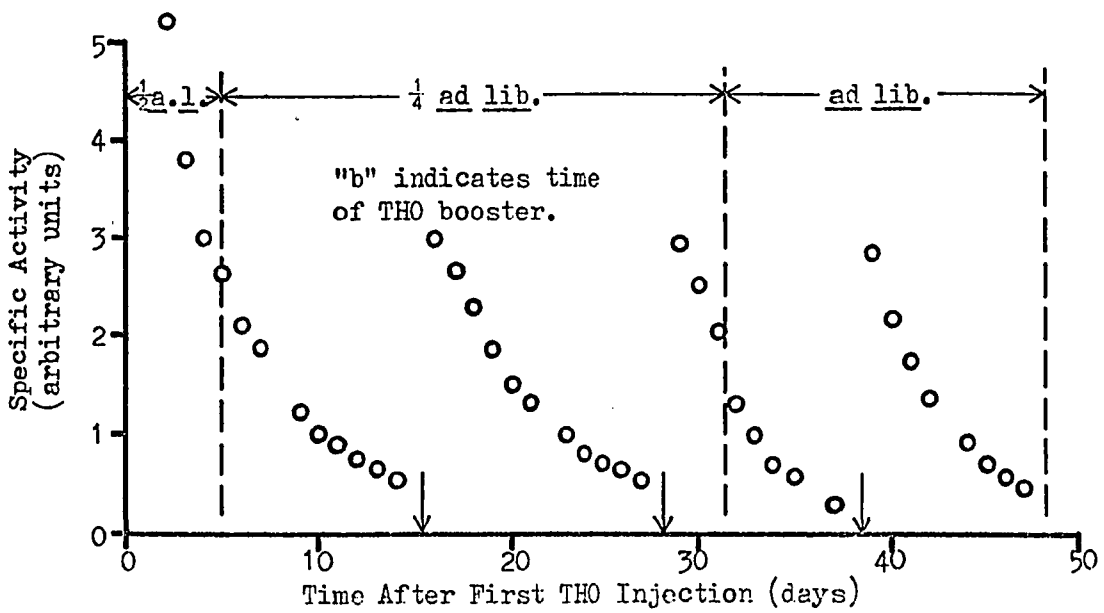


Fig. 5.16. Specific Activity During Water Acclimation Experiment in the Wild House Mouse.

points was adjusted so that the forward linear extrapolation of the end pair of data points before each THO injection agreed, at the injection time, with the backward linear extrapolation of the pair of data points immediately following the injection. It is much easier to see the long-term variation in slope on this adjusted graph. Observe that the slope in Fig. 5.17 generally becomes more negative as the animal's drinking water supply increases and that there are fluctuations in slope during each time interval of constant water supply.

It is hoped to learn something about the behavior of the water regulatory system from the data presented in Figs. 5.15-5.17. Unfortunately, with just a single specific activity observed, these data can be applied only to a one-compartment model. With this restriction in mind, the water exchange mechanisms derived in Chapter IV are combined into a one-compartment water model for the mouse in the next section.

### 5.3.2 Synthesis of Control Model

Recall from (5.1)-(5.3) that the one-compartment water model for the experimental wild house mouse, shown in Fig. 5.6, satisfies conservation equation

$$\dot{W}_1 = \phi_{1a}(t) - \phi_{al}(t)$$

$$= \phi_g(t) + \phi_{as}(t) + \phi_{a\ell}(t) - \phi_u(t) - \phi_{es}(t) - \phi_{e\ell}(t) , \tag{5.60}$$

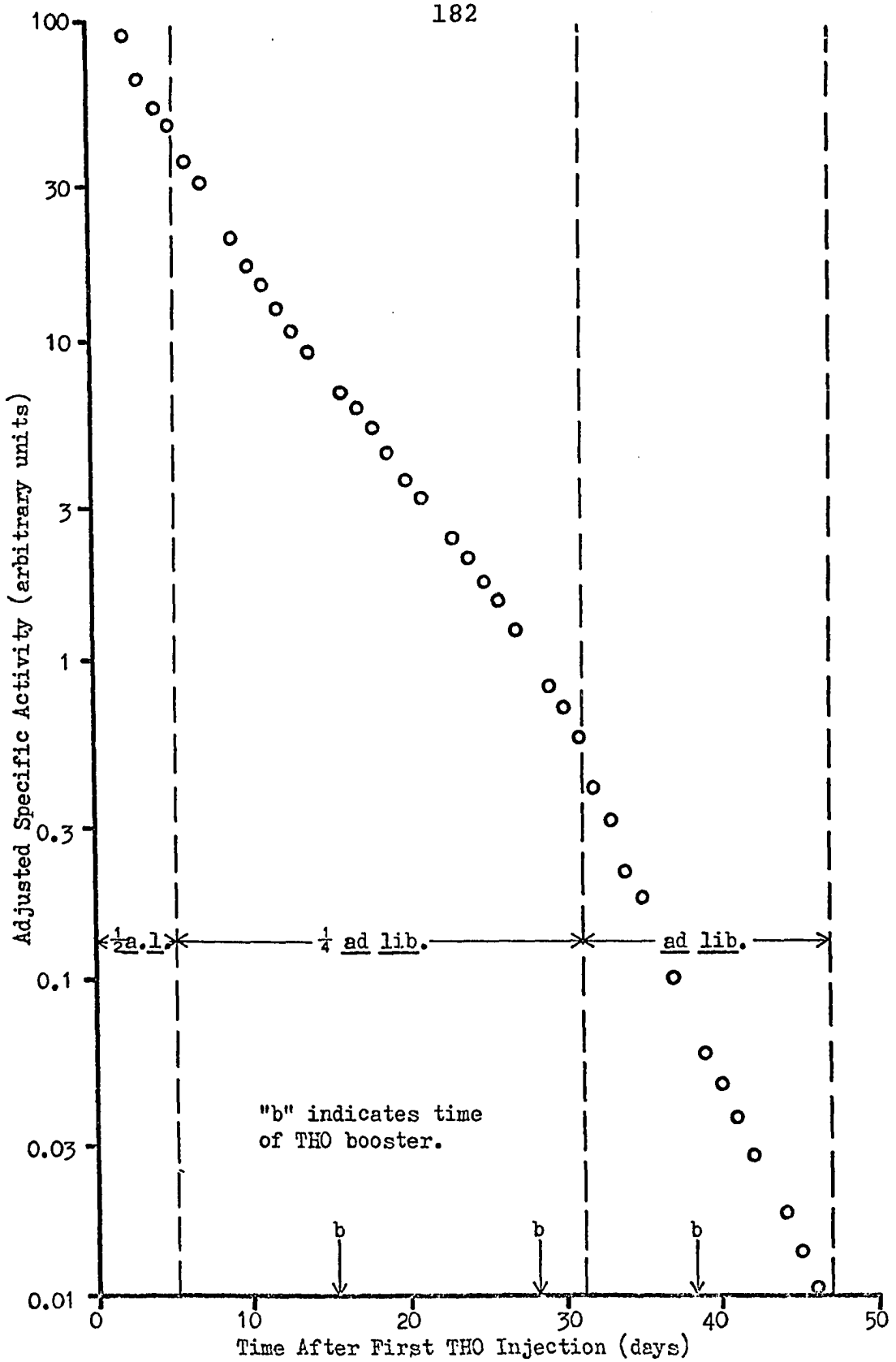


Fig. 5.17. Adjusted Specific Activity During Water Acclimation Experiment in the Wild House Mouse.

where $W_1(t) = W_B(t)$. Also recall from Section 4.2.2 of Chapter IV that the fluxes of (5.60) are as follows:

$$\phi_u(t) = \rho_g(t) f_k(t) (k_{k1} + k_{k2} W_1(t)) (1 - k_{k3} \rho_{ADH}(t) \pi_k(t)) \quad (5.61)$$

$$\phi_{as} = k_{s1} r p_{sa} \quad (5.62)$$

$$\phi_{es}(t) = k_{s1} \left( k_{s8} - \frac{k_{s9}}{\left( \frac{1}{W_1(t)} + k_{s7} \right) f_s(t)} \right) \quad (5.63)$$

$$\phi_{a\ell}(t) = r w_{sa} \dot{V}(t) \quad (5.64)$$

$$\phi_{e\ell}(t) = \dot{V}(t) \left[ c_{\ell 1} + c_{\ell 2} \beta_\ell(t) \left( T_c - \frac{k_{\ell 1}}{\left( \frac{1}{W_1(t)} + k_{\ell 2} \right) f_\ell(t)} \right) \right] . \quad (5.65)$$

For simplicity, skin model (4.24) neglecting diffusion effects is assumed in (5.63). In (5.60), water influx $\phi_g(t)$ depends partly on the animal's food intake and partly on drinking water intake, the latter being under the experimenter's control. Urinary flux, $\phi_u(t)$, is varied by control variables $\rho_g(t)$ and $f_k(t)$, which determine how much water enters the kidney from the blood, and variables $\rho_{ADH}(t)$ and $\pi_k(t)$, which regulate the fraction of water reabsorbed before leaving the kidney. Water absorption through the skin depends only on relative humidity r and air temperature through pressure term $p_{sa}$. Evaporative loss through the skin, however, can be controlled by variable $f_s(t)$, which indicates the

blood supply to the skin. Similarly, the blood supply to the respiratory surfaces, denoted by $f_\ell(t)$, affects evaporative water loss in the lungs. Other control variables affecting respiratory water loss are ventilation rate, $\dot{V}(t)$, and $\beta_\ell(t)$, a factor representing air passage geometry. Ventilation rate also influences water absorption via the lungs.

In summary, (5.60) describes a complex nonlinear first-order control system with eight control variables. If skin model (4.33) is used, there are the two additional control variables, $\gamma_d(t)$ and $\rho_s(t)$. Before continuing, system (5.60) is approximated by a bilinear model. By a suitable combination of control variables, urinary water loss is seen to have a bilinear form. Water loss by evaporation is more complex, and the suitability of a bilinear model for this process is less clear. A bilinear model, however, is the simplest form which can incorporate the "multiplicative" control modes of compartmental systems, in which substance fluxes depend on products of substance amounts and control variables. With this justification, the two evaporative loss terms in (5.60) of the form

$$f(x, u) = \frac{1}{\left(\frac{1}{x} + a\right)u} \tag{5.66}$$

are replaced by bilinear approximations derived from a two-dimensional Taylor series expansion in x and u about $x_o$ and $u_o$. That is,

$$f(x, u) \approx a_o x + b_o xu + c_o u + g_o \ , \tag{5.67}$$

where

$$a_o = \frac{2u_o}{x_o^2} f^2(x_o, u_o)$$

$$b_o = -\frac{1}{x_o^2} f^2(x_o, u_o) \tag{5.68}$$

$$c_o = -af^2(x_o, u_o)$$

$$g_o = 2ax_o f(x_o, u_o) \ .$$

Define the new control variables,

$$u_1(t) = k_{k2}\rho_g(t) f_k(t) \ , \tag{5.69}$$

$$u_2(t) = k_{k2}k_{k3}\rho_g(t) f_k(t) \rho_{ADH}(t) \pi_k(t) \ , \tag{5.70}$$

$$u_3(t) = f_s(t) \ , \tag{5.71}$$

$$u_4(t) = \dot{V}(t) \ , \tag{5.72}$$

$$u_5(t) = c_{\ell 2}k_{\ell 1}\dot{V}(t)\beta_\ell(t) \ , \tag{5.73}$$

and

$$u_6(t) = c_{\ell 2}k_{\ell 1}\dot{V}(t)\beta_\ell(t) f_\ell(t) \ . \tag{5.74}$$

Then, with bilinear approximations of form (5.67) in evaporate fluxes (5.63) and (5.65), fluxes (5.61)-(5.65) become

$$\phi_u(t) = b_{k21,11}W_1(t)u_1(t) + b_{k21,12}W_1(t)u_2(t) + c_{k21,1}u_1(t) + c_{k21,2}u_2(t) , \tag{5.75}$$

$$\phi_{as} = g_{s12} , \tag{5.76}$$

$$\phi_{es}(t) = a_{s21,1}W_1(t) + b_{s21,13}W_1(t)u_3(t) + c_{s21,3}u_3(t) + g_{s21} , \tag{5.77}$$

$$\phi_{a\ell}(t) = c_{\ell 12,4}u_4(t) , \tag{5.78}$$

and

$$\phi_{e\ell}(t) = b_{\ell 21,15}W_1(t)u_5(t) + b_{\ell 21,16}W_1(t)u_6(t) + c_{\ell 21,4}u_4(t) + c_{\ell 21,5}u_5(t) + c_{\ell 21,6}u_6(t) , \tag{5.79}$$

where the coefficients in (5.75)-(5.79) are known functions of the coefficients in (5.61)-(5.65). System (5.60), with fluxes (5.75)-(5.79), becomes a first-order bilinear system with six control variables.

### 5.3.3 Analysis of Dynamical Behavior

An important goal in studying water acclimation in the wild house mouse is to ascertain what physiological changes

take place to allow an animal to survive changes in its water supply. Light can be shed on this question by determining the dynamical behavior of the state and control variables of model (5.60) during acclimation. With a one-compartment water model, it is possible to measure the state, $W_1$, directly by weighing the animal. Fig. 5.15 contains such a record. There are, however, m = 6 unknown control variables, and little can be learned about $\bar{u}$ from the single equation (5.60) in the six unknown control variables of fluxes (5.75)-(5.79).

Tracer analysis of the one-compartment model provides more information on $\bar{u}$. With direct tracer insertion, the tracer system associated with (5.60) becomes, from (3.2),

$$\begin{aligned} \dot{a}_1 &= s_{11}(t)a_1 + \frac{1}{W_1(t)} F \\ w_1 &= a_1 \ , \end{aligned} \tag{5.80}$$

where F is the inserted tracer flux. By (3.16), system (5.80) is certainly CC-CO, and a linearly independent set of solutions reduces to the single scalar $a_1(t)$. Hence, the method developed in Section 3.2.3 for deriving tracer matrix S(t) becomes

$$s_{11}(t) = \frac{\dot{a}_1(t)}{a_1(t)} \ . \tag{5.81}$$

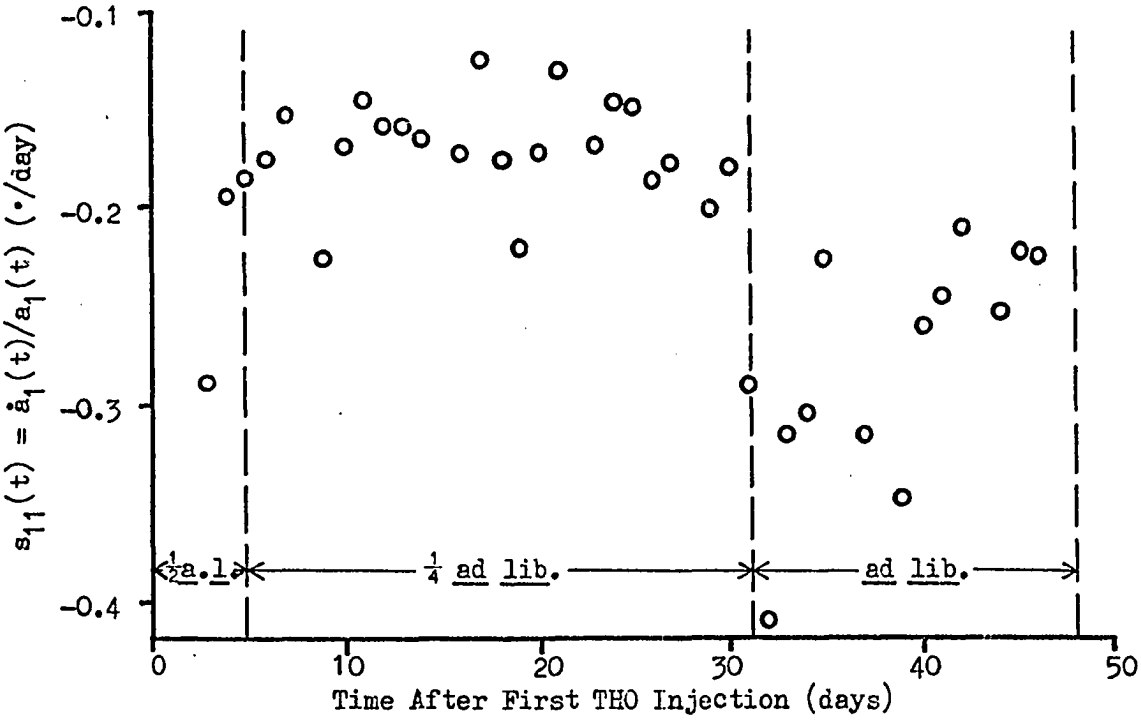


Fig. 5.18. Function $s_{11}(t)$ Versus Time During Water Acclimation Experiment in the Wild House Mouse.

A graph of $s_{11}(t)$ based on the specific activity data of Fig. 5.17 is presented in Fig. 5.18. In deriving $s_{11}(t)$, the derivative of $a_1(t)$ at each point was estimated as the slope of the line between the points on either side. It is not possible to measure total water influx $\phi_{1a}(t)$ or total efflux $\phi_{a1}(t)$ for the mouse directly, as only net evaporative fluxes can be detected. With tracer-derived function $s_{11}(t)$, however, $\phi_{1a}(t)$ and $\phi_{a1}(t)$ can be obtained, respectively, by (3.44) and (3.45). That is,

$$\phi_{1a}(t) = -W_1(t)s_{11}(t) \ , \tag{5.82}$$

and

$$\phi_{al}(t) = -\dot{W}_1(t) - W_1(t)s_{11}(t) \quad . \tag{5.83}$$

The derivative $\dot{W}_1(t)$, estimated as was $\dot{a}_1(t)$ above, is shown in Fig. 5.19. Using (5.82) and (5.83), the data in Figs. 5.16, 5.18, and 5.19 are combined to yield the graphs of $\phi_{1a}(t)$ and $\phi_{al}(t)$ in Fig. 5.20. Fig. 5.20 shows that when available drinking water, and hence water influx, $\phi_{1a}(t)$, is changed, the experimental animal adjusts its total water efflux, $\phi_{al}(t)$, to compensate for the change. Hence, for example, on the 31st day, when ad libitum drinking water was restored, both $\phi_{1a}(t)$ in Fig. 5.20a and $\phi_{al}(t)$ in Fig. 5.20b show marked increases. The graph also suggests large fluctuations in these fluxes during the first week or so after the 31st day before they settle down to more constant values.

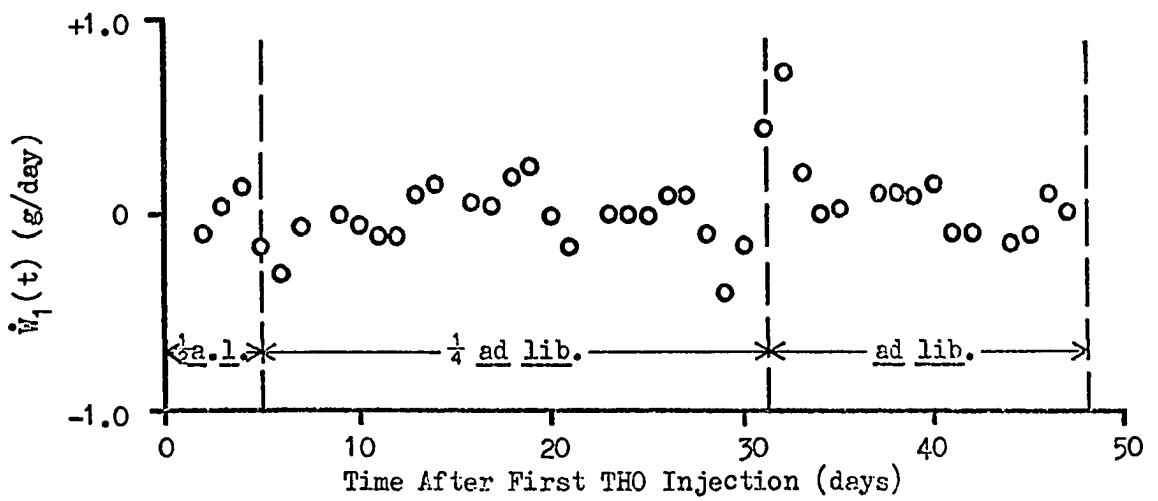


Fig. 5.19. Derivative, $\dot{W}_1(t)$, of Body Water Versus Time During Water Acclimation Experiment in the Wild House Mouse.

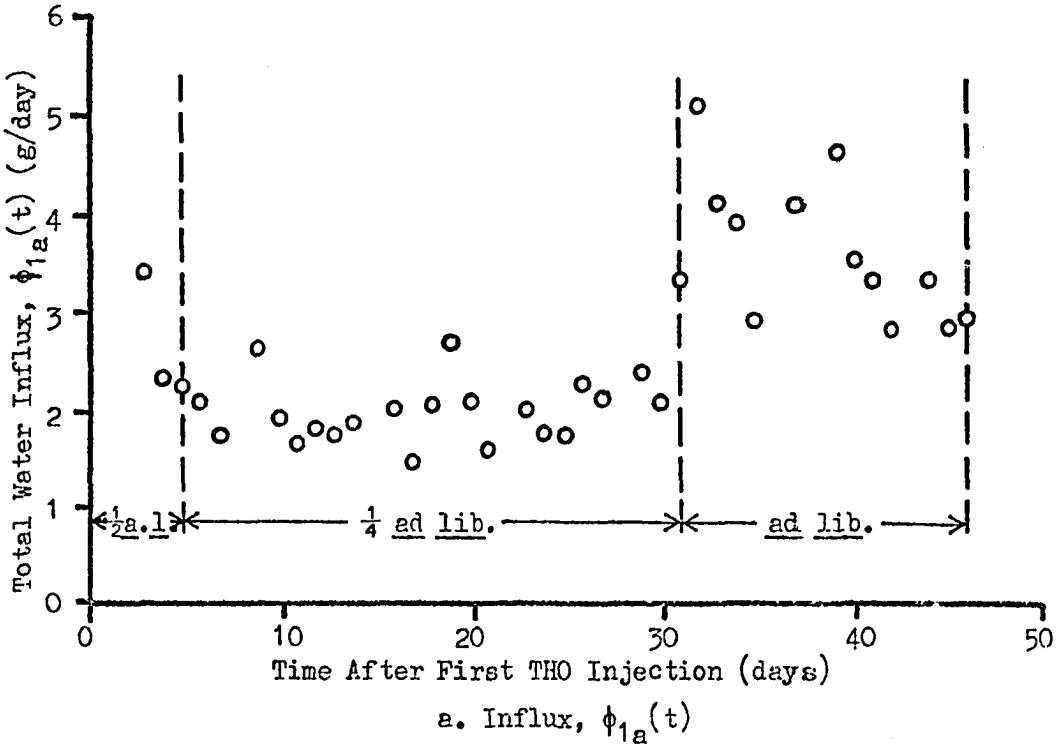


a. Influx, $\phi_{1a}(t)$

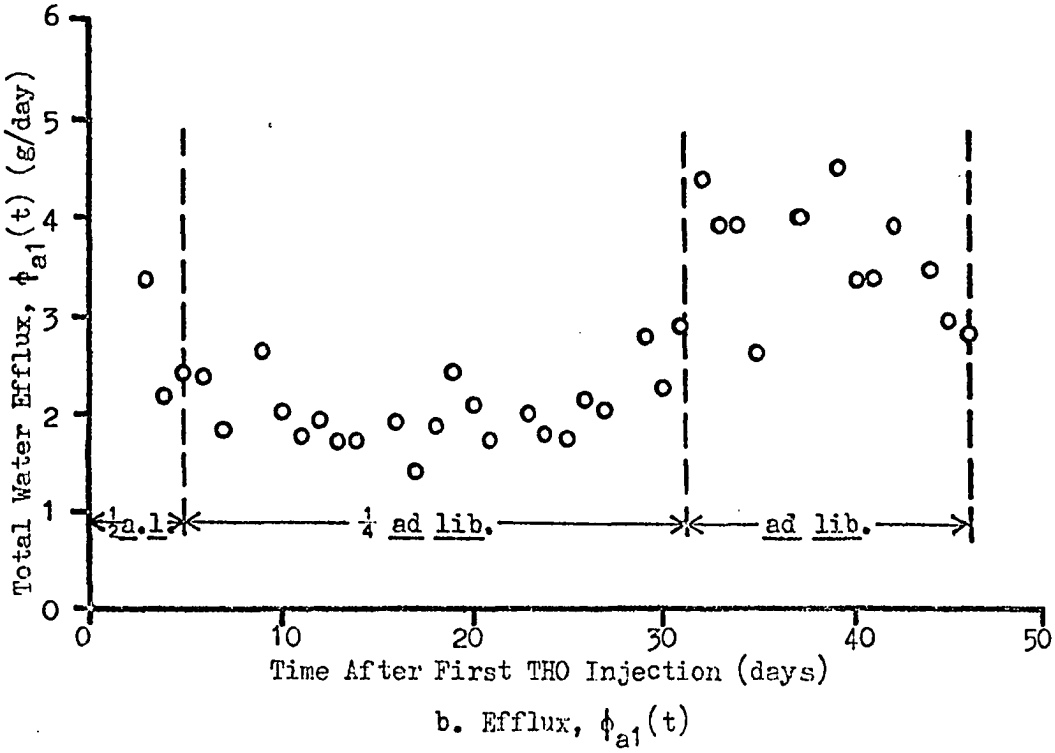


b. Efflux, $\phi_{a1}(t)$

Fig. 5.20. Total Water Fluxes Versus Time During Water Acclimation Experiment in the Wild House Mouse: a. Influx, $\phi_{1a}(t)$; b. Efflux, $\phi_{a1}(t)$.

A basic advantage of compartmental tracer analysis in studying physiological system behavior is illustrated above. That is, the net water exchange, given by the right side of (5.60) is now separated into total influx $\phi_{la}(t)$ and total efflux $\phi_{al}(t)$. Hence, rather than having to derive the behaviors of control variables $u_1, \cdots, u_6$ from the single equation (5.60), it is now possible to use the two equations

$$\phi_{la}(t) = \phi_g(t) + \phi_{as}(t) + \phi_{a\ell}(t) , \tag{5.84}$$

and

$$\phi_{al}(t) = \phi_u(t) + \phi_{es}(t) + \phi_{e\ell}(t) , \tag{5.85}$$

where the right-hand fluxes are again given by (5.75)-(5.79). In fact, it can be seen from (5.76) and (5.78) that the only control variable appearing in (5.84) is $u_4$, so that if $\phi_g(t)$ is known, the behavior of $u_4$ (lung ventilation rate) can be immediately obtained.

Because of the limited experimental data on water acclimation, it is not possible to proceed beyond the derivation of total influx $\phi_{la}(t)$ and total efflux $\phi_{al}(t)$ as shown in Fig. 5.20. Therefore, in the remainder of this section, more complete experiments are suggested, and the potential increase in information is described. First, the results of collecting more data on the one-compartment model are discussed. Then, the advantages of two- and three-compartment water

system models are demonstrated. Techniques for performing the proposed experimental measurements are either already available or could easily be implemented.

The usefulness of water influx $\phi_g(t)$ in studying control variable $u_4$ is mentioned above. Another easily measured flux is urinary-fecal flux, $\phi_u(t)$. Once this flux is measured for the one-compartment model, (5.75) provides information on control variables $u_1$ and $u_2$ (kidney control functions). Then, since $\phi_{al}(t)$ and $\phi_u(t)$ are both known, the sum of (5.77) and (5.79),

$$\phi_{es}(t) + \phi_{e\ell}(t) = \phi_{al}(t) - \phi_u(t) \ , \qquad (5.86)$$

can be used to study the three control variables, $u_3$, $u_5$, and $u_6$ (skin and lung variables). That is, the knowledge of $\phi_u(t)$, as well as $\phi_{la}(t)$ and $\phi_{al}(t)$, results in three equations in the six control variables, $u_1, \cdots, u_6$.

If two-compartment model (5.11) is applied to the mouse's water system, then the associated tracer system becomes (5.13) with S(t) matrix (5.14). Is there any advantage in using this second-order model to study water acclimation? In this case, it is necessary to measure both plasma and evaporate specific activities, $a_1(t)$ and $a_2(t)$, during the acclimation process. It is shown by (5.39) that this tracer system, with intraperitoneal (compartment 1) tracer injection, is CC if the compartmental system is in steady state. Definition (3.14) can similarly be used in (3.16) to show that the tracer system is

CC where the compartmental system is not in steady state. Therefore, the methods of Section 3.2.3 can be applied to finding the time-varying elements of S(t) from measurements on $a_1(t)$ and $a_2(t)$.

If, again, $\phi_g(t)$ and $\phi_u(t)$ are measured, time-varying versions of equations (5.46) and (5.47) can be combined with

$$\begin{pmatrix} \dot{W}_1 \\ \dot{W}_2 \end{pmatrix} = -S^*(t)\begin{pmatrix} W_1 \\ W_2 \end{pmatrix} - \begin{pmatrix} \phi_u(t) \\ \phi_e(t) \end{pmatrix} \tag{5.87}$$

to yield $W_1(t)$ and $W_2(t)$ and fluxes $(\phi_{as} + \phi_{a\ell}(t))$ and $(\phi_{es}(t) + \phi_{e\ell}(t))$. This model, then, results in the same three equations for studying control variables $u_1, \cdots, u_6$ as does the one-compartment model. As an added benefit, however, the time-varying equivalents of (5.50) and (5.51) provide intercompartmental fluxes $\phi_{12}(t)$ and $\phi_{21}(t)$. Hence, a two-compartment tracer analysis also gives information on the changes in water distribution and internal fluxes during water acclimation.

With a slight extension of the experimental apparatus and procedures developed by Dr. Haines, it is possible to extend the tracer analysis to the three-compartment water model shown in Fig. 5.21. This model is similar to the two-compartment model of Fig. 5.9 except that the compartment from which evaporation takes place is divided into a skin exchange compartment (2) and a lung exchange compartment (3).

It is assumed there is no direct exchange between the skin and lung water compartments. Specific activity data for the plasma compartment (1) are obtained in the same manner as for the two-compartment model. Skin and lung compartment specific activities are measured separately by collecting evaporate from only the body portion or only the head portion of the animal, respectively.

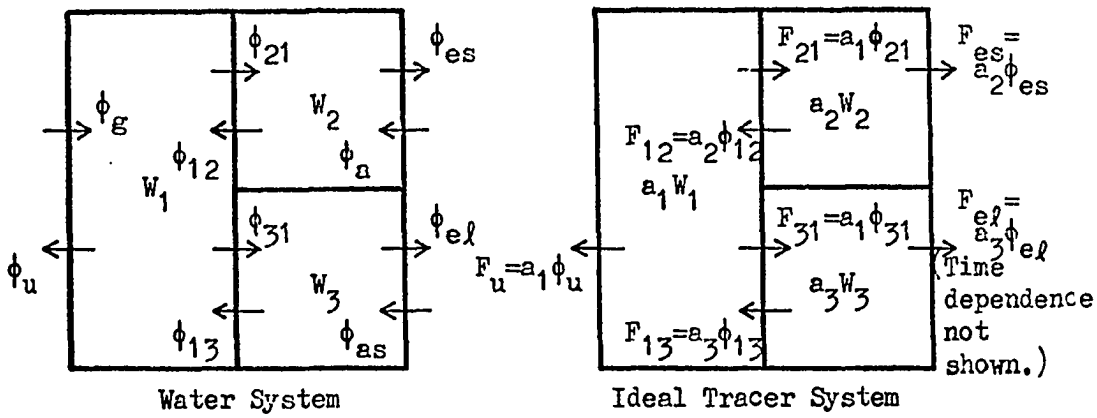


Fig. 5.21. A Three-Compartment Water Model and Associated Ideal Tracer System.

Water conservation for this three-compartment model is described by

$$\dot{W}_1 = -(\phi_{21}(t) + \phi_{31}(t)) + \phi_{12}(t) + \phi_{13}(t) - \phi_u(t) + \phi_g(t)$$

$$\dot{W}_2 = \phi_{21}(t) - \phi_{12}(t) - \phi_{es}(t) + \phi_{as} \qquad (5.88)$$

$$\dot{W}_3 = \phi_{31}(t) - \phi_{13}(t) - \phi_{el}(t) + \phi_{al}(t) \ .$$

The associated ideal tracer system has form (5.13), where $3 \times 3$ matrix $S(t)$ is

$$S(t) = \begin{pmatrix} -\frac{(\phi_{12}(t)+\phi_{13}(t)+\phi_g(t))}{W_1(t)} & \frac{\phi_{12}(t)}{W_1(t)} & \frac{\phi_{13}(t)}{W_1(t)} \\ \frac{\phi_{21}(t)}{W_2(t)} & -\frac{(\phi_{21}(t)+\phi_{as})}{W_2(t)} & 0 \\ \frac{\phi_{31}(t)}{W_3(t)} & 0 & -\frac{(\phi_{31}(t)+\phi_{a\ell}(t))}{W_3(t)} \end{pmatrix}, \tag{5.89}$$

and

$$\bar{a} = \begin{pmatrix} a_1 \\ a_2 \\ a_3 \end{pmatrix} . \tag{5.90}$$

As before, the elements of $S(t)$ in (5.89) can be derived by observing the specific activities in vector $\bar{a}(t)$. When tracer is again injected intraperitoneally (into compartment 1), the resultant experimental tracer system is shown, by evaluating (3.14), to be CC on any interval over which

$$\frac{(\phi_{13}(t)+\phi_{e\ell}(t))}{W_3(t)} + \frac{\dot{\phi}_{31}(t)}{\phi_{31}(t)} \neq \frac{(\phi_{12}(t)+\phi_{es}(t))}{W_2(t)} + \frac{\dot{\phi}_{21}(t)}{\phi_{21}(t)} . \tag{5.91}$$

When criterion (5.91) holds, the set of linearly independent vectors, $\{\bar{a}^1(0), \bar{a}^2(0), \bar{a}^3(0)\}$, can be obtained to start the three necessary tracer experiments for evaluating S(t) as discussed in Section 3.2.3. Once the elements of S(t) are obtained, (3.44) becomes

$$\begin{aligned}
(s_{11}(t) + s_{12}(t) + s_{13}(t))W_1(t) &= -\phi_g(t) \\
(s_{21}(t) + s_{22}(t) + s_{23}(t))W_2(t) &= -\phi_{as} \\
(s_{31}(t) + s_{32}(t) + s_{33}(t))W_3(t) &= -\phi_{a\ell}(t) \ ,
\end{aligned} \tag{5.92}$$

and (3.47) becomes

$$\dot{\bar{W}} = -S^*(t)\bar{W} - \begin{pmatrix} \phi_u(t) \\ \phi_{es}(t) \\ \phi_{e\ell}(t) \end{pmatrix} \ . \tag{5.93}$$

The six fluxes in (5.92) and (5.93) can be found if the net evaporative fluxes,

$$\phi_{esnet}(t) = \phi_{es}(t) - \phi_{as} \ , \tag{5.94}$$

and

$$\phi_{e\ell net}(t) = \phi_{e\ell}(t) - \phi_{a\ell}(t) \ , \tag{5.95}$$

are measured directly during the experiment. These net fluxes might be found, for example, by observing how much water must

be removed from chambers containing the animal's body and head to maintain constant temperature and humidity. To use (5.93), it is also necessary to have some boundary condition, $\bar{W}(t_*) = \bar{W}_*$. It is enough, for example, to know $\bar{W}(t_f)$, which may be estimated after the experiment by dissecting and weighing appropriate pieces of the animal before and after dehydration of the pieces. Then, (5.92)-(5.95) can be used to find fluxes $\phi_g(t)$, $\phi_{as}$, $\phi_{a\ell}(t)$, $\phi_u(t)$, $\phi_{es}(t)$, and $\phi_{e\ell}(t)$, given $\phi_g(t)$ or $\phi_u(t)$. Once these fluxes are known, equation (5.75) can be used to study $u_1$ and $u_2$, (5.77) to study $u_3$, (5.78) to study $u_4$, and (5.79) to study $u_5$ and $u_6$.

In order to evaluate the above control variables, it is necessary to know the values of the coefficients of (5.75)-(5.79) and hence of those of (5.61)-(5.65). At the present time, these are not known. The above analysis may help define some of these coefficients. For example, $k_{s1}$ in (5.62) is determined once influx $\phi_{as}$ and air temperature and relative humidity are known. Even if these coefficients are not known, however, the above analysis can at least provide qualitative information on the behaviors of the various control variables. None of the above water models results in enough equations to solve for all the control variables uniquely. If it is known physiologically, however, that some controls are fast-acting, short-term controls compared with others, then it may be possible to separate in time the effects of two or more control variables in the same equation.

## 5.4 Remarks

As with any application of theory to a practical problem, there is a gap between the theory available for the analysis of compartmental bilinear systems and the experimental data on hand and analytical needs in the above physiological research. Because of inadequate experimental data, the search for a suitable compartmental structure for the water acclimation system cannot be completed, and a one-compartment model must be assumed in the dynamic analysis. Also, the models for the various water exchange organs, based as they are on the incomplete physiological understanding of today, are necessarily open to question.

Even assuming a one-compartment structure and making gross simplifications in the water exchange models, the resultant control system plant associated with water acclimation is still quite complex. Recall that control mechanisms include neurally- and chemically-induced vasomotor activity in the circulatory systems of the kidney, skin, and breathing passages, variable breathing style and breathing passage geometry, and structural compacting of skin layers. Hormonally-induced changes in capillary wall and connective tissue permeabilities in the skin and glomerular and tubular permeabilities in the kidney provide additional control functions.

In retrospect, it can be seen that the complexity of this system is basically a consequence of the universal

presence and importance of water in living systems. Water is essential to or inextricably involved in so many bodily processes that its regulation involves multiple routes of exchange with the environment, multiple functions of the organs of exchange, and, therefore, multiple control mechanisms. In particular, in the wild house mouse, water exchange is involved in waste removal and osmotic and ionic loss via the kidnay, evaporative heat removal from the skin and lungs, and gaseous exchange in the lungs. Hence, water regulation is intimately related with, among other things, the major problems of osmotic and ionic balance, thermal balance, and carbon dioxide and oxygen regulation. This interrelatedness of control systems is reflected in the great number of control variables in the water regulatory model.

The complexity of the water regulatory system is further increased by the multifaceted and unique nature of water transport. Within the body, water not only diffuses, but also moves under the influence of hydrostatic and osmotic pressures. Water is not generally considered to be actively transported, but it does passively follow other actively moved chemical species. The most obviously complex water exchange, however, occurs at the liquid-vapor interface at the skin and lungs. Here, water transport involves a combination of diffusion, evaporation, and condensation, and, in contrast to internal transport mechanisms, temperature plays a critical role.

# CHAPTER VI

# SUMMARY, CONCLUSIONS, AND RECOMMENDATIONS

## 6.1 Summary and Conclusions

This dissertation illustrates the application of system theory in generating concepts and techniques for the study of physiological processes. Both homeostasis and compartmentation, with their inherent multiplicative modes of control, are identified as characteristic of living organisms, and are incorporated into the concept of compartmental bilinear control systems. Also, tracer techniques are recognized as a powerful tool in compartmental system analysis. A general open, nonconservative, nonsteady state compartmental structure is described mathematically, and the associated general tracer system is derived. This linear tracer system, which accounts for both direct and "natural" tracer insertion, is time-varying (time-invariant) when the compartmental system is in nonsteady (steady) state.

A procedure, based on tracer observations, is proposed for estimating the order of a bilinear model of a physiological control system with a compartmental structure. This procedure is, in fact, applicable to any control system which has a compartmental structure and in which tracers can be

used. The necessary tracer measurements can be made while the compartmental system under study is maintained in steady state, thus making the associated tracer system time-invariant. Different types of tracer experiments are formalized into corresponding linear dynamical systems. With these systems, conditions are derived on the compartmental structure and on the required tracer experiments under which tracer data can yield the order of the compartmental bilinear system. The proposed procedure applies to any compartmental structure. If, however, the state matrix of the associated tracer system has real, distinct eigenvalues, special tracer methods can be used to estimate system order. Existing criteria for compartmental structures which result in such tracer systems are generalized and developed.

A method, again using tracer measurements, is then presented for evaluating the state and control variables of a compartmental bilinear system, whether in steady state or not. In the process, the behaviors of the compartmental fluxes and nonconservative terms are also obtained. The method involves the identification of the elements of the state matrix of the associated tracer system. Several identification techniques are discussed, including the necessary tracer experiments and conditions on compartmental structure. The elements of the tracer matrix are then related to the compartmental parameters; these parameters include the state variables of the original bilinear system. Finally, it is shown that the

system control variables are linearly related to the compartmental parameters through postulated compartmental exchange and nonconservative mechanisms. Linear relations of this type hold in general for any compartmental control system linear in control.

The process of acclimation to water deprivation in the wild house mouse is investigated using the above concepts and techniques. Mathematical models, not available in the literature, are derived from physiological descriptions for water exchange processes between the mouse and its environment. Then, based on physiology and steady state tracer data, a second-order compartmental structure is developed. Models incorporating both ideal and nonideal tracer behavior are presented.

Tracer data on the dynamics of water acclimation are limited so that only a one-compartment water model can be studied. Even this one-compartment model is complex, reflecting the multiple functions of water in organisms and the complexities of water transport. Moreover, bilinear models seem more appropriate for describing internal water transport than evaporative exchange with its complex temperature dependence. Nevertheless, the analysis of water acclimation data illustrates the application of tracer data to finding compartmental parameters and the advantages of a compartmental bilinear approach in studying control behavior. Also, straightforward extensions of the present tracer experiments are proposed

which would substantially increase the information on water acclimation dynamics.

## 6.2 Recommendations for Future Work

With regard to the study of acclimation to water deprivation in the wild house mouse, it is recommended that the experiments proposed in Section 5.3.3 be performed. A more complete analysis of water acclimation would then be possible. It is also desirable to investigate experimentally the appropriateness of the water exchange models developed in Section 4.2.2 and their bilinear approximations in Section 5.3.2.

More generally, the usefulness of the concept of compartmental bilinear systems and the practicality of tracer analysis should be tested by applying them to physiological processes other than water regulation. The suitability of bilinear models of physiological transport processes should also be tested.

In the method for determining compartmental parameters from tracer measurements discussed in Section 3.2.3, only the elements of matrix S(t) of tracer system (3.2) are used. The additional use of matrix R(t) in (3.2) could be developed.

The method for identifying the elements of tracer matrix S(t) presented in Section 3.2.3 is recommended over the other identification schemes because of its simplicity. Very noisy data, however, are characteristic of physiological experiments. An important criterion, then, in an identification procedure for finding S(t) from tracer data is that the

procedure provide a good estimate of S(t) from noisy data. In fact, all of the techniques developed for the tracer analysis of compartmental bilinear systems should be extended to yield the best estimates of the desired quantities in the presence of noise and incomplete data.

More direct identification and modeling techniques for bilinear systems should also be explored and developed. These techniques should include means of estimating the number of state variables and of identifying the elements of the bilinear model from input-output data. Also, for physiological applications, it is desirable to be able to estimate the number of control variables and control variable behavior from output and/or state observations.

## LIST OF REFERENCES


1.1 Mohler, R. R., and Shen, C. N. Optimal Control of Nuclear Reactors. New York: Academic Press, 1970.

1.2 Mohler, R. R. "Natural Bilinear Systems," IEEE Trans. on Sys. Sci. and Cyber., SSC VI (1970), 192-197.

1.3 Smith, Warren D., and Mohler, R. R. "Foundations of Bilinear Compartmented Physiological Systems," 1970 SWIEEECO Record of Technical Papers (1970), 157-160.

1.4 Rink, Ray, and Mohler, R. R. "Completely Controllable Bilinear Systems," SIAM J. Control, VI (1968), 477-486.

1.5 Mohler, R. R., and Rink, Ray. "Control with a Multiplicative Mode," J. Basic Engr., XCI (1969), 201-206.

1.6 Mohler, R. R., and Moon, Sang F. "Computation of Optimal Trajectories for a Class of Nonlinear Control Processes," Proc. 1970 IFAC Symposium on Computer Control (1970).

1.7 Bruni, DiPillo, and Koch. "On the Mathematical Models of Bilinear Systems," Ricerche di Automatica (forthcoming).

1.8 Milsum, J. H. Biological Control Systems Analysis. New York: McGraw-Hill Book Co., 1966.

1.9 Alvi, Z. M. "Predictive Aspects of Monitored Medical Data." Ph.D. dissertation, Department of Engineering, University of California, Los Angeles, 1968.

1.10 Snyder, W. S.; Fish, B. R.; Bernard, S. R.; Ford, M. R.; and Muir, J. R. "Urinary Excretion of Tritium following Exposure of Man to HTO - a Two Exponential Model," Phys. Med. Biol., XIII (1968), 547-559.

1.11 Langer, G. A., and Brady, A. J. "The Effects of Temperature upon Contraction and Ionic Exchange in Rabbit Ventricular Myocardium," J. Gen. Physiol., LII (1968), 682-713.

1.12 Hart, H. E. "Analysis of Tracer Experiments: VII General Multi-Compartmented Systems Imbedded in Non-Homogeneous Inaccessible Media," Bull. Math. Biophys., XXVIII (1966), 261-282.

1.13 Wise, M. E.; Osborn, S. B.; Anderson, J.; and Tomlinson, R. W. S. "A Stochastic Model for Turnover of Radiocalcium Based on the Observed Power Laws," Math. Biosci., II (1968), 199-224.

1.14 DiStefano, J. J., III. "A New Model of the Thyroid Hormone Regulator and a Proposal for its Experimental Validation." Ph.D. dissertation, Department of Engineering, University of California, Los Angeles, 1966.

1.15 Fried, J. "Compartmental Analysis of Kinetic Processes in Multicellular Systems: A Necessary Condition," Phys. Med. Biol., XIII (1968), 31-43.

1.16 Sheppard, C. W., and Householder, A. S. "The Mathematical Basis of the Interpretation of Tracer Experiments in Closed Steady-State Systems," J. Appl. Phys., XXII (1951), 510-520.

1.17 Hill, T. L., and Kedem, O. "Studies in Irreversible Thermodynamics, III. Models for Steady State and Active Transport Across Membranes," J. Theoret. Biol., X (1966), 399-441.

1.18 Iberall, A. S. "Human Body as an Inconstant Heat Source and Its Relation to Determination of Clothes Insulation, I. Descriptive Models of the Heat Source," J. Basic Engr., LXXXII (1960), 82.

1.19 Grodins, F. S. Control Theory and Biological Systems. New York: Columbia Press, 1963.

1.20 Robertson, James S. "Mathematical Treatment of Uptake and Release of Indicator Substances in Relation to Flow Analysis in Tissues and Organs," Handbook of Physiology, Sec. 2: Circulation, Vol. I (1962), 617-644.

1.21 Sheppard, C. W. Basic Principles of the Tracer Method. New York: John Wiley and Sons, Inc., 1962.

1.22 Solomon, A. K. "Compartmental Methods of Kinetic Analysis," Mineral Metabolism, Vol. I, Part A. Edited by C. L. Comar and F. Bronner. New York: Academic Press, 1960.

1.23 Sheppard, C. W. "The Theory of the Study of Transfers with a Multi-Compartment System Using Isotopic Tracers," J. Appl. Phys., XIX (1948), 70-76.

1.24 Berman, M., and Schoenfeld, R. "Invariants in Experimental Data on Linear Kinetics and the Formulation of Models," J. Appl. Phys., XXVII (1956), 1361-1370.

1.25 Hearon, J. Z. "Theorems on Linear Systems," Ann. N.Y. Acad. Sci., CVIII (1963), 36-68.

1.26 Hearon, J. Z. "The Washout Curve in Tracer Kinetics," Math. Biosci., III (1968), 31-39.

1.27 Berger, E. Y. "Intestinal Absorption and Excretion," Mineral Metabolism, Vol. I, Part A. Edited by C. L. Comar and F. Bronner. New York: Academic Press, 1960.

2.1 Chen, Chi-Tsong. Introduction to Linear System Theory. New York: Holt, Rinehart, and Winston, 1970.

2.2 Gantmacher, F. R. Applications of the Theory of Matrices. New York: Interscience Publishers, Inc., 1959.

2.3 Isidori, Alberto. "A Comparison Between the Algorithms for Computing the Order of Linear Systems," Proc. 1970 Kyoto IFAC (1970), 40-45.

2.4 Solomon, A. K. "Compartmental Methods of Kinetic Analysis," Mineral Metabolism, Vol. I, Part A. Edited by C. L. Comar and F. Bronner. New York: Academic Press, 1960.

2.5 Parsons, D. H. "Biological Problems Involving Sums of Exponential Functions of Time: A Mathematical Analysis That Reduces Experimental Time," Math. Biosci., II (1968), 123-128.

2.6 Gardner, Donald G. "Resolution of Multi-Component Exponential Decay Curves Using Fourier Transforms," Ann. N.Y. Acad. Sci., CVIII (1963), 195-203.

2.7 Lancaster, Peter. Theory of Matrices. New York: Academic Press, 1969.

2.8 Hearon, John Z. "Theorems on Linear Systems," Ann. N.Y. Acad. Sci., CVIII (1963), 36-68.

2.9 Goldberg, Karl. "A Matrix with Real Characteristic Roots," J. Res. Nat. Bur. Stand., LVI (1956), 87.

2.10 Stern, Thomas E. Theory of Nonlinear Networks and Systems, An Introduction. Reading, Mass.: Addison-Wesley, 1965.

2.11 Parter, S. "On the Eigenvalues and Eigenvectors of a Class of Matrices," J. SIAM, VIII (1960), 376-388.

2.12 Indritz, Jack. Methods in Analysis. New York: The Macmillan Co., 1963.

2.13 Sheppard, C. W., and Householder, A. S. "The Mathematical Basis of the Interpretation of Tracer Experiments in Closed Steady-State Systems," J. Appl. Phys., XXII (1951), 510-520.

3.1 Sheppard, C. W., and Householder, A. S. "The Mathematical Basis of the Interpretation of Tracer Experiments in Closed Steady-State Systems," J. Appl. Phys., XXII (1951), 510-520.

3.2 Berman, M., and Schoenfeld, R. "Invariants in Experimental Data on Linear Kinetics and the Formulation of Models," J. Appl. Phys., XXVII (1956), 1361-1370.

3.3 Robertson, James S. "Mathematical Treatment of Uptake and Release of Indicator Substances in Relation to Flow Analysis in Tissues and Organs," Handbook of Physiology, Sec. 2: Circulation, Vol. I (1962), 617-644.

3.4 Chen, Chi-Tsong. Introduction to Linear System Theory. New York: Holt, Rinehart, and Winston, 1970.

3.5 D'Angelo, Henry. Linear Time-Varying Systems: Analysis and Synthesis. Boston: Allyn and Bacon, 1970.

3.6 Balakrishnan, A. V., and Peterka, V. "Identification in Automatic Control Systems," Automatica, V (1969), 817-829.

3.7 Sage, Andrew P. Optimum Systems Control. Englewood Cliffs, N.J.: Prentice-Hall, Inc., 1968.

3.8 Lee, E. Stanley. Quasilinearization and Invariant Imbedding. New York: Academic Press, 1968.

3.9 Gantmacher, F. R. Applications of the Theory of Matrices. New York: Interscience Publishers, Inc., 1959.

3.10 Shields, Paul C. Linear Algebra. Reading, Mass.: Addison-Wesley Publishing Co., Inc., 1964.

4.1 Neely, W. A.; Turner, M. D.; and Taylor, A. E. "Bidirectional Movement of Water through the Skin of a Non-sweating Animal," J. Surg. Res., VII (1967), 323-328.

4.2 Personal communication with Dr. Howard Haines, Department of Zoology, University of Oklahoma, 1970.

4.3 Ruch, T. C., and Patton, H. D. Physiology and Biophysics, 19th edition. Philadelphia: Saunders, W. B., 1965.

4.4 Chew, Robert M. "Water Metabolism of Mammals," Physiological Mammalogy, Vol. II. Edited by William V. Mayer and Richard G. Van Gelder. New York: Academic Press, 1965.

4.5 Fertig, Daniel S., and Edmonds, Vaughan. "The Physiology of the House Mouse," Sci. Am., CCXXI, No. 4 (Oct., 1969), 103-110.

4.6 Folk, G. Edgar, Jr. Introduction to Environmental Physiology. Philadelphia: Lee and Febiger, 1966.

4.7 Muntwyler, Edward. Water and Electrolyte Metabolism and Acid-Base Balance. St. Louis: The C. V. Mosby Co., 1968.

4.8 Hyman, Libbie Henrietta. Comparative Vertebrate Anatomy. Chicago: University of Chicago Press, 1956.

4.9 Romer, Alfred Sherwood. The Vertebrate Body. Philadelphia: W. B. Saunders Co., 1956.

4.10 Goodman, A. B., and Wolf., A. V. "Insensible Water Loss from Human Skin as a Function of Ambient Vapor Concentration," J. Appl. Physiol., XXVI (1969), 203-207.

4.11 Shortley, George, and Williams, Dudley. Elements of Physics. Englewood Cliffs, N.J.: Prentice-Hall, Inc., 1953.

4.12 Hardy, James D. "Physiology of Temperature Regulation," Physiol. Rev., XLI (1961), 521-606.

4.13 Jackson, Donald C., and Schmidt-Nielsen, Knut. "Countercurrent Heat Exchange in the Respiratory Passages," Proc. N.A.S., LI (1964), 1192-1197.

5.1 Personal communication with Dr. Howard Haines, Department of Zoology, University of Oklahoma, 1970.

5.2 Pinson, Ernest A. "Water Exchanges and Barriers as Studied by the Use of Hydrogen Isotopes," Physiol. Rev., XXXII (1952), 123-134.

A.1 Stern, Thomas E. Theory of Nonlinear Networks and Systems, An Introduction. Reading, Mass.: Addison-Wesley, 1965.

A.2 Gantmacher, F. R. Applications of the Theory of Matrices. New York: Interscience Publishers, Inc., 1959.

A.3 DeRusso, Paul M.; Roy, Rob J.; and Close, Charles M. State Variables for Engineers. New York: John Wiley and Sons, Inc., 1967.

B.1 Wolf, George. Isotopes in Biology. New York: Academic Press, 1964.

B.2 Guinn, V. P. "Special Features of Tritium as a Tracer in Industrial Research," Advances in Tracer Methodology, Vol. I. Edited by Seymour Rothchild. New York: Plenum Press, 1963.

B.3 Burr, John G., Jr. Tracer Applications for the Study of Organic Reactions. New York: Interscience Publishers, Inc., 1957.

B.4 King, Vinetia. "A Study of the Mechanism of Water Transfer across Frog Skin by a Comparison of the Permeability of the Skin to Deuterated and Tritiated Water," J. Physiol., CC (1969), 529-538.

B.5 Thomson, J. F. Biological Effects of Deuterium. New York: The Macmillan Co., 1963.

B.6 Sepall, O., and Mason, S. G. "Vapor/Liquid Partition of Tritium in Tritiated Water," Can. J. Chem., XXXVIII (1960), 2024-2025.

B.7 Van Hook, W. Alexander. "Vapor Pressure of the Isotopic Waters and Ices," J. Phys. Chem., LXXII (1968), 1234-1244.

## APPENDIX A

## LINEAR INDEPENDENCE OF SOLUTIONS

Consider the time-invariant homogeneous linear nth-order system,

$$\dot{\bar{x}} = A\bar{x} \ , \tag{A.1}$$

where n-square real matrix A has n distinct real eigenvalues, $\lambda_i$, $i = 1, \cdots, n$. Assume that response $\bar{x}(t)$ to (A.1) from initial condition $\bar{x}(t_o)$ is known over interval $I = [t_o, t_f]$. It is desired to show that the vectors $\bar{x}(t_i)$, $i = 1, \cdots, n$, for $t_i \in I$, distinct, comprise a linearly independent set.

Note first that for the A matrix defined above, there corresponds to each eigenvalue an eigenvector, $\bar{e}^i$, such that the set $\{\bar{e}^i\}$ is linearly independent [A.1, p. 558]. Hence, any solution to (A.1) can be expressed as

$$\bar{x}(t) = \sum_{j=1}^{n} c_j e^{\lambda_j t} \bar{e}^j \ , \tag{A.2}$$

where the real constants $c_j$, $j = 1, \cdots, n$, depend only on initial condition $\bar{x}(t_o)$. By (A.2) and the definition of linear independence, a set $\{\bar{x}(t_i)\}$ of n vectors at distinct

times $t_1, \cdots, t_n$ from a single solution of (A.1) is linearly independent if and only if the condition

$$\sum_{i=1}^{n} \sum_{j=1}^{n} d_i c_j e^{\lambda_j t_i} \bar{e}^j = \bar{0} \tag{A.3}$$

implies that $d_i = 0$, $i = 1, \cdots, n$. Since $\{\bar{e}^j\}$ is a linearly independent set, (A.3) requires that

$$c_j \left( \sum_{i=1}^{n} d_i e^{\lambda_j t_i} \right) = 0 , \quad j = 1, \cdots, n . \tag{A.4}$$

Clearly, for system of equations (A.4) to have the unique solution $d_i = 0$, $i = 1, \cdots, n$, it is necessary that $c_j \neq 0$, $j = 1, \cdots, n$, and that matrix

$$\left( e^{\lambda_j t_i} \right) \equiv \begin{pmatrix} e^{\lambda_1 t_1} & \cdots & e^{\lambda_n t_1} \\ \vdots & & \vdots \\ e^{\lambda_1 t_n} & \cdots & e^{\lambda_n t_n} \end{pmatrix} \tag{A.5}$$

be nonsingular. Matrix (A.5), however, is a generalization of the Vandermonde matrix and is known to be nonsingular if and only if $\lambda_p \neq \lambda_q$ and $t_p \neq t_q$, $p, q = 1, \cdots, n$, $p \neq q$ [A.2, pp. 118-119].

In conclusion, then, assume that nth-order homogeneous linear system (A.1) has an A matrix with distinct real eigenvalues. Then, the set $\{\bar{x}(t_i)\}$ of n solution vectors taken from the same response at distinct times $t_1, \cdots, t_n$ is linearly

independent, provided all the response modes are represented ($c_j \neq 0$, $j = 1, \cdots, n$, in (A.2)).

For second-order systems, it can further be shown by means of phase portraits [A.1, p. 274, A.3, p. 470] that linearly independent solution vectors can sometimes be obtained even when the A matrix of (A.1) has repeated eigenvalues. If the eigenvalues are not distinct, then one of the two types of degenerate nodes shown in Fig. A.1 results. When only a single eigenvector direction exists, producing a node such as the one in Fig. A.1a, no two distinct vectors, $\bar{x}(t_1)$ and $\bar{x}(t_2)$, of any trajectory are colinear unless they are on the eigenvector. On the other hand, if matrix A of the second-order system has two linearly independent eigenvectors, the node assumes the form in Fig. A.1b. Hence, in this case, every vector on any trajectory is colinear with initial condition $\bar{x}(t_o)$, and no two vectors in the same solution are ever linearly independent.

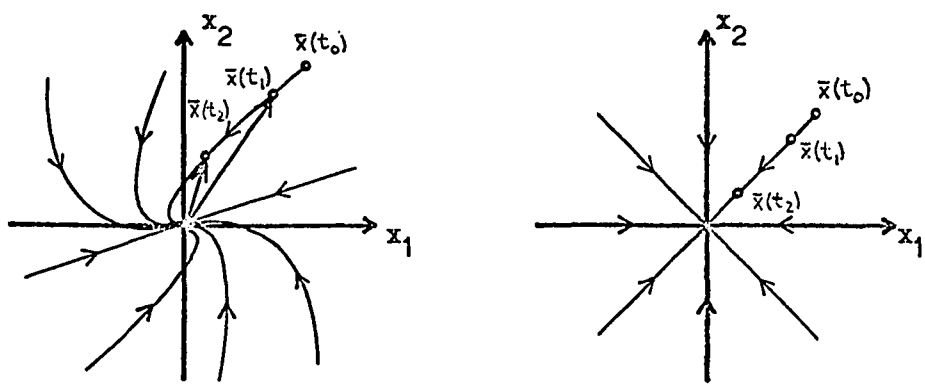


a. One Eigenvector b. Two Eigenvectors

Fig. A.1. Phase Portraits for Second-Order Systems with Repeated Negative Eigenvalues: a. One Eigenvector; b. Two Eigenvectors.

## APPENDIX B

## TRITIUM AS A TRACER FOR WATER IN BIOLOGICAL SYSTEMS

The radiation emitted by radioisotopic tracers such as THO can disturb the biological system under study by causing ionization within the cells. Generally, if a few cell molecules are altered by radiation, there will be no noticeable change in cell behavior, because the cellular machinery will quickly replace them. The important exception to the operation of this replacement mechanism is, of course, the genetic molecules. A radiation-induced change in a DNA molecule will result in a permanent change in the processes in the cell. (It is generally assumed that about 50 roentgens (R) per kilogram tissue mass gives rise to genetic damage [B.1, p. 53]; a dose of tritium of 140 μc/kg gives radiation equivalent to 0.3 R/week [B.1, p. 54].

Fortunately, because of its weak β-radiation (maximum energy of 18.5 kev, average energy of 5.6 kev, half-life of 12.5 years), non-localization in the body, and rapid excretion from the body, tritium ($T,H^3$) is relatively harmless [B.2, p. 227]. Beta-radiation is the least dangerous radiation to tissue, being readily absorbed by a few millimeters of the aqueous medium surrounding the radiating $H^3$ atoms

[B.1, p. 51]. Possible radiation damage in radioisotopic tracer experiments is further minimized because only small amounts of tracer need be used. Using a liquid scintillator, for example, the minimum detectable specific activity of $H^3$ in aqueous samples is $190 \times 10^{-6}$ μc/g [B.2, p. 230]. This need for only small amounts of tracer also reduces the possibility of other unwanted disruptions or damage to the biological system by the tracer. Hence, it can be assumed that the use of THO as a tracer does not disturb the system under study.

The chemical equivalence of isotopes (both radioactive and stable) suggests that a chemical or biological system might not strongly differentiate between an isotopic tracer and the unlabeled substance being traced. Differences in the behaviors of isotopes, called isotope effects, do arise, however, because of their unequal atomic masses. Although isotopes can form the same types of chemical bonds, their different masses cause differences in the rates of bonding and, therefore, differences in chemical reaction velocities and equilibria of reactions. Isotope effects become less noticeable as the mass-ratio of the isotopes in question decreases; in practice they are appreciable only with isotopes of hydrogen, carbon, and nitrogen [B.3, p. 3]. The ratio of bonding rates, however, can be much greater than the isotopic mass-ratio might indicate. For example, carbon-deuterium bonds break about 3 to 10 times more slowly than carbon-hydrogen

bonds, even though the deuterium-hydrogen mass-ratio is only 2. The difference between the behavior of tritium and hydrogen is even greater [B.3, p. 3].

Isotope effects can be especially significant in biological systems, both because their magnitudes cumulatively increase through the complex biochemical reactions and because the reactions do not usually go to completion, so that equilibria are not established [B.1, p. 47]. Unfortunately, chemical and physical processes are so varied and complex in living organisms that it is difficult to predict and evaluate the isotopic effects in a particular physiological system. Nevertheless, some biological processes might be better understood if life scientists considered such effects.

As previously indicated, primary kinetic isotope effects between tritium and hydrogen can be much larger than the ratio of masses, 3:1, would suggest. There are three factors which contribute to lowering the bonding activity of tritium as compared with hydrogen: the difference in free energy of activation, the velocity effect of the mass difference, and the possibility for hydrogen of "non-classical" penetration of the potential energy barrier [B.4, p. 530]. Activation energy comparisons between tritiated and ordinary hydrogen compounds are not available. It is known, however, that rate constants for hydrogen and deuterium substituted species can differ by more than a factor of 10 [B.4, p. 530]; the difference between hydrogen and tritium behavior would be expected to be

even greater. But, even if the relative reactivity rates of tritium and hydrogen were known for the reactions of various chemical compounds, their relationship still could not be calculated for the complex and poorly understood processes of living organisms.

Water transport mechanisms in living organisms include bulk flow; diffusion through aqueous media; passage through membranes by diffusion, filtration and perhaps other undetermined processes; and evaporation and condensation. In order to evaluate tritiated water as a tracer of ordinary water, the behaviors of tritiated and ordinary water must be compared for each of the above processes. Very low concentrations of tritium are assumed in order to avoid solvent effects and the questions of radiation and other biological damage (e.g., organisms die when given high concentrations of deuterium in their water, and deuterium is not even radioactive [B.5, p. 89]).

Little difference would be expected in the behaviors of tritiated and ordinary water in bulk aqueous media, for their diffusion rates are inversely proportional to the square roots of their atomic masses [B.4, p. 529]. Therefore, tritiated water diffuses about 5% slower than $H_2O$ in aqueous solutions.

The processes of water transfer through biological membranes are still poorly understood. If the water is transported through aqueous pores in the membrane, an isotope

effect for tritium on the order of that for aqueous diffusion would be expected. If, on the other hand, water passes through the membrane by the repeated making and breaking of O-H bonds of the hydration water within the membrane, then tritium may exhibit very large isotopic effects [B.4, p. 530], as mentioned above. Isotopic effects are usually small in equilibrium reactions, so if water passes through the membrane in quasi-equilibrium, tritiated water would not behave much differently from ordinary water. More rapid water transfer through the membrane, however, would tend to increase observable isotopic effects [B.4, p. 531].

Because of this uncertainty regarding water transport in membranes, King [B.4] compares the passage of deuterated (DHO) and tritiated water across frog skin membranes. She finds that for pH values of the external bath solution ranging from 5 to 8, the effective permeabilities, P, for THO and DHO do not differ significantly (e.g., $P_{THO} = 3.66$, $P_{DHO} = 3.62$ ($10^{-3}$ cm. $min^{-1}$) [B.4, p. 537]); that is, no isotope effects are observable in her work. This means that either an insufficient number of chemical reactions takes place in passage through the membrane to cause a significant isotope effect or that membrane structures are so fluid and inert that water can pass through without chemical reactions [B.4, p. 537]. Therefore, even though it was not possible to compare hydrogen and tritium behavior directly, King concludes that

the use of hydrogen isotopes as markers for measurements of water transfer across biological membranes appears valid.

The exchange of water between a mouse and its environment via the skin and lungs differs from water transfer across internal biological membranes. In the former water is in a liquid state within the animal but in a vapor state in the surrounding air. This change of state of the water can result in differences in the tritium concentrations in the liquid and vapor phases of an $H_2O$-THO mixture. In a saturated vapor-liquid system of tritiated water, for example, the isotopic ratios of the vapor and liquid states are given in Table B.1 (from [B.6, p. 2024]). Alternately, vapor pressures of several isotopic waters are given in Fig. B.1 (from [B.7, p. 1235]). Note, either from Table B.1 or Fig. B.1, that the vapor pressure of THO is lower than that of ordinary water. That is, evaporation of tritiated water tends to leave the tritium behind in the liquid phase. Hence, in contrast to the observation of Pinson quoted in Chapter V, tritium may exhibit an isotope effect when used as a tracer for water undergoing evaporation. For example, from the results of Table B.1, the THO specific activity of the evaporate from the skin (with, say, a skin temperature of 30°C) of the wild house mouse could be on the order of 10% less than that of the water in the skin.

Table B.1. Isotopic Ratios in Tritiated Water Vapor and Liquid in a Saturated System.

| Temperature °C | $\frac{[H^3]/[H^1]\ \text{vapor}}{[H^3]/[H^1]\ \text{liquid}}$ |
|---|---|
| 0 ± .5 | .86 ± .005 |
| 14 | .90 |
| 20 | .91 |
| 30 | .92 |
| 50 | .94 |
| 70 | .96 |
| 90 | .97 |

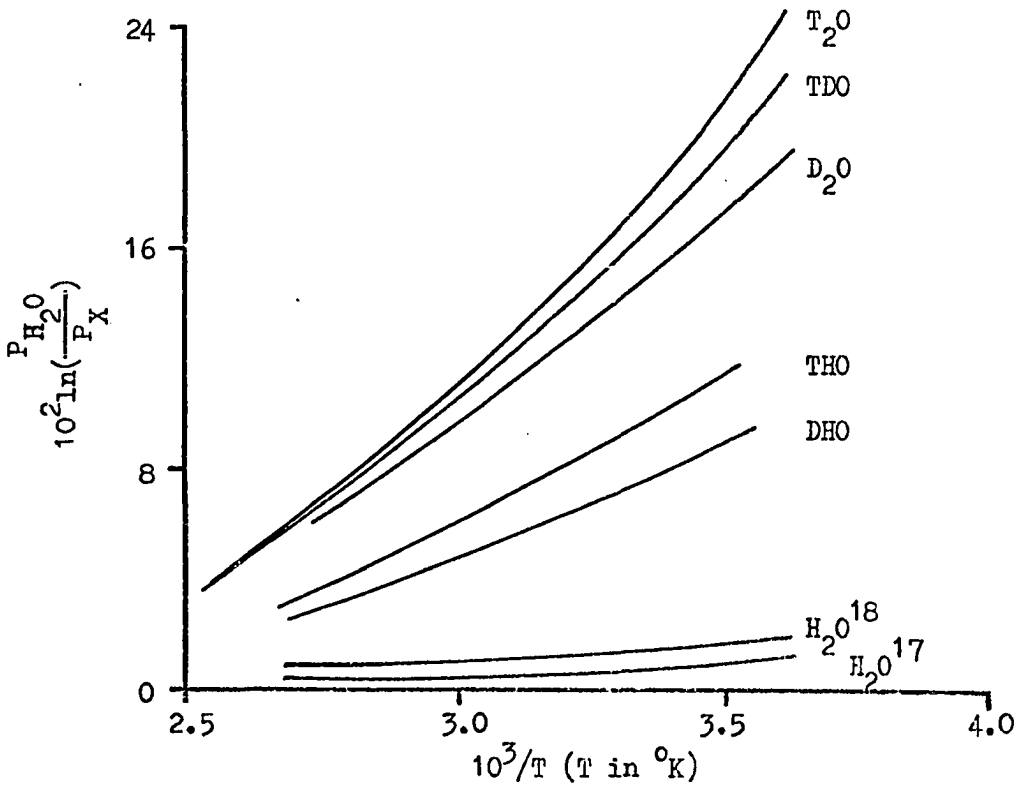


Fig. B.1. Vapor Pressures, P, of Several Isotopic Waters Versus Temperature, T.